

NBS

PUBLICATIONS

A11102 593368

NAT'L INST OF STANDARDS & TECH R.I.C.



A1102593368

Technical activities 1986 : Molecular Sp
QC100 .U56 NO.86-3483 1986 V19 C.1 NBS-P

NE

Technical Activities 1986 Molecular Spectroscopy Division

A. Weber, Chief

U.S. DEPARTMENT OF COMMERCE
National Bureau of Standards
National Measurement Laboratory
Center for Chemical Physics
Molecular Spectroscopy Division
Gaithersburg, MD 20899

November 1986

QC

100

.U56

86-3483

1986

C. 2

for:

DEPARTMENT OF COMMERCE

National Bureau of Standards

Gaithersburg, MD 20899

NBSIR 86-3483

TECHNICAL ACTIVITIES 1986
MOLECULAR SPECTROSCOPY DIVISION

A. Weber, Chief

U.S. DEPARTMENT OF COMMERCE
National Bureau of Standards
National Measurement Laboratory
Center for Chemical Physics
Molecular Spectroscopy Division
Gaithersburg, MD 20899

November 1986

Prepared for:
U.S. DEPARTMENT OF COMMERCE
National Bureau of Standards
Gaithersburg, MD 20899



U.S. DEPARTMENT OF COMMERCE, Malcolm Baldrige, *Secretary*
NATIONAL BUREAU OF STANDARDS, Ernest Ambler, *Director*

ABSTRACT

This report summarizes the technical activities of the NBS Molecular Spectroscopy Division during the Fiscal Year 1986. The activities span experimental and theoretical research in high resolution molecular spectroscopy, quantum chemistry and laser photochemistry, and include the development of frequency standards, critically evaluated spectral data, applications of spectroscopy to important scientific and technological problems, and the advancement of spectroscopic measurement methods and techniques. A listing is given of publications and talks by the Division staff.

FOREWORD

This report is a summary of the technical activities of the NBS Molecular Spectroscopy Division for the period of October 1, 1985 to September 30, 1986. The report was prepared as part of the Annual Report of the Center for Chemical Physics within the National Measurement Laboratory of NBS. The Molecular Spectroscopy Division is organized into three working groups comprised of permanent staff, post-doctoral fellows, guest scientists, and support personnel. An organizational chart of the Division is given at the end of this Foreword.

The goals and activities of the Division and the general nature of its technical programs are described in the Introduction, Section 1. Sections 2-4 present the descriptions of technical work done by the High Resolution Spectroscopy, Laser Photochemistry, and Quantum Chemistry Groups. Each group report gives project objectives, details of results obtained during the past year, and plans for future work. A mini-table of contents precedes each group report to afford a quick overview of the group's activities.

The technical descriptions are followed by Sections 5 and 6 which list the publications and talks given during the past year, while Section 7 lists the seminars hosted by the Division. The Division has had a number of visiting scientists during the past year; these are identified in Section 8.

This report was prepared during the period July-August, 1986. While anticipating some of the accomplishments that resulted from the work done during the remainder of the reporting period, the report clearly can not

do justice to the full range of activities and accomplishments that actually did take place. Some of these will be presented in the report for the following year.

Further information on the activities of the Division can be obtained by contacting the scientists identified in each project report, or by writing to Dr. Alfons Weber, Chief, Molecular Spectroscopy Division, Physics Building, B268, National Bureau of Standards, Gaithersburg, MD 20899.

Staff of the Molecular Spectroscopy Division

A. Weber, Chief

A. Flynt, Secretary

C. V. Kurtz, Division Technician

Laser Photochemistry

Stephenson, J. C., Group Leader
Elwell, L. B.
King, D. S.
Casassa, M. P.
Heilweil, E. J.
Woodward, A. M. (P.D.)
Bodaness, R. (G. S.)
Cavanagh, R. R. *
Burgess, D. (P.D.)*

Quantum Chemistry

Krauss, M., Group Leader
Goldgaber, N. I.
Julienne, P. S.
Mies, F. H.
Stevens, W. J.
Jasien, P. (P.D.)
Basch, H. (G.S.)
Beveridge, S. (G.S.)
Fink, W. (G.S.)
Lengsfeld, B. H. (G.S.)
Konowalow, D. D. (G.S.)
Mezei, M. (G.S.)
Miller, K. J. (G.S.)
Osman, R. (G.S.)
Vahala, L. (G.S.)

High Resolution Spectroscopy

Maki, A. G., Group Leader
Fraser, G. T. (P.D.)
Hougen, J. T.
Jacox, M. E.,
Lafferty, W. J.
Lovas, F. J.
Olson, W. B.
Pine, A. S.
Rotter, G. L.

Suenram, R. D.
Thompson, G. A. (P.D.)
Weber, A.
Craig, N. (G.S.)
Hollis, J. M. (G.S.)
Gillies, C. W. (G.S.)
Jennings, D. E. (G.S.)
Ohashi, N. (G.S.)
Sattler, N. (G.S.)
Zozom, J. (G.S.)

P. D. - Post Doc

G. S. - Guest Scientist

* - Surface Science Division

do justice to the full range of activities and accomplishments that actually did take place. Some of these will be presented in the report for the following year.

Further information on the activities of the Division can be obtained by contacting the scientists identified in each project report, or by writing to Dr. Alfons Weber, Chief, Molecular Spectroscopy Division, Physics Building, B268, National Bureau of Standards, Gaithersburg, MD 20899.

Staff of the Molecular Spectroscopy Division

A. Weber, Chief

A. Flynt, Secretary

C. V. Kurtz, Division Technician

Laser Photochemistry

Stephenson, J. C., Group Leader
Elwell, L. B.
King, D. S.
Casassa, M. P.
Heilweil, E. J.
Woodward, A. M. (P.D.)
Bodaness, R. (G. S.)
Cavanagh, R. R. *
Burgess, D. (P.D.)*

Quantum Chemistry

Krauss, M., Group Leader
Goldgaber, N. I.
Julienne, P. S.
Mies, F. H.
Stevens, W. J.
Jasien, P. (P.D.)
Basch, H. (G.S.)
Beveridge, S. (G.S.)
Fink, W. (G.S.)
Lengsfeld, B. H. (G.S.)
Konowalow, D. D. (G.S.)
Mezei, M. (G.S.)
Miller, K. J. (G.S.)
Osman, R. (G.S.)
Vahala, L. (G.S.)

High Resolution Spectroscopy

Maki, A. G., Group Leader
Fraser, G. T. (P.D.)
Hougen, J. T.
Jacox, M. E.,
Lafferty, W. J.
Lovas, F. J.
Olson, W. B.
Pine, A. S.
Rotter, G. L.

Suenram, R. D.
Thompson, G. A. (P.D.)
Weber, A.
Craig, N. (G.S.)
Hollis, J. M. (G.S.)
Gillies, C. W. (G.S.)
Jennings, D. E. (G.S.)
Ohashi, N. (G.S.)
Sattler, N. (G.S.)
Zozom, J. (G.S.)

P. D. - Post Doc

G. S. - Guest Scientist

* - Surface Science Division

TABLE OF CONTENTS

Abstract	i
Foreword	iii
Staff of the Molecular Spectroscopy Division	v
1. Introduction.	1
A. Goal	1
B. Organization	2
C. Division Programs.	2
D. Collaborations	5
E. Other Agency Support	5
2. High Resolution Spectroscopy Group.	7
A. Introduction	9
B. Calibration and Data Center Activities	9
C. Spectroscopy for Environmental Studies	12
D. Spectroscopy of Hydrogen-bonded and van der Waals Complexes	22
E. Matrix Isolation Spectroscopy.	32
F. General Spectroscopy and Theory.	36
3. Laser Photochemistry Group.	43
A. Introduction	44
B. Condensed Phase Energy Transfer.	44
C. Laser Diagnostics of Surface Dynamics.	52
D. Dynamics of van der Waals Molecules.	57
E. Photophysical Studies of Photosensitizers.	61

4.	Quantum Chemistry Group	63
	A. Introduction	65
	B. Theoretical Calculations on Biomolecules	66
	C. Quantum Chemistry of Small Molecules	73
	D. Scattering in the Presence of Radiation.	76
	E. Atomic and Molecular Scattering Theory	79
5.	Publications.	83
6.	Talks	91
7.	Molecular Spectroscopy Division Seminars.	97
8.	Visiting Scientists	101

MOLECULAR SPECTROSCOPY DIVISION

A. Weber, Chief

SUMMARY OF ACTIVITIES

Fiscal Year 1986

1. INTRODUCTION

A. Goal

This Division is a discipline oriented unit and its goal is to be at the forefront of modern theoretical and experimental spectroscopy in order to:

Advance spectroscopic measurement methods and techniques

Develop models, theoretical concepts and quantum theoretical methods for predicting molecular properties and interactions

Obtain reliable reference spectroscopic data for NBS, government, research community and industrial needs

Understand and model fundamental chemical processes

Provide state-of-the-art frequency standards

Transfer forefront spectroscopic expertise to other NBS Divisions, other government agencies, industry and the research community.

Within the framework of these general goals the Division also follows three specific thrusts which are part of the overall program of the Center for Chemical Physics - Properties of Weakly Bonded Systems, Biotechnology, and Energy Transfer. Properties of weakly bonded systems are obtained for small atomic and molecular complexes held together by van der Waals and hydrogen bond forces in order to develop a data base to understand conformation, thermodynamics, and reactivity of such systems. The objectives of our thrust in biotechnology are to develop and implement methods for the study of metal interactions in proteins and nucleic acids using primarily quantum mechanical techniques, while the major effort of the third thrust is directed to the study of vibrational energy transfer.

This summary contains a report of the activities of each of the three groups within the Division during the past year and demonstrates how they are meeting the above objectives.

B. Organization

To carry out its work the Molecular Spectroscopy Division is organized into three working groups: High Resolution Spectroscopy (HRS), Laser Photochemistry (LPC), and Quantum Chemistry (QC). The permanent Division staff is augmented by that of postdoctoral fellows and guest scientists. During the past year we have had fourteen guest scientists and four post doctoral fellows engaged in Division projects. In addition, two members of the Surface Science Division participated in the work of the LPC group. A list of the guest scientists, their permanent affiliations, and their activities is given in Section 8 of this report.

C. Division Programs

To be able to respond to the present and projected needs of NBS, the Center for Chemical Physics (CCP), and the user community, a significant fraction of the Division's effort is directed toward achieving and maintaining the expertise of its staff in their discipline oriented fields, and into maintaining its experimental facilities at the state-of-the-art level. We must remain at this level of expertise in spectroscopic measurements, theory, and interpretation in order to respond quickly to provide standards, serve national technical needs, and to insure adequate response to future, unknown problems. This approach is justified by the past and present applications of experimental and theoretical spectroscopy by our Division. These applications also provide much of the direction and motivation for our efforts. Remote sensing for industrial and atmospheric monitoring, laser chemistry, and combustion diagnostics are a few of the many important high technology areas that depend on modern spectroscopic techniques.

As described in Section 2, the work of the HR group involves experimental and theoretical applications of molecular spectroscopy for characterizing gas phase molecules, primarily in the infrared (rotation-vibrational) and microwave (rotational) spectral regions, the development of frequency standards for the infrared, and the development and application of new experimental techniques for high resolution spectroscopy. The emphasis of these studies is in the applications of our expertise to problems in structural chemistry, atmospheric chemistry, chemical analysis, radio astronomy and the properties of weakly bound molecular species.

The environmental problem posed by the pollutants of the earth's atmosphere, especially the role played by trace constituents in the chemistry of the upper atmosphere, are of major concern and a portion of the group's activities is devoted to providing critically needed data to help solve some of these problems. In this effort our activities are guided by the needs of the environmental research community, and are conducted with the support of NASA and AFGL. These efforts will continue to play an important role in the work of the HR group during the coming years.

Weakly bound molecular complexes, i.e., van der Waals and hydrogen bonded molecules have received considerable attention in our laboratory during the past year and will continue to do so in the future. The Division is in a unique position of having available personnel and instrumentation that permits such studies to be performed using any and all of the facilities from the microwave to the near infrared region of the spectrum in a concerted attack on the problems posed by these weakly bound systems. These experimental efforts are buttressed by the analytical and computational theoretical expertise available in the Division.

The Division is the home of the NBS Molecular Spectra Data Center. This Center, supported by the Office of Scientific Reference Data and staffed by members of the HR group provides evaluated data on molecular rotational spectra in the microwave region and develops evaluated infrared spectra to be used as standards in calibrating diode lasers and infrared laser spectrometers. This work is based on the needs of the user community. Thus the work on infrared standards is a response to requests from the instrumentation industry, industrial research laboratories, applied technological user groups, and government agencies and laboratories. Improvements in the stability of diode lasers have emphasized the need for accurate calibration standards. The absorption frequencies of N_2O that involve the lower energy levels are now being tied to the cesium frequency standard. This work has been made possible through the joining of the unique facilities of the Time and Frequency Division of NBS/Boulder with our spectroscopic expertise. Other collaborations, with non-U.S. research groups exist as well in an effort to develop the most extensive and accurate set of frequency calibration data. A recent activity is the critical evaluation and tabulation of the vibrational and electronic energy levels of transient molecules. Section 2.B of the HR group report describes the various activities of the Data Center.

The LPC group primarily does quantum-state specific studies of molecular dynamics. A common factor in the research of this group is the role of energy transfer in the spectroscopy and kinetics of molecules. Three major activities are pursued: Condensed Phase Energy Transfer, Laser Diagnostics of Surface Dynamics, and Dynamics of van der Waals Molecules. As described in Section 3.B, in the first of these the direction taken is the study of vibrational energy transfer. This research was extensively discussed in the Annual Report for FY85 and the research outlined and proposed there has been pursued successfully during the past year in the determination of the rates of energy transfer from vibrationally excited chemical bonds in liquids, solids, and on molecules bound to surfaces.

In the second major activity the goal is to obtain an understanding of the energy transfer and chemical dynamics occurring at metal surfaces at a fundamental level. This work is done in close collaboration with staff members of the Surface Science Division. This collaboration has resulted in the creation of an experimental facility to perform state-resolved studies of

thermally and laser desorbed molecular processes at well characterized surfaces. Details about this year's accomplishments are presented in Section 3.C.

The capability to perform time resolved spectroscopic measurements at the picosecond level has been turned to good advantage in the study of vibrational predissociation of van der Waals molecules. The experiments are performed in the time domain and thereby yield a direct measure of the lifetimes of the predissociating states. This work is described in Section 3.D of the LPC group report.

The field of Quantum Chemistry continues to experience new developments which extend the range of reliable and useful calculations to complex polyatomic systems. The stabilities, conformations, spectroscopy and reactivity of complex molecules, clusters, ions, radicals, and transition states, among others, are successfully investigated by the Quantum Chemistry group. The ability of the QC group to attack large scale computational problems using ab-initio rather than semi-empirical methods is significantly enhanced by the dedicated IBM 4381 superminicomputer located in the Molecular Structure and Modeling Facility of the Molecular Spectroscopy Division.

A major effort of the QC group described in Section 4.B is in the field of theoretical calculations on biomolecules. The goal of this program is the theoretical calculation of the energetics, spectroscopy, and reaction behavior of biomolecules with emphasis on the role of metal interactions in biomolecules. Ab initio methods are used to the exclusion of semi-empirical methods to insure predictability. The program is developed on three levels. At the first and fundamental level is the development of an ab initio electronic structure, reaction field method and code which will allow quantum mechanical calculations on systems of the order of 1000 atoms. Molecular and statistical mechanics is used to provide conformation for quantum models and to determine the environment for a reaction field approach. At the second level accurate ab initio calculations of small prototype systems provide data on a wide range of properties which also contributes to the large theoretical data base required in the reaction field code. At the third and applied level, model calculations that relate to specific problems of current interest are undertaken. The reaction field code development is the major thrust of this program.

During the last few years the three groups have been engaged in the study of the properties of van der Waals and hydrogen bonded complexes. This activity is continued using the experimental and theoretical expertise represented in each group and the individual group reports give detailed description of the work done. Only free complexes (i.e., gas phase) are investigated in order to obtain clearly interpretable data on molecules which are unperturbed by molecular interactions that exist in the condensed phase. Thus the HR group reports on its studies of the resolved microwave rotation and infrared rotation-vibration spectra while the LPC focusses its attention on the dynamics of vibrational pre-dissociation. In many cases the interpretation of the experimental results is aided by the analytical and

computational theoretical studies performed in the HR and QC groups. The work done by the three groups on weakly bound complexes constitutes therefore a Division wide effort in which the groups are participating in a mutually supportive and beneficial manner. The study of weak molecular interactions as exemplified by the van der Waals and hydrogen bonded molecules is a field of considerable present and future interest and our Division is expected to fully participate in these investigations during the coming years (cf. the Pimentel Report "Opportunities in Chemistry," National Academy Press, Washington, D.C., 1985, and the more recent Brinkman report on "Physics Through the 1990s," National Academy Press, 1986).

D. Collaborations

The Division staff conducts its research in collaboration with postdoctoral associates, members of the Surface Science and Time and Frequency Divisions as well as with many non-NBS visiting scientists. Some of these use the facilities of the Division and are appointed Guest Scientists at NBS. Section 8 of this reports lists the names, affiliations, and activities of the guest scientists who collaborated with us during the past year. Further collaborations exist with other scientists associated with universities from the U.S. and abroad whose names are given in the various project descriptions and appear as co-authors of many of the publications and talks listed in Sections 5 and 6 of this report.

E. Other Agency Support

Among the several goals of the Division are the services provided to various agencies of the government and private industry which in turn support some of the work done in the Division. The various agencies of the Department of Defense (ONR, ARO, AFGL, AFOSR), NASA, DOE, as well as the National Foundation for Cancer Research are among those that sponsored some of the research done during the past year.

In the remainder of this Annual Report are the individual group reports (Sections 2, 3, 4), the listings of publications and talks (Section 5, 6), Division seminars (Section 7), and guest scientists (Section 8).

2. HIGH RESOLUTION SPECTROSCOPY GROUP

N. Craig, G. T. Fraser, C. W. Gillies, J. T. Hougen, M. E. Jacox, W. J. Lafferty, F. J. Lovas, A. G. Maki, W. B. Olson, A. S. Pine, G. Rotter, R. D. Suenram, G. A. Thompson, A. Weber, and J. Zozom.

A. Introduction

B. Calibration and Data Center Activities

1. N₂O Frequency Measurements Extending Calibration Data into the 2800 cm⁻¹ Region
2. OCS Heterodyne Measurements for Calibration from 1866 to 1920 cm⁻¹
3. Recommended Rest Frequency List
4. Microwave Spectral Tables
5. Update of Landolt-Börnstein Structural Tables of Free Polyatomic Molecules
6. Vibrational and Electronic Energy Levels of Transient Molecules
7. Future Plans

C. Spectroscopy for Environmental Studies

1. N₂- and Air-Broadening in the Fundamental Bands of HF and HCl
2. Measurements of Collisional Interference in Nitrous Oxide
3. Heterodyne Frequency Measurements for Nitric Oxide (NO)
4. New Measurements and Analysis for Nitric Acid (HNO₃)
5. Rotational Intensity Dependence Measured for ClO
6. Analysis of the Spectrum of H₂O₂
7. Future Plans

- D. Spectroscopy of Hydrogen-bonded and van der Waals Complexes
1. Rotational Spectrum and Structure of $\text{CF}_3\text{H-NH}_3$
 2. Rotational Spectrum of the Hydrogen-bonded Formamide-water Dimer
 3. Microwave Spectrum and Properties of the Methanol-Formamide Dimer
 4. Microwave Spectra and Structures of the van der Waals Complexes Ar-Formamide and Ar-Methanol
 5. Nearly Free Internal Rotation in Ar- CH_3Cl Determined from its Microwave Spectrum
 6. The Microwave Spectrum of the $K=0$ States of Ar- NH_3
 7. Van der Waals Potentials from the Infrared Spectra of Rare Gas-HF Complexes
 8. NATO-Advanced Research Workshop
 9. Future Plans
- E. Matrix Isolation Spectroscopy
1. Fluorine-Atom Reaction Study
 2. Excited Argon-Atom Reaction Studies
 3. Reaction Intermediates in the Decomposition of Energetic Materials
 4. Future Plans
- F. General Spectroscopy and Theory
1. Fourier Transform Measurements of High Temperature Species; Infrared Gas Phase Spectra of LiCl, LiH, and LiD
 2. Hydrogen Migration Tunneling Effects in the Rotational and Vibrational Spectrum of Protonated Acetylene C_2H_2^+
 3. The Torsional-Wagging Tunneling Problem and the Torsional-Wagging Rotational Problem in Methylamine
 4. Far-Infrared Spectrum of Methylamine
 5. Transfer Optics System Design
 6. Analysis of Infrared Spectra of SiH_3D
 7. Future Plans

A. Introduction

The work of this group spans a variety of spectroscopic topics many of which are a part of programmatic efforts. Accordingly the activity reports are grouped into five separate sections: Calibration and Data Center Activities, Spectroscopy for Environmental Studies, Spectroscopy of Hydrogen-bonded and van der Waals Complexes, Matrix Isolation Spectroscopy, as well as General Spectroscopy and Theory. Each section is concluded with a brief statement of work planned for the coming year. The descriptions list the scientists active on the projects. These include NBS staff, guest scientists, as well as, outside collaborators.

B. Calibration and Data Center Activities

We collect under this heading the work of the group connected most closely with the core mission of NBS, namely the production and dissemination of compilations of accurately measured frequencies or wavenumbers for use as secondary standards, and of critically evaluated molecular constants for use in other disciplines. Occasionally, spectral fitting programs, for use in reducing data in other laboratories are also proceeded. The group devotes a significant portion of its effort each year to this program, and frequently collaborates with workers in other laboratories. Outputs of the program serve needs spanning the microwave to the ultraviolet spectral regions.

1. N_2O Frequency Measurements Extending Calibration Data into the 2800 cm^{-1} Region
(A. G. Maki, J. S. Wells, and A. Hinz)

In a continuation of our collaborative work with Joe Wells (NBS, Boulder) we have this year measured the frequency of several important hot band transitions in the 1257 to 1335 cm^{-1} region. These data were used to provide a finer comb of calibration features in this region, but their most important contribution has been to tie more energy levels of N_2O to the cesium frequency standard. From these accurate energy level determinations, it is possible to obtain accurate transition frequencies outside the area of direct measurement. In particular, these new frequency measurements allow us to extend our calibration tables to the 2800 cm^{-1} region, which was the primary goal of this year's work.

This work has also given us the opportunity to compare our frequency measurements with frequencies derived from wavelength measurements coming from various other laboratories. It appears that the recent work reported by Toth (JPL) using the Brault interferometer at Kitt Peak gives wavenumber values that are consistently close to those we measure. Toth's accuracy seems to be largely due to the calibration procedure he has been using based on frequency measurements of several bands.

Some of the hot band measurements that were made this past year will assume greater importance next year if we are able to measure some of the other transitions that are on our agenda. These measurements will provide frequency values for new energy levels and this will lead to new calibration bands in the 2300 to 3000 cm^{-1} region. This work is supported by NASA.

2. OCS Heterodyne Measurements for Calibration from 1866 to 1920 cm^{-1}
(A. G. Maki, J. Wells, and A. Hinz)

Another advance in the development of OCS absorption lines as convenient frequency standards was made by the heterodyne measurement of a number of transition frequencies in the 1866 to 1915 cm^{-1} region. These measurements have allowed us to prepare an improved calibration table for this region and also provide a good measure of the energy levels for the $12^{\circ}0$ state from which other transition frequencies can be calculated. This work is supported by NASA.

3. Recommended Rest Frequency List
(F. J. Lovas and G. Rotter)

The first revision of the paper originally entitled "Recommended Rest Frequencies for Observed Interstellar Molecular Microwave Transitions - 1984 Revision" was published in the January 1986 issue of J. Phys. Chem. Ref. Data. While the manuscript was in the publication process, we continued to update the spectral entries through 1985 so the title was modified to "- 1985 Revision" to reflect the content more accurately.

The next revision of this paper is planned for 1988, so the literature search of radio astronomy papers and data evaluation of new microwave studies of these species will continue. Last year preprints were widely distributed and very favorable responses were received. Since the manuscript was published in January, several requests for magnetic tape copies have been received and very recently Professor K. R. Lang of Tufts University requested permission to reproduce the frequency list in a forthcoming book Astrophysical Formulae.

4. Microwave Spectral Tables
(F. J. Lovas, G. Rotter, and R. S. Suenram)

The general search for all papers dealing with microwave spectral data continues. Reprints or photocopies of all pertinent reports are obtained and filed according to empirical formula. These files are the source of data for spectral evaluation reported in the various publication series which the data center produces.

Work continues on the Part III of the Microwave Spectral Table series. This involves the spectra of simple hydrocarbon species C_xH_y . During the current year we have been carrying out evaluations on species exhibiting internal rotation from methyl groups. This project is slated for completion in September 1986 and appears to be on schedule. This is

part of the long range plan to develop a microwave spectral atlas, so care is taken to keep all the coding compatible with previous compilations in this series.

We continue to up-date our computer files on diatomic and triatomic species. Since the publication of Part I. Diatomic Molecules, 21 new species have been added and the spectra for 34 species have been augmented. Similarly for Part II. Triatomic Molecules, spectra for 15 new species have been added and the data on 30 other species have been updated.

5. Update of Landolt-Börnstein Structural Tables of Free Polyatomic Molecules
(J. H. Callomon, E. Hirota, K. Kuchitsu, and W. J. Lafferty)

A project to update the Landolt-Börnstein compilation, "Structure Data of Free Polyatomic Molecules," has just been completed. This effort includes all structural data of gas phase molecules reported in the literature since the last volume was published in 1976 up to the end of 1985. It includes structures obtained by microwave, infrared, Raman, and visible spectroscopy as well as electron diffraction techniques. About 1500 new or improved structures are included in this work which has been a collaboration between workers in England, Japan, and the United States. The new volume is expected to be in press in early 1987.

6. Vibrational and Electronic Energy Levels of Transient Molecules
(M. E. Jacox)

All of the data previously compiled on the ground-state vibrational energy levels of polyatomic transient molecules have been transferred to a new IBM PC-AT computer system. This system not only is much more efficient, but also will facilitate possible future development of a version of the tables amenable to digital search. The tables of ground-state vibrational energy levels have been kept current; new or revised tables have resulted for approximately 75 molecules per year.

Matrix effects on the electronic spectra of diatomic molecules have been surveyed in a paper entitled, "Comparison of the Electronic Energy Levels of Diatomic Molecules in the Gas Phase and in Inert Solid Matrices," to be published in a forthcoming issue of Journal of Molecular Structure honoring Professor George C. Pimentel. Electronic band origins and vibrational band spacings in excited electronic states have been compared for the approximately 230 electronic transitions of diatomic molecules which have been observed both in the gas phase and in rare-gas or nitrogen matrices. With few exceptions, valence transitions and the associated vibrational band spacings are shifted by less than about 1% in neon matrices. Somewhat larger shifts, often to longer wavelengths, result from isolation of the molecule in a heavier rare gas or a nitrogen matrix. The perturbation of Rydberg transitions by the matrix, the effects of charge-transfer interaction with the heavier rare-gas matrices, and the behavior of the potential curve of the matrix-isolated molecule in the vicinity of the dissociation continuum are discussed.

With partial support from the NBS Office of Standard Reference Data, experimental data are being critically evaluated and compiled for the electronic energy levels of transient molecules possessing from 3 to 6 atoms. Both gas-phase and inert matrix data will be included. A wide variety of observation techniques, including high resolution absorption spectroscopy, laser-excited fluorescence, multiphoton ionization, and photoelectron spectroscopy, are being surveyed. Energies of band origins, fundamental vibration frequencies, rotational constants (A, B, C), and radiative lifetimes are among the properties now being entered. When complete, the tables will include well over 150 molecules.

7. Future Plans

Further work in our frequency standards effort is to systematically develop the N₂O spectrum and energy levels for use as frequency calibration bench marks by heterodyne frequency measurements of the 10⁰⁰-02⁰⁰ transitions near 1060 cm⁻¹ and the 10⁰⁰-01¹⁰ transitions near 1635 cm⁻¹. When combined with other frequency measurements made earlier in this program, these new measurements will provide the first frequency data on the 02⁰⁰-00⁰⁰ transitions near 1168 cm⁻¹ and thereby will provide improved data for the 10⁰⁰ and 01⁰⁰ levels of N₂O.

Evaluation of microwave spectra data will continue to focus on the two major projects in progress. The radio astronomy literature is continually searched for new observations to be included in the next revision of the Recommended Rest Frequency compilation. When the current work on the Microwave Spectral Tables - Part III on simple hydrocarbons is finished, we will begin evaluation of the next group, hydrocarbons containing oxygen.

The compilation of the electronic spectral data tables is nearing completion. It is planned to submit these tables to the Journal of Physical and Chemical Reference Data late in FY87.

Revisions and additions to the tables of ground-state vibrational energy levels will continue to be kept current. It is also planned to submit a supplement to these tables to the Journal of Physical and Chemical Reference Data late in FY87. This supplement will include a master index, in order to facilitate a complete search of the experimental literature on the vibrational and electronic spectra of polyatomic transient molecules.

C. Spectroscopy for Environmental Studies

Many small molecules play a significant role in the chemistry of the earth's atmosphere. As such, they are of significant interest to agencies like NASA, DOD and the CMA (Chemical Manufacturer's Association). The interest of these agencies generally focusses on molecular spectroscopy as a remote sensing tool and for the determination of concentration profiles. Consequently, the emphasis in this section is on band analyses as well as the important information on line intensities, line widths, line shapes, and the effect of pressure on these quantities. As in all

branches of spectroscopy, the very narrow band width of infrared laser sources now permits quite reliable studies of phenomena involved in spectroscopic concentration determinations.

1. N_2 - and Air-Broadening in the Fundamental Bands of HF and HCl
(A. S. Pine)

N_2 - and air-broadened lineshapes of HF and HCl transitions in the $v=1\leftarrow 0$ bands have been measured at $T=295$ and 202 K with a high-resolution difference-frequency laser spectrometer. Pressure broadening and shifts and collisional narrowing parameters have been extracted by least squares fitting of several collisional profiles to the spectra. Figure 2.1 shows the observed lineshape of the R(0) line of HF as a function of N_2 pressure fit to Voigt and Galatry (soft collision model) profiles. At low pressures, the collisional, or Dicke, narrowing effect causes deviations from the Voigt profile having a Doppler-fixed Gaussian component and yields a measure of the diffusion constants for the hydrogen halides in the buffer gases. The pressure broadening parameters, Γ , were effectively linear with pressure for the Galatry collisional narrowing model as they should be, whereas the Voigt fits were highly nonlinear as shown by the ratios of Γ for the two models in Fig. 2.1. At high J, where the pressure shifts are comparable to or larger than the broadenings, a slight asymmetry is observed in the lineshapes which is attributed to statistical correlation between velocity- and state-changing collisions. Fig. 2.2 indicates this asymmetry for the P(9) line of HF at $P(N_2) \sim 54$ Torr fit to the formally symmetric Voigt, soft and hard collisional narrowing profiles.

The ratio of air-to- N_2 broadening varies systematically with rotational levels and is always somewhat larger than that given by the relative quadrupolar contributions of O_2 and N_2 . The temperature variations in the broadening coefficients are also J dependent, deviating significantly from $T^{-1/2}$ and exhibiting opposite behavior for HF and HCl. These effects are summarized in Fig. 2.3 as a function of the rotational index m. This work is supported by NASA.

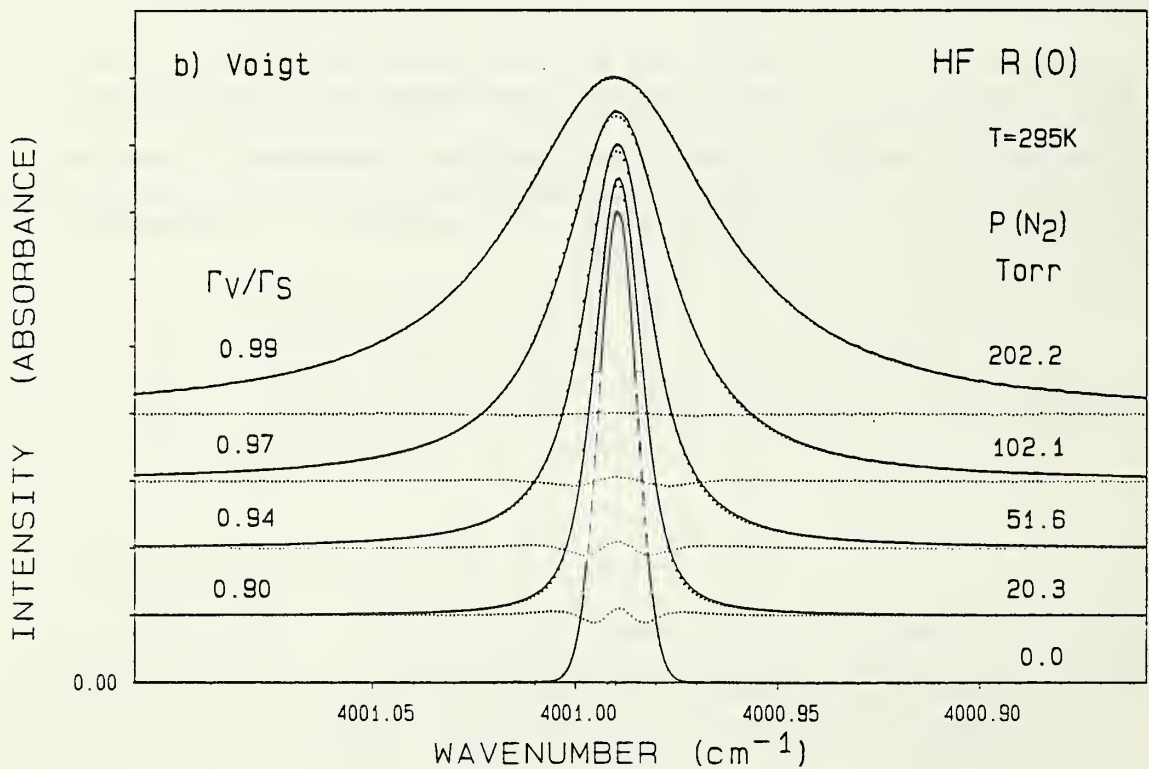
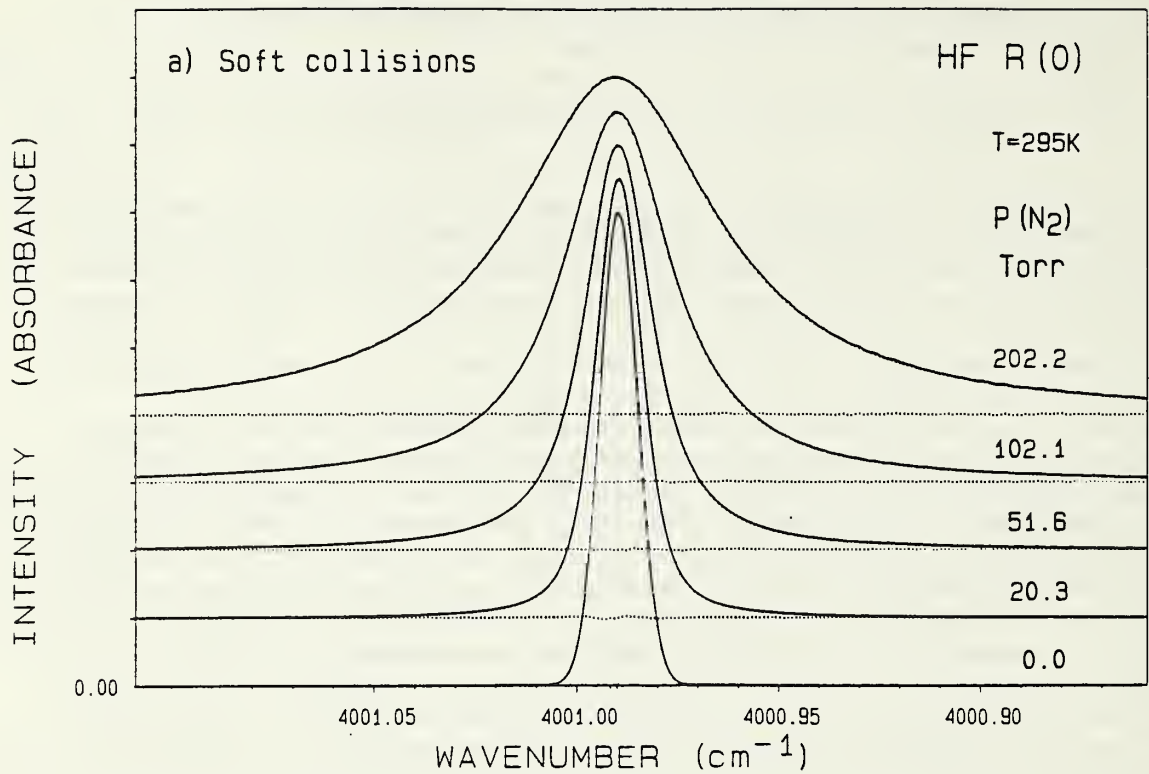


Fig. 2.1 Lineshape of HF as a function of N₂ pressure fit to Voigt and soft collision models.

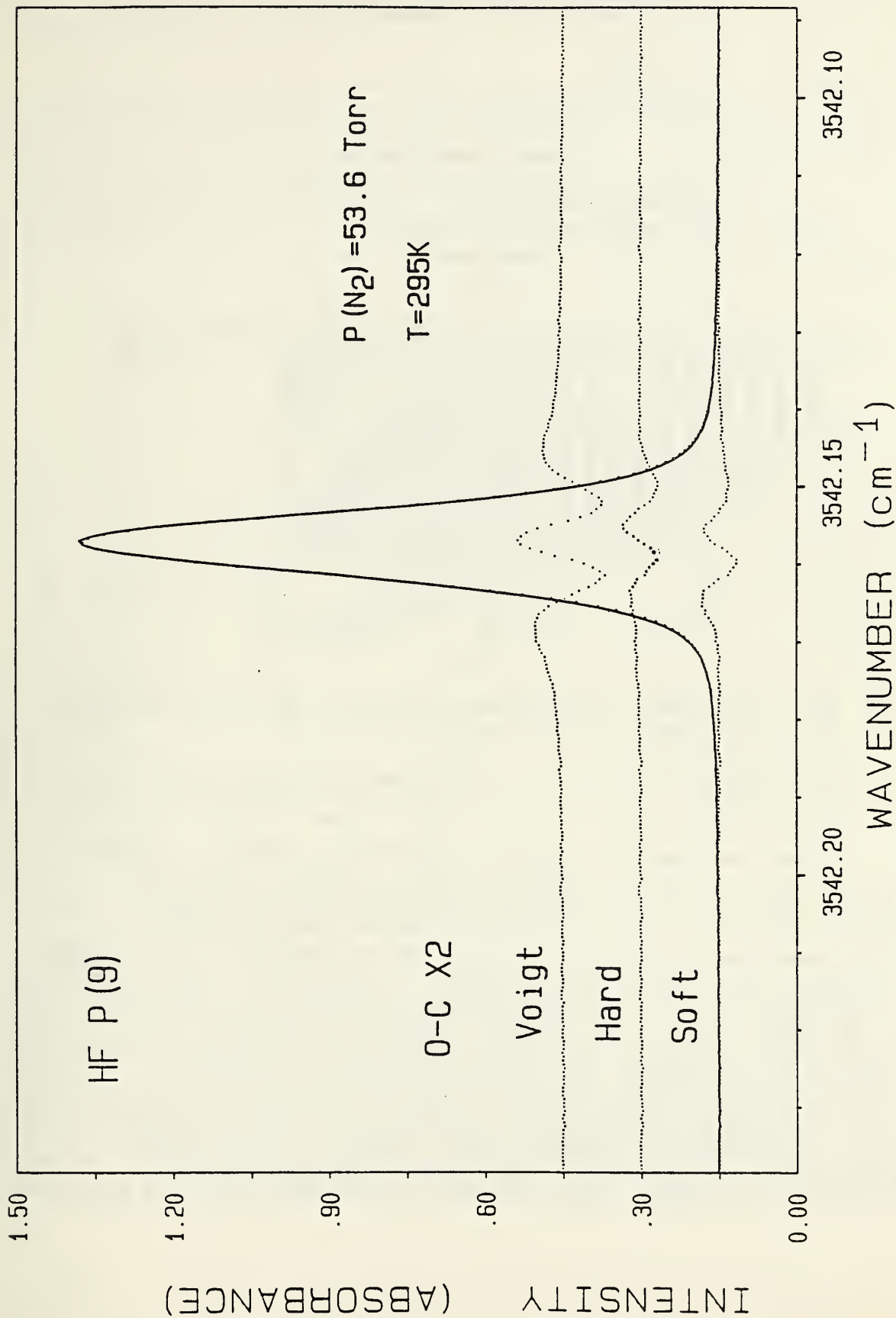


Fig. 2.2 The P(9) line of HF shown fit to the Voigt, hard, and soft collisional narrowing models.

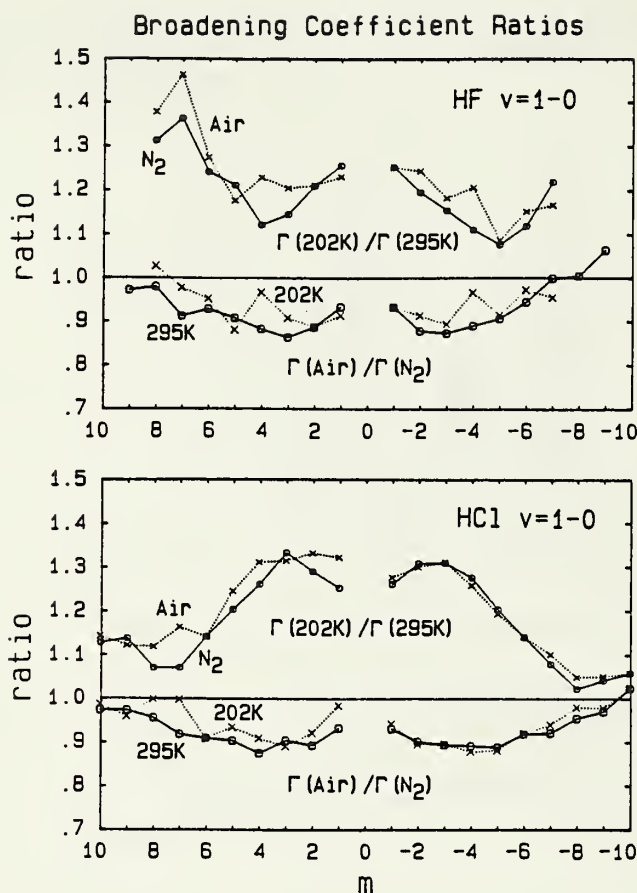


Fig. 2.3 Ratio of the air-to-N₂ broadening of HF and HCl as a function of temperature and rotational index, M.

2. Measurements of Collisional Interference in Nitrous Oxide (A. S. Pine)

We have been making a number of collisional lineshape studies in support of a NASA program to monitor the upper atmosphere for trace contaminants using sensitive infrared techniques. One of the major uncertainties is how to interpret the observed profile of a dense unresolved spectrum, such as occur for the strong, characteristic Q-branch and band-head features used for monitoring various species. When spectral lines overlap due to collisional broadening, the resulting envelope may not be the simple addition of individual component lineshapes if the collisions actually transfer excitation between energy levels involved in the unresolved transitions. This nonadditivity is a collisional interference effect, akin to motional narrowing, variously known as line coupling, line mixing or rotational collapse, and is well known for densities approaching the condensed phase. However, in the range of pressures below 10^5 Pa, pertinent to atmospheric and stratospheric conditions, the deviations from additivity are typically small and subtle

and require exceptionally high resolution, good signal-to-noise ratio and wide linear dynamic range as well as precise scanning control in order to be reliably measured.

Collisional interference at subatmospheric pressures has been observed recently using high resolution coherent Raman gain techniques for the Q branches of N_2 , CO and NO and in the infrared for Q branches of CO_2 using diode lasers and Fourier transform interferometers. In the present work we have performed measurements on N_2O with a precision tunable difference-frequency laser system. Preliminary transmission spectra of the Q branch of the $\nu_1 + \nu_2$ combination band of N_2O as a function of pressure are shown in Fig. 2.4 illustrating the high quality of the data.

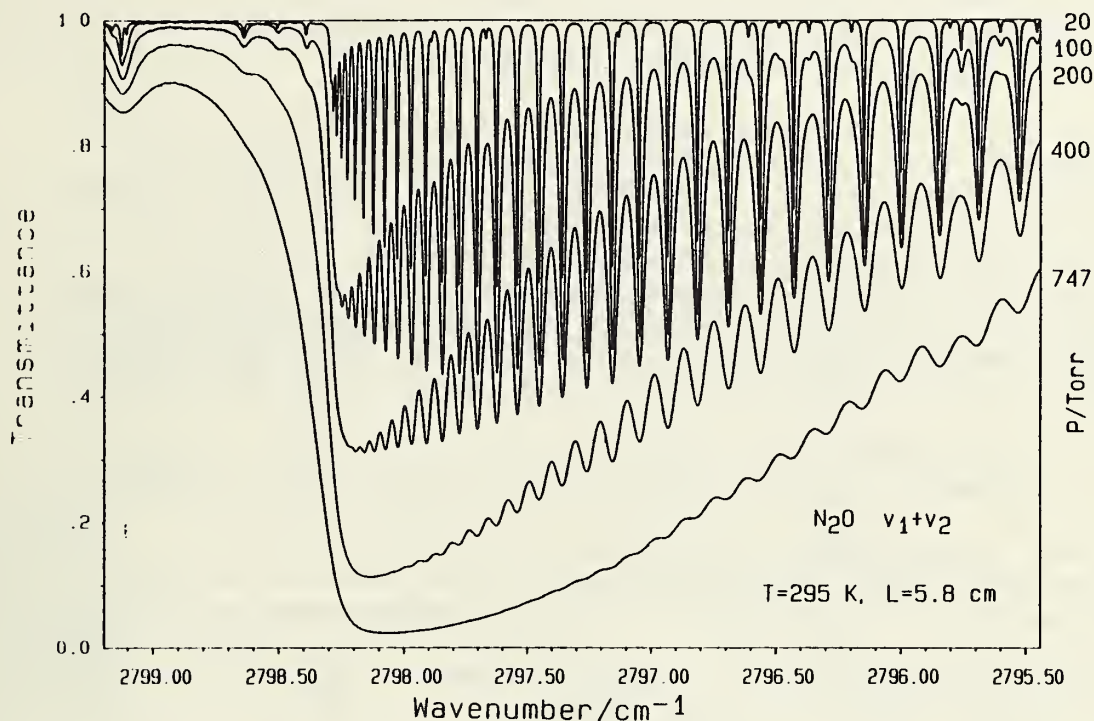


Fig. 2.4 Transmission spectra of the Q branch of the $\nu_1 + \nu_2$ combination band of N_2O as a function of pressure.

The wavenumber scale is linear and reproducible to $\leq 5 \times 10^{-5} \text{ cm}^{-1}$ using digital scanning servo control; the signal-to-noise ratio and the linear dynamic range are $\geq 1000:1$ using real-time division of the transmitted light by the incident light. The 0% transmission baseline is stable to within 0.1% and the 100% transmission baseline is reproducible to within 1%. This latter baseline uncertainty is the principal source of error in these measurements, particularly for the higher pressure traces where the troughs between the lines exhibit strong absorption and there is no clue as to the position of the baseline over an extended spectral range. The baseline is then determined from a sequential empty cell trace. However,

trace-to-trace variations in the relative sample and reference beam channels arise predominantly due to drifts in the interference fringes of the two detectors windows and filters (the sample cell windows are mounted at Brewster's angle to minimize reflections) and to beam wander from pressure-induced displacements and from thermal drifts of the phasematching oven for the LiNbO_3 nonlinear optical mixing crystal. The phasematching fluctuations are peculiar to the difference-frequency laser, but the other problems are common to any high-resolution transmission measurements. We are now developing a digitally-tuned F-center laser system with enough power to do direct optoacoustic absorption (rather than transmission) spectroscopy in order to improve the baseline reproducibility for collisional interference and for wing measurement. This work is supported by NASA.

3. Heterodyne Frequency Measurements for Nitric Oxide (NO)
(A. G. Maki, J. S. Wells, and A. Hinz)

For certain measurement applications, especially those involving laser techniques, it is often important to know quite accurately the frequencies of the absorption lines of NO. By using heterodyne frequency counting techniques we have measured 28 transitions of NO from 1750 to 1930 cm^{-1} . With the help of other measurements in the literature, especially microwave and radio frequency measurements, we have determined an improved set of constants to describe the infrared spectrum of NO. With these constants, very accurate tables of energy levels and transition frequencies have been prepared for NO. This work is supported by NASA.

4. New Measurements and Analysis for Nitric Acid (HNO_3)
(A. G. Maki, A. Fayt, J. Wells, Wm. B. Olson, and A. Goldman)

Over the past several years we have been involved in the measurement and analysis of the spectrum of nitric acid with the goal of producing an atlas or compilation of transition frequencies and intensities. Such a compilation is very useful for the analysis of remote sensing data being accumulated in various programs run by NASA and other agencies. As an example, Dr. Linda Brown (JPL) has taken our latest line-list for the ν_2 band of HNO_3 (near 1723 cm^{-1}) and added it to the data bank she has accumulated to help her in the analysis of ATMOS data. She was very pleased with the accuracy and completeness of our data. Dr. A. Goldmann (University of Denver) has also been very anxious to use our data on nitric acid and from time to time requests an updated copy of our latest data.

This past year new diode measurements were completed on the high rotational transitions of the ν_5 band of HNO_3 . These measurements, when combined with microwave and earlier infrared measurements from this laboratory, provided a more accurate set of ro-vibrational constants for the ν_2 band that enabled us to calculate an improved line-list. This improved line-list, consisting of about 12,000 entries, has been

circulated to various interested parties and will be included in the next version of the AFGL-trace gases tape, which is the major data source for most atmospheric workers.

The analysis of the highly perturbed ν_5 and $2\nu_9$ bands has been successfully accomplished by using a new computer program which fits data for two asymmetric rotor bands that are coupled through Fermi resonance and certain other resonances. This analysis allows us to fit even the most highly perturbed transitions with an overall standard deviation of 0.0007 cm^{-1} which is the accuracy expected since a number of transitions used in the fit are known to be overlapped even though a diode laser with nearly Doppler limited resolution was used for the measurements. Fig. 2.5 shows a particularly clean portion of the P-branch region of ν_5 in which the transitions are identified. In this figure it is easy to see how the perturbation shifts the $K_a < 13$ transitions to high frequencies while it shifts the $K_a > 13$ transitions to low frequency.

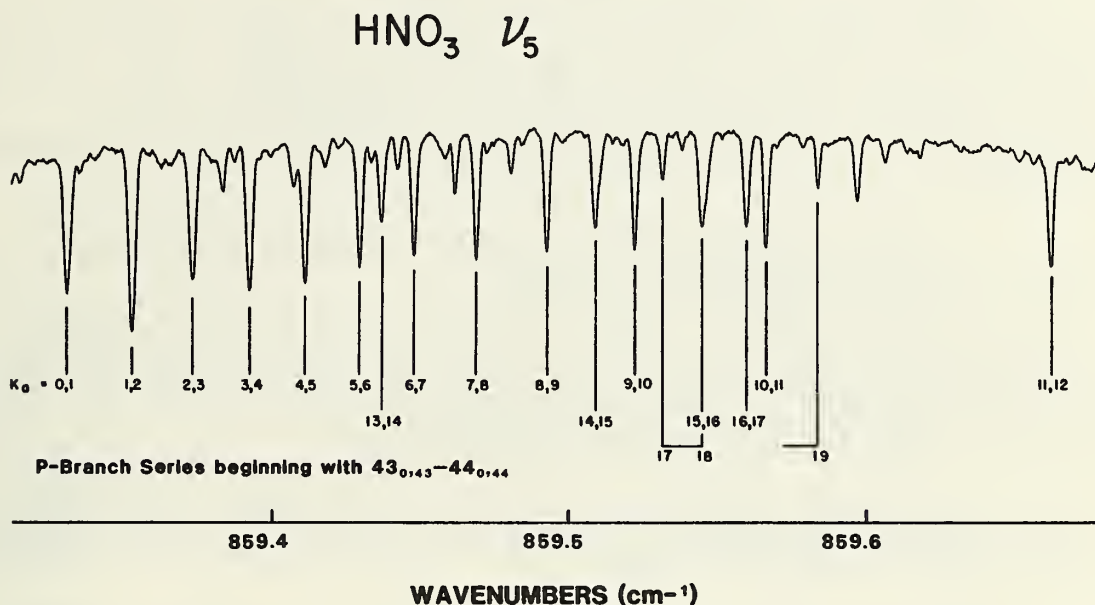


Fig. 2.5 Region of the P-branch in the ν_5 band of nitric acid.

Because of a high degree of correlation between some constants, this work will not be complete until a few more carefully chosen transitions are measured to try to reduce the correlation as much as possible. Then it will be necessary to test a new computer program which has been written to prepare an atlas of line positions and intensities for these two bands. We can anticipate that a complete line-list will be ready for the $850 - 930 \text{ cm}^{-1}$ region of HNO_3 within the next year. An important part of this work will be the determination of the relative signs and magnitudes of the transition moments for ν_5 and $2\nu_9$. This work is supported by NASA.

5. Rotational Intensity Dependence Measured for ClO
(A. G. Maki, J. B. Burkholder, P. D. Hammer, C. J. Howard,
G. Thompson, and C. Chackerian)

New frequency and relative intensity data on ClO have been determined using some diode laser measurements from this laboratory and some FTS measurements from the NOAA-Environmental Research Laboratory in Boulder, CO. Last year we described the reasons for this work, namely the need to verify the line positions and intensities in a search for the reason for discrepancies between infrared and microwave measurements of atmospheric ClO. After the work was begun here, it was learned that NOAA was making similar measurements and we joined forces.

One of the goals of this work was to measure the rotational dependence of the intensities of the fundamental infrared band of ClO. The rotational dependence is related to the ratio of the dipole moment of ClO to the vibrational transition moment. Since the transition moment seems to be small and the dipole moment is known to be fairly large, it was expected that the rotational dependence would be significant and could, in fact, be used to determine the transition moment. Our measurements did not require a knowledge of the concentration of ClO whereas all previous techniques had involved a measurement of the concentration of ClO in the absorption cell; a difficult and controversial measurement.

This work is now completed and a manuscript has been prepared but the results can be summarized as follows:

- o The ClO line frequencies are now known with greater accuracy, especially for the P-branch lines. While the new line positions are different from the old by as much as 20 MHz, the difference is not enough to reconcile the problems with the field measurements.

- o The rotational dependence of the line intensities is now known, but it only affects the derived concentration of ClO by 10 to 15% whereas the discrepancy is larger than that.

- o From the rotational dependence, the transition moment has been derived and it agrees with the previous value of $11.8 \text{ cm}^{-2} \text{ atm}^{-1}$, although the present results are not as accurate as we had hoped for.

- o By several arguments, including a determination of the temperature from intensity measurements, it has been shown that the laboratory measurements involve ClO that is in thermodynamic equilibrium at room temperature.

- o It has been shown that both the infrared and microwave field measurements involve ClO transitions that originate from the same vibronic state which is the lowest vibronic state.

The net results of this work is that we are unable to explain the problems with the field measurements, but the problems do not come from the laboratory data. This work is supported by NASA.

6. Analysis of the Spectrum of H_2O_2

(W. B. Olson, R. H. Hunt, A. G. Maki, and J. W. Brault)

Rotational constants of the OG and 1G torsional states and the matrix element coupling these states have been determined by fitting to a model of two coupled asymmetric rotors. The fitted data were primarily combination differences. Those for the OG torsional state were formed from published values of submillimeter wave transitions for low values of K_a , and those for high K_a (up to $K_a = 10$) were obtained from assigned transitions in the ν_5 OH stretching band. There are as yet no assigned submillimeter transitions involving the 1G torsional state, and all of the combination differences for this torsional state were obtained from the assigned transitions in the torsional hotband $\nu_5 + \nu_4(1U) - (1G)$.

Combination differences alone do not supply enough information to determine all the relevant parameters, i.e., they do not give direct information on the energy difference between the origins of the OG and 1G torsional states. The rotational-torsional energies of the OG state for $K_a = 8$ are only about 3 cm^{-1} above those for $K_a = 6$ in the 1G torsional state at low J , but because of the perturbation the levels of the two states are pushed apart, the separation increasing with increasing J to about 7 cm^{-1} at $J = 25$. Mixing of the wavefunctions of the OG, $K_a = 8$ levels with those of 1G, $K_a = 6$ through the perturbation leads to perturbation enhanced transitions from 1G, $K_a = 6$ to the ν_5 state with $K_a = 7$. Although these could be considered normally allowed transitions of a difference band, no transitions can be observed at J values lower than 15. It is only at this and higher values of J (to 25) that the wavefunction mixing is sufficiently large so as to provide sufficient intensity that the transitions may be observed. Differences between the normal transitions from OG, $K_a = 8$ to $K_a = 7$ in ν_5 , and the perturbation enhanced transitions from 1G, $K_a = 6$ to the same upper state levels provides direct information on the separation of the lower torsional state origins.

We obtained valuable supplementary information by assignment of the weak spectrum of the sum band from the OG state to $\nu_5 + \nu_4(1U)$. Direct differences between levels of the OG and 1G torsional states were obtained by differences of transitions with the same J and K_a in the OG and 1G torsional states to the same upper state level in the $\nu_5 + \nu_4(1U)$ vibrational-torsional state. Final constants are not yet available, but the fit is quite satisfactory at the present stage of refinement. The origin of the 1G torsional state is 254.550 cm^{-1} , about 0.35 cm^{-1} above the value obtained from the medium resolution far infrared spectrum. Our experimental value for the matrix element for the interaction of the OG and 1G torsional states proves to be only 15% higher than the value calculated by Hunt, Leacock, Peters, and Hecht [J. Chem. Phys. 42, 1931

(1965)]. Considering the complexity of their model and uncertainties in parameters required for input for their calculations, the agreement with our experimental value may be considered excellent.

7. Future Plans

In the coming year an atlas of absorption line frequencies and intensities will be completed for the ν_2 and ν_9 bands of HNO_3 near 880 cm^{-1} . This atlas will include all the transitions to these two states from the ground state including those transitions that are strongly perturbed by the effects of the Fermi resonance between these two states. We also expect to complete a paper describing the analysis of the spectrum of the ν_5 and $2\nu_9$ bands and also to complete a paper on the analysis of the ν_3 and ν_4 bands near 1300 cm^{-1} . This work is needed by various laboratories that are studying the concentration of nitric acid and nitrogen oxides in the atmosphere in connection with the ozone problem as well as the greenhouse effect.

By using a long path cell we should also like to make some heterodyne measurements on some of the weaker bands of OCS such as 11^10-00^00 (1372 cm^{-1}) 03^10-00^00 (1573 cm^{-1}) and 00^01-02^00 (1015 cm^{-1}). These measurements would locate more energy levels with respect to the ground state and would give us frequency data for the 520 cm^{-1} and 2100 cm^{-1} regions, as well as other regions.

We also expect to have new Fourier transform spectra of the lowest frequency fundamental band of SO_2 near 500 cm^{-1} . Both frequency and relative intensity measurements will be made on this band and the goal will be to produce a set of band constants that will enable us and others to accurately calculate the infrared spectrum of SO_2 in the $400-600 \text{ cm}^{-1}$ region for any temperature appropriate to an atmospheric path. Understanding atmospheric SO_2 , is, of course, important for understanding the acid rain problem.

D. Spectroscopy of Hydrogen-bonded and van der Waals Complexes

The program of study of hydrogen-bonded and van der Waals complexes initiated several years ago now represents a significant fraction of the group's total effort. Continuing studies using a difference frequency laser spectrometer in the 3 micron region, the BOMEM Fourier transform spectrometer in both the mid- and far- infrared, and studies using the pulsed beam Fourier transform microwave spectrometer are reported. The major efforts this year deal with structural determinations of weakly bound dimers from microwave spectra and potentials derived from extensive infrared spectra. This program has benefitted greatly this past year from collaborations with guest workers. We certainly plan to continue work in this direction for the foreseeable future.

1. Rotational Spectrum and Structure of $\text{CF}_3\text{H-NH}_3$
(G. T. Fraser, F. J. Lovas, R. D. Suenram, D. D. Nelson, Jr.,
and W. Klemperer)

The rotational spectrum of $\text{CF}_3\text{H-NH}_3$ has been obtained using a pulsed nozzle Fourier transform microwave spectrometer. A symmetric top spectrum is observed that is consistent with free internal rotation of the NH_3 subunit against the CF_3H subunit. Rotational transitions have been measured for both the ground and first excited internal rotor state of the complex. The spectroscopic constants which have been obtained include: $B_0 = 1996.903(2)$ MHz, $D_J = 3.46(12)$ kHz, and $eQ_q^N = -3.186(8)$ MHz. From the quadrupole coupling constant of the nitrogen nucleus, eQ_q^N , the bending amplitude of the NH_3 unit is determined to be $22.57(10)^\circ$. The hydrogen bond length is $2.314(5)$ Å and the weak bond stretching force constant is $0.066(2)$ mdyn/Å. The bond length and stretching force constant for $\text{CF}_3\text{H-NH}_3$ are similar in value to those determined for HCCH-NH_3 (2.33 Å and 0.070 mdyn/Å, respectively).

2. Rotational Spectrum of the Hydrogen-bonded Formamide-water Dimer
(R. D. Suenram, F. J. Lovas, G. T. Fraser, J. Zozom, and C. W. Gillies)

The characterization of hydrogen bonding between peptides and water molecules is one of the most challenging problems in modern science. The fundamental peptide-water hydrogen bonding may be exemplified by the prototypical formamide-water species. To date most of the information available on these systems has been provided by ab initio calculations. Now for the first time the complex of these two species has been investigated experimentally by employing a pulsed molecular beam Fabry-Perot microwave spectrometer with a heated pulsed nozzle.

Based on the ab initio calculations of Jasien and Stevens, [J. Chem. Phys. 84, 3271 (1986)], we have investigated the rotational spectrum of the lower energy form of the formamide-water complex. A planar cyclic double hydrogen bonded structure was calculated to be the lowest energy form, and the observed spectrum is in excellent agreement with this conclusion. The rotational constants obtained are listed in Table 2.1. Comparison of the ^{14}N nuclear electronic quadrupole coupling constants between the complex and formamide indicates that the complex is slightly non-planar with an angle of 16.8° between the planes of the subunits. The structure of the complex is illustrated in Fig. 2.6.

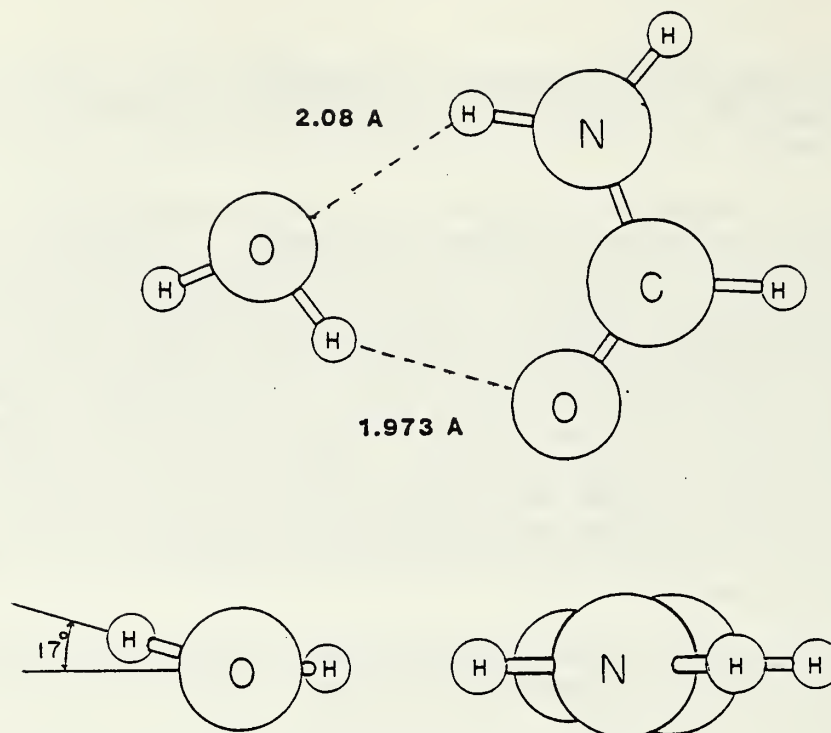


Fig. 2.6 Structure of the formamide-water dimer.

Table 2.1 Molecular constants determined from the microwave spectra of $\text{NH}_2\text{CHO}\cdots\text{H}_2\text{O}$ and $\text{NH}_2\text{CHO}\cdots\text{HOCH}_3$

Parameter	$\text{NH}_2\text{CHO}\cdots\text{H}_2\text{O}$ Value (MHz)	$\text{NH}_2\text{CHO}\cdots\text{HOCH}_3$ Value (MHz)
A	11227.913(34)	10186.69(15)
B	4586.997(2)	2088.86(8)
C	3258.872(3)	1764.18(6)
eQq_{aa}	1.330(5)	1.287(7)
eQq_{bb}	2.038(5)	2.026(6)
eQq_{cc}	-3.3685(5)	-3.313(6)
$\Delta (=I_c - I_a - I_b)$	-0.1095 μA^2	-5.05 μA^2

3. Microwave Spectrum and Properties of the Methanol-Formamide Dimer
(F. J. Lovas, R. D. Suenram, G. T. Fraser, J. Zozom, and C. W. Gillies)

Recent *ab initio* calculations on formamide-water and formamide-methanol performed by Jasien and Stevens of the Quantum Chemistry Group [J. Chem. Phys. 84, 3271 (1986)] indicated that the most stable form of each is a double hydrogen bonded planar ring structure. The results of the formamide-water study discussed above are quite consistent with the theoretical structure, although evidence for slight non-planarity is given.

Since the methanol complex is expected to have a structure similar to that of the water complex, we have examined formamide-methanol. The spectra were obtained in a pulsed beam Fabry-Perot microwave spectrometer with a heated nozzle containing liquid formamide. Rotational assignments were considerably aided by the unique hyperfine structure. The rotational analysis provided the rotational and hyperfine constants shown in Table 2.1. The rotational constants are consistent with the ring structure, but the out-of-plane moment and hyperfine constants indicate that the complex is non-planar (disregarding the methyl group).

With the monomer geometries fixed, a rotation of 15° about the HO axis (moving the CH_3 group out of the plane of the remaining atoms) provides good agreement with the observed moments of inertia. The structure of the complex is shown in two views Figs. 2.7. The internal rotation of the methyl group has also been observed. Analysis of the A-E splittings provides a barrier to internal rotation of 231 cm^{-1} , which is about 38% lower than in free methanol.

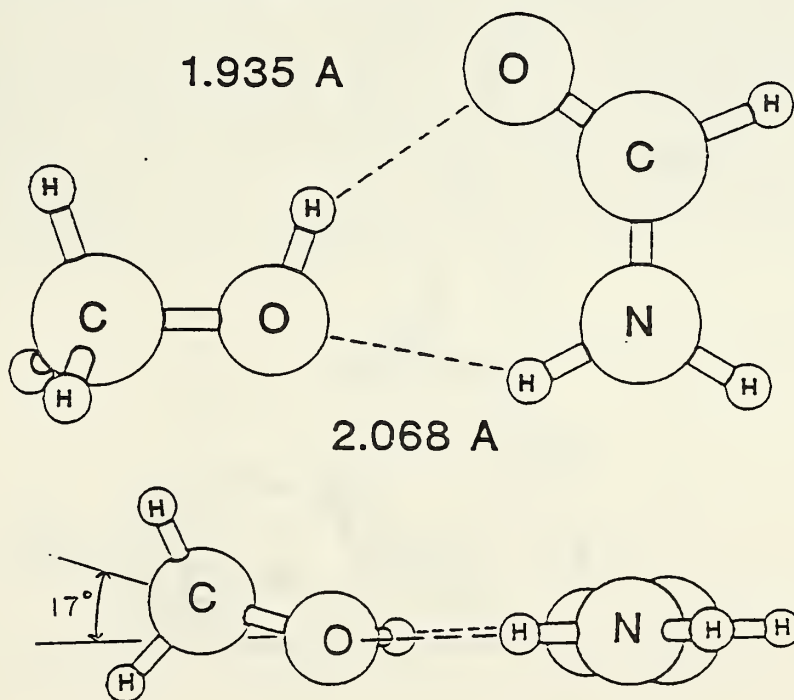


Fig. 2.7 Structure of the formamide-methanol dimer (a) top view (b) side view.

4. Microwave Spectra and Structures of the van der Waals Complexes
Ar-Formamide and Ar-Methanol
(C. W. Gillies, J. Zozom, G. T. Fraser, R. D. Suenram, and F. J. Lovas)

During the course of characterizing the formamide-water and formamide-methanol complexes, we detected the spectra of two additional complexes. One of these showed ^{14}N nuclear quadrupole hyperfine structure while the second exhibited no splittings. By using Ne as the carrier gas in place of Ar in the pulsed beam expansion, it was clear that each species contained Ar.

Assignment of the hyperfine structure on the first species provided a unique rotational state assignment for the Ar-formamide complex. Spectral fitting provides the distortion free rotational constants $A = 10725.32$ MHz, $B = 1771.58$ MHz and $C = 1549.53$ MHz. These constants indicate a non-planar structure as shown in Fig. 2.8 with the Ar at 45° to the formamide plane.

Based on chemical evidence we identify the second species as Ar-methanol and have assigned the $J = 3 - 2$ and $J = 4 - 3$ a-type R-branch transitions. The rotational constants are consistent with a T-shape structure as illustrated in Fig. 2.9. A number of strong unassigned lines remain which we believe is evidence for near free internal rotation of the methanol subunit.

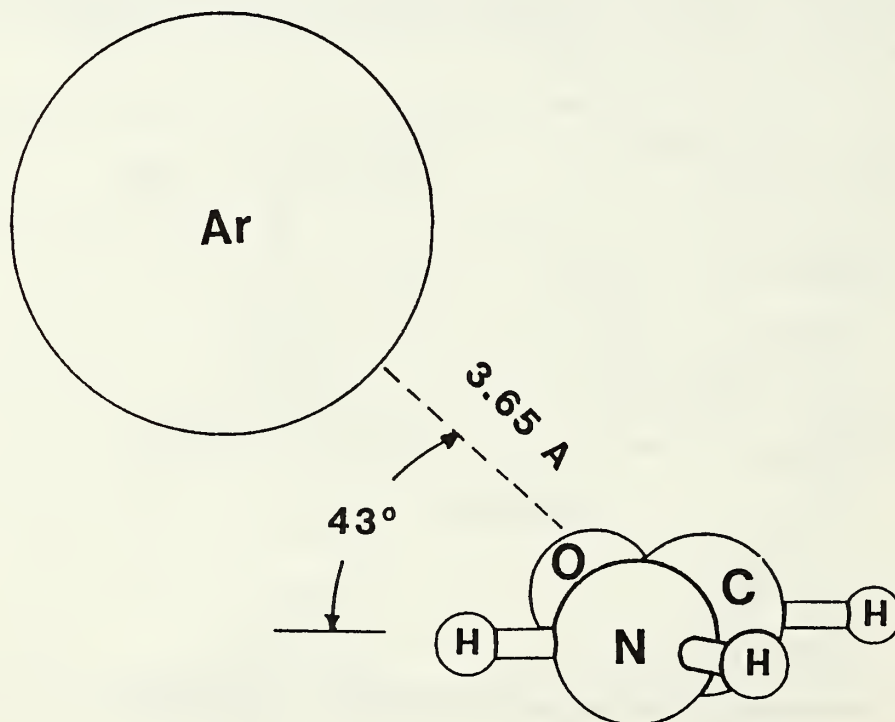


Fig. 2.8 Structure of the Argon formamide complex.

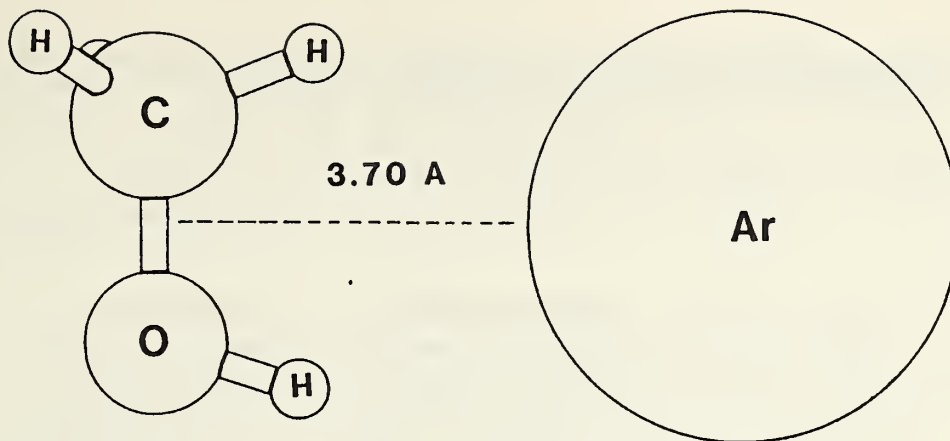


Fig. 2.9 Structure of the Argon-methanol complex.

5. Nearly Free Internal Rotation in Ar-CH₃Cl Determined from its Microwave Spectrum
(G. T. Fraser, R. D. Suenram, and F. J. Lovas)

Rotational spectra of Ar-CH₃Cl, for both Cl isotopes, have been observed, at 4 kHz resolution, using a pulsed nozzle Fourier transform microwave spectrometer. The observed spectra are consistent with a T-shaped complex in which the methyl group is undergoing nearly free internal rotation. Analysis of the ground (A-state) internal rotor state spectrum for Ar-CH₃Cl using an asymmetrical top Hamiltonian produces the spectroscopic constants listed in Table 2.2 for both the ³⁵Cl and ³⁷Cl isotopic forms. A combined analysis of the ground and excited internal rotor states (E-state) places an upper bound of 20 cm⁻¹ on the three fold barrier to internal rotation. The Coriolis interactions in the E-state also allow the determination of $|eQq_{ab}|$ for Ar-CH₃³⁵Cl as 13.0(3) MHz. The symmetry axis of the CH₃Cl subunit is nearly perpendicular (-82°) to the line joining the centers of mass of the two binding partners. The isotopic data indicate that the Cl end of the methyl chloride is tilted toward the argon. The distance between the centers of mass of the two subunits is 3.7825 Å for Ar-CH₃³⁵Cl and 3.7839 Å for Ar-CH₃³⁷Cl implying an Ar-Cl distance of 3.750 Å. Centrifugal distortion analysis yields a weak bond stretching force constant of 0.0157 mdyn/Å and stretching frequency of 34.6 cm⁻¹ for Ar-CH₃³⁵Cl.

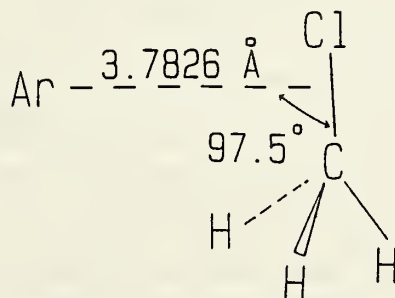


Fig. 2.10 Structure of the Argon-methylchloride complex.

Table 2.2 Asymmetric rotor constants (in MHz) for the A internal rotor states of $\text{ArCH}_3^{35}\text{Cl}$ and $\text{ArCH}_3^{37}\text{Cl}$.

	$\text{ArCH}_3^{35}\text{Cl}$	$\text{ArCH}_3^{37}\text{Cl}$
A	13633.020(14) ^a	13436.8700(56) ^a
B	1593.5683(79)	1565.075(12)
C	1420.4572(52)	1395.6126(36)
Δ_J	0.01216(14)	0.01280(41)
Δ_{JK}	0.1381(48)	0.1392(13)
δ_J	0.00096(17)	0.00150(15)
H_{JK}	-0.00058(25)	. . .
eQq_{aa}	34.895(30)	27.432(27)
eQq_{bb}	-72.185(25)	-56.799(19)
eQq_{cc}	37.290(35)	29.367(25)

a. Experimental uncertainties are reported as two standard deviations from the least squares fits.

6. The Microwave Spectrum of the $K=0$ States of Ar-NH_3
(D. D. Nelson, Jr., G. T. Fraser, K. I. Peterson, K. Zhao,
W. Klemperer, F. J. Lovas, and R. D. Suenram)

The microwave spectrum of Ar-NH_3 has been obtained using molecular beam electric resonance spectroscopy and pulsed nozzle Fourier transform microwave spectroscopy. The spectrum is complicated by nonrigidity and most of the transitions are not yet assigned. A $\Delta J=0$, $K=0$ progression is assigned, however, and from it the following spectroscopic constants are obtained for $\text{Ar-}^{14}\text{NH}_3$: $(B + C)/2 = 2876.849(2)$ MHz, $D_J = 0.0887(2)$ MHz, $eQq_{aa} = 0.350(8)$ MHz, and $\mu_a = 0.2803(3)$ D. For $\text{Ar-}^{15}\text{NH}_3$ we obtain: $B + C)/2 = 2768.701(1)$ MHz, and $D_J = 0.0822(1)$ MHz. The distance between the Ar atom and the $^{14}\text{NH}_3$ center of mass, R_{CH} , is calculated in the free internal rotor limit and obtained as 3.8358 Å. The weak bond stretching force constant is 0.00840(2) mdyn/Å which corresponds to a weak bond stretching frequency of 34.6(1) cm^{-1} . The NH_3 orientation in the complex is determined primarily on the basis of the measured dipole moment projection and the quadrupole coupling constant. It is concluded that the Ar-NH_3 intermolecular potential is nearly isotropic and that the NH_3 subunit undergoes practically free internal rotation in each of its angular degrees of freedom. Spectroscopic evidence has been obtained which indicates that the NH_3 subunit also inverts within the complex. These conclusions concerning the internal dynamics in the Ar-NH_3 complex

are in complete agreement with the model initially proposed in preliminary report concerning the microwave and infrared spectra of this species (Fraser et al., J. Chem. Phys. 82, 2535 (1985)).

7. Van der Waals Potentials from the Infrared Spectra of Rare Gas-HF Complexes
(G. T. Fraser and A. S. Pine)

The rare gas-hydrogen halide (Rg-HX) van der Waals complexes provide a simple, systematic series for studying weak molecular interactions pertinent to collisional and condensed phase properties. Last year we reported high-resolution tunable infrared laser spectra of the rare gas-HCl species including the observations of rotational predissociation, manifest as a sharp cutoff of the J progression within a band, and of the large-amplitude bending or librational motion from the anomalously strong bend-stretch combination band. In the present work we have extended the study to the rare gas-HF species using a difference-frequency laser to record the HF stretching fundamentals, ν_1 , of Ar-, Kr- and Xe-HF under thermal equilibrium conditions at $T \approx 211$ K for path lengths up to 80 m. The observed Xe-HF spectra are shown in Fig. 2.11 along with simulations calculated from the measured and predicted rovibrational constants for the ν_1 fundamental and $\nu_1 + \nu_3 - \nu_3$ hot band.

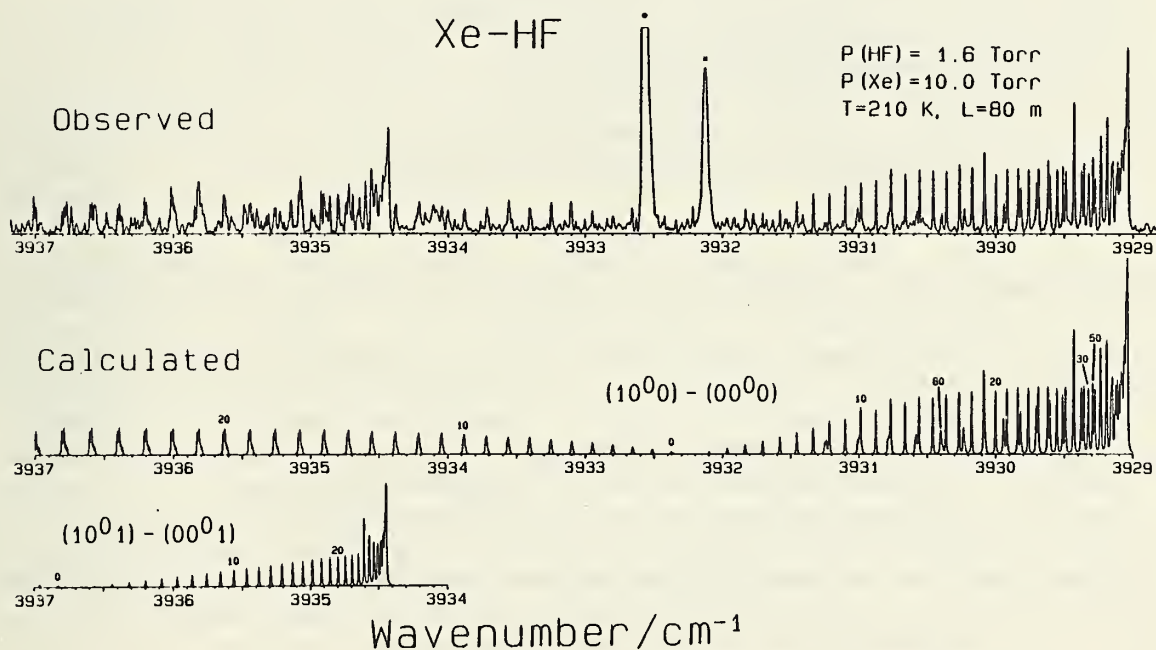


Fig. 2.11 Spectrum of the Xe-HF van der Waals complex for an absorption path length of 80 m and a temperature of $T = 211$ K; observed (top) and calculated (bottom).

Rotational structure has been observed up to or approaching rotational predissociation, permitting us to model the effective radial van der Waals potentials for these complexes. For example, Ar-HF is found to predissociate by tunneling through the centrifugal barrier at $J=40$ in the ground vibrational state, leading to the empirical potentials shown in Fig. 2.12. These potentials provide good estimates for the binding energies, D_0 , and the van der Waals stretching frequencies, ν_3 , in the

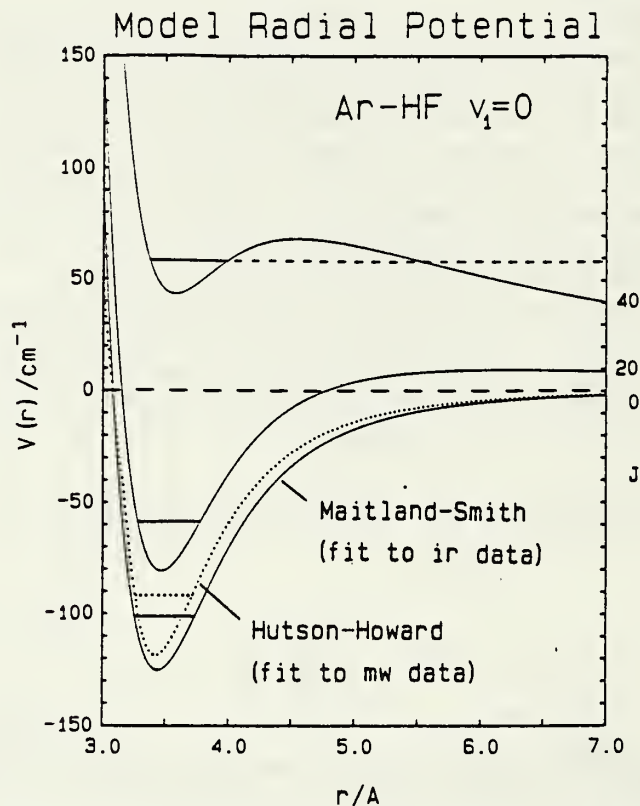


Fig. 2.12 Empirical potentials for Ar-HF derived from spectroscopic data.

ground ($\nu_1=0$) and excited ($\nu_1=1$) states of the molecules. For $\nu_1=0$ in Ar-HF, Kr-HF and Xe-HF, we find $D_0 = 102, 133, \text{ and } 181 \text{ cm}^{-1}$ and $\nu_3 = 39.2, 41.1, \text{ and } 43.4 \text{ cm}^{-1}$ respectively. The ν_3 modes characterized by the model potentials aid in the assignment of the $\nu_1 + \nu_3 - \nu_3$ hot bands observed in our spectra. The band centers for the ν_1 fundamentals are all down-shifted in frequency from the isolated HF monomer by $\Delta\nu = -9.654, -17.518 \text{ and } -29.185 \text{ cm}^{-1}$ for the Ar, Kr, and Xe complexes respectively, indicating that the van der Waals bonds are some 10 to 15% stronger in the excited vibrational state. This increased vibrational attraction also results in a contraction of the van der Waals radial coordinate manifest in the larger rotational constants observed for ν_1 ; $\Delta B/B_0 = +0.35, +1.00 \text{ and } +1.75\%$ for Ar-, Kr-, and Xe-HF. We have also observed the Q branch of the $\nu_1 + \nu_2$ stretch-bend combination band in Ar-HF some 70.2 cm^{-1} above the ν_1 fundamental with a large negative $\Delta B/B_0 = -2.00\%$ implying a strong anisotropy in the potential.

8. NATO-Advanced Research Workshop (A. Weber)

A NATO-Advanced Research Workshop on "Structure and Dynamics of Weakly Bound Molecules Complexes" was conducted in Acquafredda di Maratea, Italy in September 1986. The purpose of this Workshop was to bring together researchers active in the field of high resolution spectroscopy and dynamics of van der Waals and hydrogen-bonded molecular complexes in order to assess the present state of knowledge, to communicate directions and progress of research already underway and to indicate directions, potential and level of effort needed for future research. Seventy scientists from nearly all NATO countries participated in this Workshop. The topics taken up included the determination of structures by microwave, molecular beam electric resonance, high resolution infrared, and visible spectroscopy, rotational and vibrational predissociation determined from spectral line widths and from time dependent photodissociation experiments, determination of potential energy surfaces from experimental data and from ab initio calculations, as well as stability and dissociation dynamics. The proceedings of the Workshop will be published in the NATO-ASI series of publications.

9. Future Plans

During the past year the pulsed beam Fourier transform microwave spectrometer (FTMWS) has provided rotational spectra of both new dimers and van der Waals complexes. Further work in this direction will continue next year. A number of dimer studies have been started, but are not yet complete due to the complexity of the observed spectra. These include studies of $\text{CH}_3\text{NH}_2\text{-H}_2\text{O}$, $\text{CH}_3\text{OH-NH}_3$ and several new species observed in Ar/03 expansions. We hope to complete the assignment of these spectra during the coming year.

We will also test several new molecular beam designs. One design allows mixing two beams in the nozzle exit channel for the study of dimers of species which react, e.g., ammonium halides. A second design will provide a dc electric discharge in the beam exit channel which we hope will generate free radical species.

One of the major thrusts during FY87 will be the development of a pulsed laser ablation system which can be used in conjunction with the FTMWS to study molecular species that are normally non-volatile. The high power pulsed laser has been ordered and the pumping system is in place. All that remains is to design a vacuum chamber to allow the laser-target to be interfaced with a pulsed nozzle and the FTMWS.

A second area of major emphasis will be to investigate the feasibility of incorporating a cryogenically cooled, extremely low noise mixer device in the FTMWS. Theoretically improvements in signal-to-noise with this type of device could be two or three orders of magnitude.

Infrared investigations will also be performed on molecular-beam adiabatically-cooled systems. A pulsed molecular beam apparatus is now under construction and will be used for absorption spectroscopy with the aid of various tunable lasers. A cw-molecular-beam laser resonance apparatus is now under development and scheduled for completion during the coming year for vibrational predissociation measurements. Also under development is a high resolution tunable F-center laser system for high power excitation of van der Waals complexes for vibrational predissociation studies.

E. Matrix Isolation Spectroscopy

1. Fluorine-Atom Reaction Study (M. E. Jacox)

Some years ago, the infrared spectra of cis- and trans-HOCO were obtained in this laboratory by the reaction of photolytically generated OH with a CO matrix. These species are of considerable interest to the combustion scientist, since the OH + CO reaction is the principal process by which CO₂ is formed in combustion systems. Because HOCO can hydrogen-bond to the CO matrix, it was desirable to obtain the spectra of its rotamers in an argon matrix. However, molecules cannot diffuse through solid argon under the conditions necessary for effective matrix isolation. Therefore, it was not feasible to study the OH + CO reaction in solid argon. Preliminary studies, outlined in the Annual Report for FY85, have shown that the reaction of F atoms with HCOOH provides a suitable source of trans-HOCO. Early in FY86, further isotopic studies on the F + HCOOH system were conducted using the Beckman IR-9 infrared spectrophotometer.

2. Excited Argon-Atom Reaction Studies (M. E. Jacox)

As was reported in the Annual Report for FY85, a good yield of trans-HOCO can also be obtained by codepositing the Ar:HCOOH sample with a beam of argon atoms excited in a low-power microwave discharge. This method of preparation of trans-HOCO has the advantage of eliminating contributions of HOCO...HF from the spectrum. Detailed isotopic studies of trans-HOCO formed in this system were also performed using the Beckman IR-9. However, the product yield on deuterium substitution was relatively low. Therefore, completion was deferred until the BOMEM Fourier transform system can be used. The greater frequency accuracy of this experimental system will be valuable for the determination of carbon-13 and oxygen-18 isotopic shifts. In turn, these isotopic data will permit derivation of an improved vibrational potential function for trans-HOCO.

The accessibility of the near infrared spectral region using the BOMEM system made possible a detailed series of experiments on the interaction of excited argon atoms with acetylene. Previous studies in this laboratory have shown that this sampling configuration provides a

consistently high yield of the HC_2 free radical, an important intermediate in astrophysical and combustion systems. Extensive deuterium- and carbon-isotopic substitution studies spanning the $700\text{--}7900\text{ cm}^{-1}$ spectral region were conducted at a resolution of 0.2 cm^{-1} .

The mid-infrared studies yielded a more precise value of 1846.2 cm^{-1} for the CC -stretching frequency of HC_2 . Several weak absorptions between 2100 and 3400 cm^{-1} were also assigned to HC_2 . An absorption at 3610 cm^{-1} has previously been assigned (M. E. Jacox, *Chem. Phys.* 7, 424 (1975)) as the CH stretching fundamental of HC_2 . Although this value is anomalously high for a CH -stretching fundamental, the observation of Fermi resonance with the first overtone of the CC -stretching fundamental for $\text{H}^{12}\text{C}^{13}\text{C}$ and for H^{13}C_2 indicates that the energy level of HC_2 which contributes this absorption must be of Σ^+ vibronic symmetry.

Recently, Curl, Carrick, and Merer (R. F. Curl, P. G. Carrick, and A. J. Merer, *J. Chem. Phys.* 82, 3479 (1985)) have assigned prominent gas-phase absorptions at 3796 , 4012 , and 4108 cm^{-1} observed by color-center laser spectroscopy in a discharge through polyacetylene to combination bands arising from the ground state of HC_2 . Counterparts of these three bands at 3806 , 4022 , and 4134 cm^{-1} are prominent in the matrix experiments, consistent with such an assignment. The corresponding absorptions for the carbon-13 substituted species were also observed in the matrix experiments.

The matrix studies have provided the first observation of the $\text{A } ^2\Pi - \text{A } ^2\Sigma^+$ absorption band system of HC_2 in the $4200\text{--}7900\text{ cm}^{-1}$ spectral region. As is evident from Fig. 2.13, a rich spectrum is obtained. The product absorptions shown in trace (b), the spectrum obtained in an

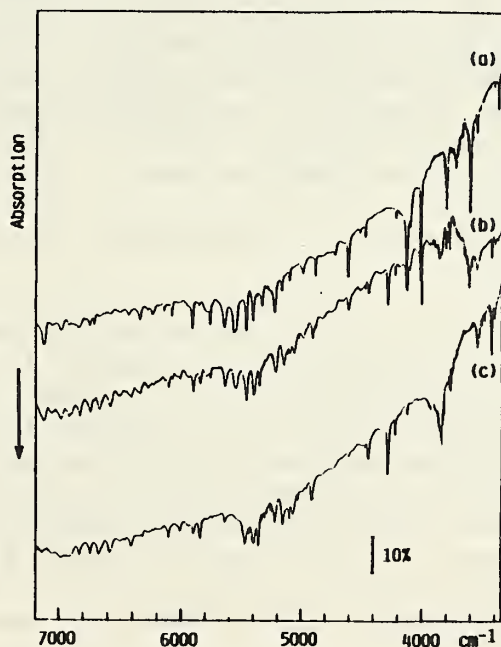


Fig. 2.13 HC_2 (DC_2) absorption spectrum between 3400 and 7200 cm^{-1} observed on codeposition of $\text{Ar}:\text{C}_2\text{H}_2\text{-d}_n$ sample with a beam of excited argon atoms. (a) $\text{Ar}:\text{C}_2\text{H}_2 = 800 + \text{Ar}^*$; (b) $\text{Ar}:\text{HCCD} = 200 + \text{Ar}^*$; (c) $\text{Ar}:\text{C}_2\text{D}_2 = 150 + \text{Ar}^*$.

experiment using an HCCD sample, are the sum of those characteristic of C_2H_2 samples (trace (a)) and C_2D_2 samples (trace (c)), supporting the assignment of all of the peaks in this spectral region to HC_2 and DC_2 . There are concentrations of peaks at intervals of approximately 1500 cm^{-1} , appropriate for a progression in the upper-state CC-stretching frequency. The superposed structure is contributed by extensive perturbation by high vibrational levels of the ground state. Although the ground-state bending vibration has not yet been directly observed, both it and the bending fundamental of HC_2 in the $A\ ^2\Pi$ state are expected to occur at very low frequencies, as has been observed (C. Fridh and L. Asbrink, *J. Electron Spectrosc. Relat. Phenom.* 7, 119 (1975)) for the isoelectronic species HCN^+ . Such perturbations in the spectrum of NO_2 are well known. Their occurrence for HC_2 helps to explain the properties of the emission spectrum observed on photolysis of acetylene in the gas phase. Depending on the photolysis wavelength, several workers have observed unstructured emission by HC_2 at wavelengths from the near ultraviolet to the cutoff of an InSb detector in the mid-infrared. Anomalously long lifetimes, between about 5 and 30 μs , are typical. Douglas (A. E. Douglas, *J. Chem. Phys.* 45, 1007 (1966)) has considered the increase in fluorescence lifetime which is associated with extensive interaction between two electronic states.

Although a detailed assignment of all of the matrix data has not been possible, the shifts on carbon-13 substitution appear to be sufficiently regular that correlations can be made with reasonable certainty. The isotopic shifts indicate that most of the peaks involve CC-stretching excitations. Of particular interest is a peak at 4622 cm^{-1} , which shifts by 103 cm^{-1} for $H^{13}C_2$. It is difficult to explain such a large shift except by postulating that two quanta of CC-stretching vibration are excited in the transition. Such an assignment would place the origin of the transition some 3000 cm^{-1} lower, or near 1600 cm^{-1} . A definitive assignment must await rotational analysis of the gas-phase absorption spectrum. Because all of the absorptions which are observed in the matrix experiments must arise from the X(000) state of the molecule, the data should be useful in the analysis of spectra of HC_2 obtained in future gas-phase studies in other laboratories.

3. Reaction Intermediates in the Decomposition of Energetic Materials (M. E. Jacox)

As a part of a project on the spectroscopic characterization of reaction intermediates in the decomposition of energetic materials, supported in part by the Army Research Office, studies of the products of the $H + HCN$ reaction were also conducted on the BOMEM system. This reaction is of especial interest because H_2CN is a potential intermediate in the decomposition of the solid propellants HMX and RDX. Preliminary studies had provided evidence for the formation of CN and of three CH_2X species (presumably H_2CN and cis- and trans- $HCNH$) when H atoms produced by a microwave discharge through an $Ar:H_2$ mixture react with HCN in an argon matrix. BOMEM observations between 700 and 4000 cm^{-1} were conducted with

a resolution of 0.2 cm^{-1} . The peak at 1336.6 cm^{-1} , which appeared even when low-energy H atoms were formed by the mercury-arc photolysis of HI, was shifted by only 0.1 cm^{-1} on carbon-13 substitution, but by 3.0 cm^{-1} on nitrogen-15 substitution. This behavior is similar to that of the 1500 cm^{-1} CH_2 "scissors" fundamental of H_2CO . Since H_2CN is calculated to be the most stable isomer and since it has been identified in earlier studies of the esr spectrum of products of the mercury-arc photolysis of Ar:HCN:HI samples, the assignment of the 1336.6 cm^{-1} peak to the CH_2 "scissors" fundamental of H_2CN is strongly indicated. The carbon-13 isotopic shift of the 3104 cm^{-1} peak, tentatively attributed to a HCNH species, requires its assignment to a CH-stretching fundamental. Carbon-13 and nitrogen-15 isotopic shifts were also observed for the 886.3 cm^{-1} absorption, contributed by a photochemically unstable HCNH species, probably the cis-rotamer. Despite the greater sensitivity of the BOMEM interferometer, other infrared absorptions which can be assigned to these three products have not been identified. The interferometer system was also used for survey scans of the $4000\text{-}8000\text{-}$ and $10,000\text{-}20,000 \text{ cm}^{-1}$ spectral regions, but no absorptions which could be assigned to the analog of the red bands of the isoelectronic species HCO were detected.

In a preliminary Ebert scan of the ultraviolet spectrum which results on 122-nm photolysis of an Ar:HCN sample, moderately intense absorptions appeared at 34990 (overlapped by the OH A-X 1-0 absorption) and 35436 cm^{-1} . These two peaks correspond closely with gas-phase absorptions previously attributed to H_2CN , formed on flash photolysis of several more complicated precursor molecules. Several less intense peaks extending to 37764 cm^{-1} may have been contributed by previously unidentified bands of H_2CN . Further studies are needed to confirm this identification.

In an earlier study in this laboratory, the nitromethyl free radical, CH_2NO_2 , was stabilized by the reaction of F atoms with CH_3NO_2 in an argon matrix, and the first spectroscopic data for this species were reported. Most of the vibrational fundamentals were observed for five isotopic species of nitromethyl, and a tentative vibrational assignment was proposed. The wealth of data available from these experiments suggested that a detailed normal coordinate analysis should be feasible. Among the important questions which such an analysis would address are whether the molecule is asymmetric, as had been proposed as a result of a recent ab initio calculation, and whether the unpaired electron contributes to partial double-bond character for the CN bond. A least-squares force constant adjustment calculation has recently been conducted. All of the observed frequencies can be fitted very well for a planar C_{2v} molecular structure. The vibrational assignment proposed in the earlier experimental paper has been somewhat revised. The magnitude of the CN-stretching force constant is appropriate for a single bond. A manuscript presenting the detailed results of the normal coordinate calculations is being prepared for publication.

A manifold has been designed and constructed to permit matrix isolation sampling of low vapor pressure materials by controlling the pressure of argon with which they are in equilibrium. This manifold will be used for studies of the spectra of products of the photolysis of phenol and nitrobenzene, also a part of the current ARO project.

4. Future Plans

During the coming year, highest priority must be given to the completion of a number of important projects which have already been discussed. These projects include BOMEM studies of the infrared spectrum of trans-HOCO and Ebert studies of the electronic spectra of the H + HCN reaction products. Detailed studies of products of the photolysis of benzene, phenol, and nitrobenzene be conducted using the BOMEM system. Studies of the products of the reaction of O atoms with these three molecules will also be conducted.

Studies begun in 1985 on the reaction of SiH₄ with H, Cl, and O atoms produced in a discharge are also planned. The potential stabilization of SiH_n and SiH_nO species is of interest in relation both to basic chemical research and to applied studies of plasma etching.

Infrared studies of interesting and important F-atom reaction systems- e.g., F + cyclopropane--will continue to be conducted. However, emphasis will now be placed on UV-visible studies of F-atom reaction products, for which there is a substantial backlog.

For some time, it has been planned to use a beam of excited neon atoms as a source of 16.6-16.8 eV energy for the production of small molecular ions, to be trapped in a neon matrix. This energy range should make possible the preparation of significant concentrations of such small molecular cations as HCO⁺, H₂O⁺, NH₃⁺, and CH₄⁺, not accessible in the 11.5-11.8 eV energy range provided by a beam of excited argon atoms. It is hoped that later in FY87 the excited neon atom experiments, which may provide much previously inaccessible information on the vibrational and electronic spectra of molecular ions, can begin.

F. General Spectroscopy and Theory

In addition to the previously described programmatic activities a variety of research problems are pursued in response to special opportunities, and special interests of the staff and outside guest scientists. The following are descriptions of such projects of a general nature.

1. Fourier Transform Measurements of High Temperature Species;
Infrared Gas Phase Spectra of LiCl, LiH, and LiD
(W. B. Olson, G. A. Thompson, A. G. Maki, and A. Weber)

The new transfer optics for the BOMEM described below have allowed us to make high temperature measurements of the infrared spectrum of several compounds produced in a high temperature oven. So far we have measured the $\Delta v=1$ transitions of the two species LiH and LiD and the four naturally abundant isotopic species of LiCl.

A portion of the spectrum of LiCl containing 95% ^6Li is shown in Fig. 2.14. The complete spectrum contained over 2500 identified transitions for the various isotopic species. Vibrational transitions ranged from $v=1-0$ to $v=8-7$ and rotational transitions for J values up to 75. These transitions were fit to a set of Dunham potential constants that included 9 isotopically invariant terms and 4 terms to allow for isotopic shifts due to the break-down in the Born-Oppenheimer approximation. The standard deviation of the fit was 0.00027 cm^{-1} which is what we expect considering the slightly larger than normal Doppler linewidth of these high temperature spectra.

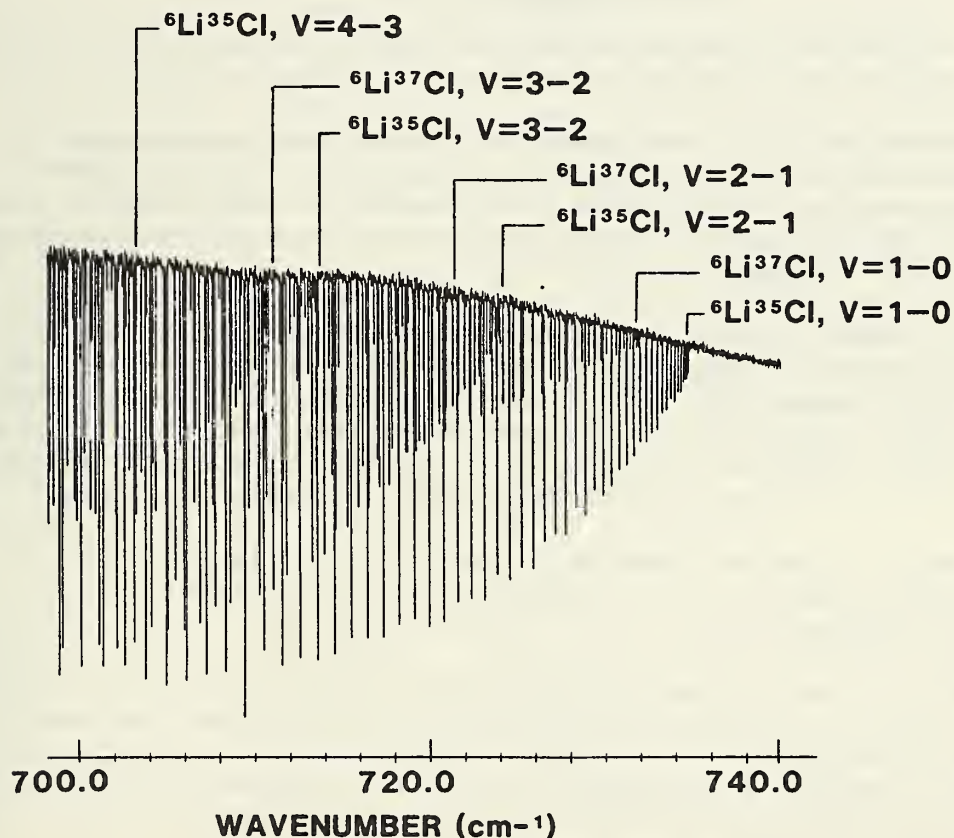


Fig. 2.14 A portion of the spectrum of $^6\text{LiCl}$ at 830°C . The locations of a number of band heads are indicated above the spectrum.

A portion of the spectrum of LiD is shown in Fig. 2.15. This spectrum is much more sparse than that of LiCl and shows the advantage of

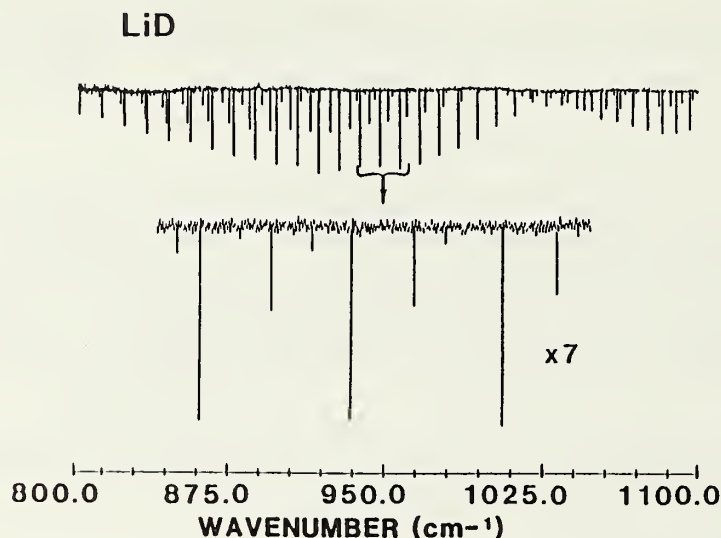


Fig. 2.15 A portion of the absorption spectrum of LiD at 750°C. The wave number scale applies to the upper spectrum.

using a broad-scanning FTS instrument for making these measurements. Earlier measurements using a diode laser spectrometer were very slow because the lines were so far apart, the electronic tuning range of the spectrometer was quite small, temperature tuning was slow, and there were many gaps in the coverage.

The standard deviation of the fit of the LiH and LiD spectra (0.0076 cm^{-1}) was worse than that of LiCl because the Doppler width was larger and there seems to be more of a problem with break-down of the Born-Oppenheimer approximation. To investigate this further, we hope to measure the pure rotational spectrum of LiH at high J values to get better measurements on the higher centrifugal distortion constants.

2. Hydrogen Migration Tunneling Effects in the Rotational and Vibrational Spectrum of Protonated Acetylene C_2H_3^+ (J. T. Hougen)

The influence of a possible hydrogen atom migration in protonated acetylene, C_2H_3^+ , on the high-resolution vibration-rotation spectrum of this ion was investigated. The migration model, which derives from ab initio calculations, consists of a planar structure with the three hydrogen atoms moving on an elliptical path around the two carbon atoms. Symmetry considerations for this ion were considered in terms of the permutation-inversion group G_{24} . A method for calculating energy levels for a highly idealized model of this ion can be found in the early

microwave literature. In this idealized model, an equilateral triangle of three hydrogen atoms performs internal rotation about a dumbbell of two carbon atoms, with all atoms remaining in the same plane. This model gives rise to a symmetric rotor top, an asymmetric rotor frame, and a six-fold barrier to the internal rotation motion. An alternative method of calculating the energy levels of this ion, involving a more recently proposed algebraic tunneling formalism, shows that qualitatively similar results are obtained even when the hydrogens do not retain the form of a rigid equilateral triangle during their migration motion. Energy level diagrams, nuclear spin statistical weights, selection rules for electric dipole transitions, etc. were developed. It is hoped that the patterns described in the present work will aid in identifying and interpreting any spectrum of $C_2H_3^+$ obtained as a result of ongoing efforts elsewhere to record its spectrum.

3. The Torsional-Wagging Tunneling Problem and the Torsional-Wagging Rotational Problem in Methylamine (N. Ohashi and J. T. Hougen)

A theoretical formalism is presented for fitting rotational energy levels in isolated (unperturbed) vibrational states of methylamine. This formalism is obtained by recasting and extending theoretical studies in the earlier literature, which were undertaken to help analyze the methylamine microwave spectrum. The present formalism is applicable when both the NH_2 umbrella (wagging) motion and the CH_3 internal rotation (torsion) motion take place near the high-barrier limit and leads to the usual Fourier sine and cosine series expansions for molecular energy levels. The derivation is separated into two parts, one treating the large-amplitude vibrational problem (the torsional-wagging problem) by itself, the other treating the torsional-wagging-rotational problem. In both treatments, permutation-inversion group and extended group ideas are used to determine the allowed terms in an effective rotational-tunneling Hamiltonian operator and to block diagonalize the matrix representation of this operator for a near-prolate symmetric top. Application of the method in detail to the methylamine spectrum is planned for a later study.

4. Far-Infrared Spectrum of Methylamine (N. Ohashi, W. J. Lafferty, and W. B. Olson)

The far-infrared spectrum of CH_3NH_2 has been recorded in the region 50 to 350 cm^{-1} on the NBS BOMEM Fourier transform spectrometer with a resolution of about 0.004 cm^{-1} . The torsional band as well as pure rotational transitions originating in higher K_a levels fall in this region of the spectrum. This molecule is of more than passing interest since it has two large amplitude motions, the NH_2 -wag and the CH_3 -torsion, and the spectrum is rather complex as a result. Assignment of the pure rotational transitions is complete at this point, and the stronger $B_1(B_2)+B_2(B_1)$ and E_1+E_1 components of the torsional band have been assigned. A small portion of the spectrum of the torsional band is given in Fig. 2.16 where the line assignment of two components of the r_{Q_4} - and r_{Q_5} - transitions is

indicated. Ohashi and Hougen have recently derived approximate energy level formulas for CH_3NH_2 , and a computer program is being written to fit the data and extract the molecular constants. Preliminary fits show that the torsional splitting in the torsional vibrational state is about 30 times larger than in the ground state, and, somewhat suprisingly, the inversion splitting in the excited state is about 3 times greater than it is in the ground state.

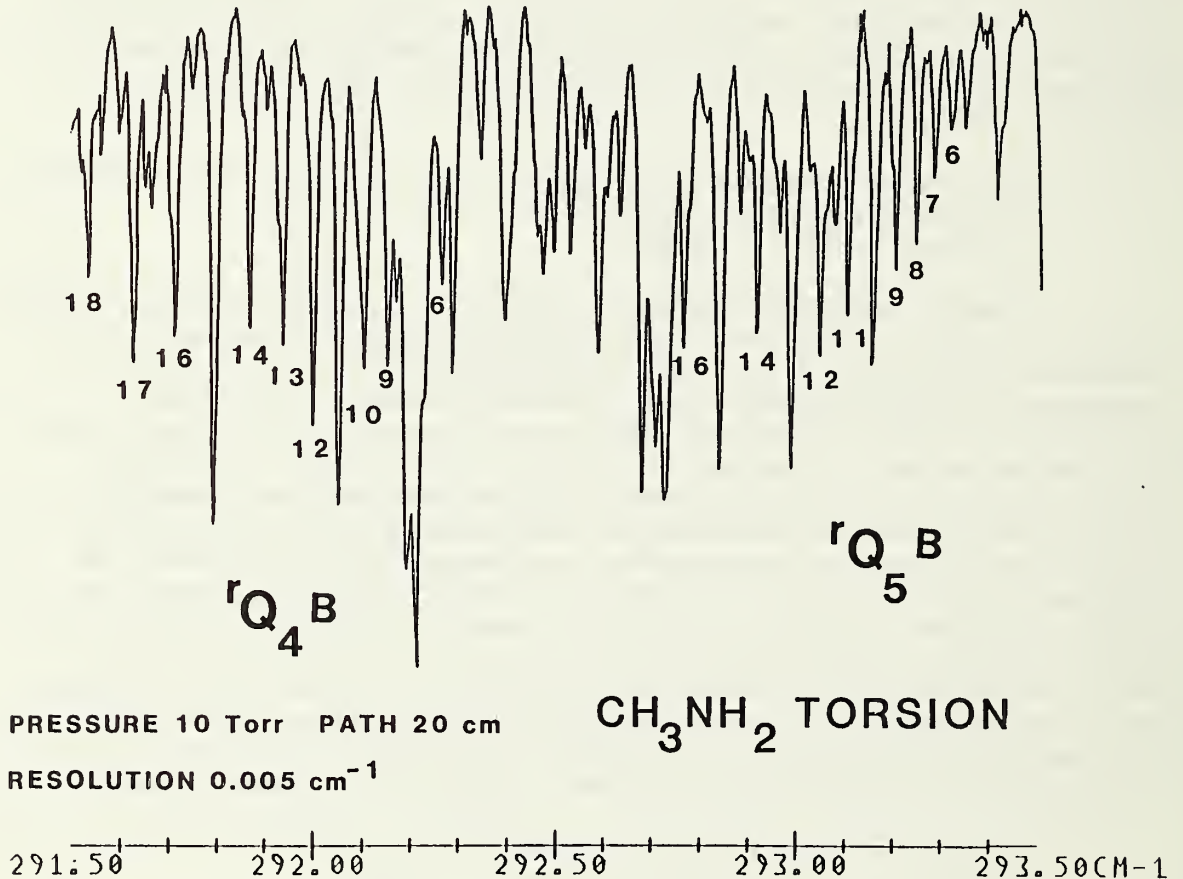


Fig. 2.16 A small portion of the torsional band of CH_3NH_2 taken with a resolution of 0.005 cm^{-1} showing the line assignments of the Q-branches of two components of the $K=5-4$ and $K=6-5$ subbands.

5. Transfer Optics System Design (W. B. Olson)

An efficient transfer optics system has been designed and constructed to couple the BOMEM FTS to an existing heat pipe in order to obtain infrared absorption spectra of species which can only be seen in

the gas phase at high temperatures. This system has enabled the high resolution observation of several bands of LiCl and LiH leading to improved vibrational and rotational constants for these species.

The necessity of efficient and practical transfer optics for the heat pipe was the "mother of the invention" of a fairly general and powerful approach to transfer optics design via a "system" concept of first order design, through analytical equations directly coupling required throughput or entendue to the ray transfer matrix of an optical system. The necessary ray transfer matrix for the system is uniquely determined (except for sign), and one can relatively rapidly calculate required distances and focal lengths of spherical mirrors required to implement a practical system.

With a single optical element, in our applications a concave spherical mirror, one has no degrees of freedom with which to make the design convenient. With each added optical element one gains two degrees of freedom to adjust features. With three optical elements one can specify all four distances in the system to convenient or practical values, and from these calculate the focal lengths required for each of the three mirrors. This is the method used for the heat pipe transfer optics system design. The resultant optical system for the heat pipe works well, but no precise explanation can be given of the function of the individual optical elements in simple, familiar terms.

6. Analysis of Infrared Spectra of SiH_3D (R. Schaefer, R. Lovejoy, W. B. Olson, and G. Tarrago)

An analysis of the ν_2 parallel band of $^{28}\text{SiH}_3\text{D}$ has been nearly completed through the collaborative efforts of Ron Schaefer and Roland Lovejoy of Lehigh University, W. B. Olson of NBS, and Ginette Tarrago of the University of Paris, South. For a complete analysis the interactions of ν_2 with the parallel and perpendicular components of $2\nu_6$ had to be taken into account by simultaneous solution of a secular determinant containing all three vibrational states. Three different types of perturbations giving readily evident displacements of absorption line positions in ν_2 were found to be due to perturbations with the perpendicular component of $2\nu_6$.

The perpendicular component of $2\nu_6$ proved difficult to assign because it was so weak, and additional spectra were run with a pressure-pathlength product a factor of ten higher than that used for the initial runs. This also increased the intensity of many other weak lines from unidentified hot bands and silicon isotopes. Two techniques for getting assignments, and checking them through the quality of the least squares fit, and the success of using molecular parameters from the fit to calculate new line positions at higher values of J and K eventually lead to a reasonably complete set of assignments for this weak band. Many of

the strongest lines in $2\nu_6$ are actually perturbation allowed transitions which get their intensity from the parallel component of $2\nu_6$ through the l-type doubling matrix element.

The secular determinant used for this work contained all possible matrix elements through the fourth order of the twice transformed Hamiltonian. A number of the higher order terms were found to be insignificant, while others of high order are significant, but did not make major contributions to the energies of any of the levels.

The values of the major low order molecular parameters of $2\nu_6$ are in quite satisfactory agreement with those of the ν_6 fundamental. The origin of the ν_2 band is at 1593.962 cm^{-1} , and that of $2\nu_6$ is at 1557.258 cm^{-1} . An article describing this work in detail is being prepared for publication.

7. Future Plans

In the coming year we plan to exploit the optical system used for the high temperature Fourier transform experiments to obtain Fourier transform measurements of other systems unstable under normal room temperature conditions. We shall try to observe the far infrared spectrum of several systems such as the pure rotational spectrum of LiH and the spectrum of compounds with low frequency vibrations (e.g., NaCl). We shall also try to observe the spectrum of compounds produced in an electric discharge with the hope that this may enable us to look at the spectrum of some metal oxides or hydrides.

Theoretical studies will focus further on large amplitude motions. Topics to be examined are the CH_3NH_2 microwave and far infrared spectra both in terms of pure rotational spectra and torsional spectra. The water dimer Hamiltonian and spectral consequences will be examined in further detail.

3. LASER PHOTOCHEMISTRY GROUP

D. F. R. Burgess, Jr., M. P. Casassa, R. R. Cavanagh, L. B. Elwell,
E. J. Heilweil, D. S. King, and J. C. Stephenson

- A. Introduction
- B. Condensed Phase Energy Transfer
- C. Laser Diagnostics of Surface Dynamics
 - 1. Adsorbate-Adsorbate Interactions: (NO + NH₃)/Pt(111) Thermal Desorption
 - 2. Laser-induced Desorption: NO/Pt(foil)
 - 3. Future Plans
- D. Dynamics of van der Waals Molecules
- E. Photophysical Studies of Photosensitizers

A. Introduction

This group primarily does quantum-state specific studies of molecular dynamics. A common factor in the research described below is the role of energy transfer in the spectroscopy and kinetics of molecules. Research on molecular dynamics of molecules on surfaces is done in collaboration with the Surface Science Division.

B. Condensed Phase Energy Transfer

(M. P. Casassa, R. R. Cavanagh, L. B. Elwell, E. J. Heilweil, and J. C. Stephenson)

The major effort in the condensed phase energy transfer program has been directed at the study of vibrational energy transfer (VET). During the past year we have successfully measured the rates of energy transfer from vibrationally excited chemical bonds in liquids, solids, and in molecules bound to surfaces.

This research area was extensively discussed in the 1985 Annual Report. The present report does not repeat last year's lengthy discussion of experimental detail and program rationale. In summary, we used a picosecond infrared pump/probe method to perform time-resolved measurements of the vibrational energy relaxation rate (T_1^{-1}) for the high frequency modes of species chemisorbed on a silica (SiO_2) surface in a variety of chemical environments. Previously, energy transfer rates have been measured for the vibrations of many molecules in the gas phase, and for a few molecules in liquids and low temperature solids. However, our experiments were the first to measure vibrational energy transfer rates for vibrations on surfaces.

A summary of some surface T_1 results is given in Table 3.1. These data were limited to vibrations with frequencies $\nu > 2500 \text{ cm}^{-1}$ since the psec ir pulses necessary to cause transient bleaching of the surface vibrations were generated in a Nd-YAG-pumped LiNbO_3 OPA (LiNbO_3 only transmits $\nu > 2500 \text{ cm}^{-1}$). The data suggest the following conclusions. T_1 times are longer than most people expected prior to these measurements. Energy relaxation rates (T_1^{-1}) are much slower by factors of 100-2000, than would be deduced from spectral bandwidths of these surface vibrations. At the vacuum interface, the MOH (M=B, Si, Al, Zn) and MOD stretching vibrations relax via anharmonic coupling to spatially adjacent vibrational modes, particularly the M-O-H bending mode. One reason BOH relaxes faster than SiOH is that its local accepting modes are higher in frequency and hence a better match to the OH stretch. The faster relaxation of NH_2 and OCH_3 vibrations is consistent with energy transfer from the NH stretches to the NH_2 bend and similarly from the CH stretches to the CH bends (with which the CH stretches are known to couple strongly via Fermi resonance). It is reasonable that T_1 of OH in the commercial zeolite ZSM-5

Table 3.1 T_1 decay times at room temperature for various surface vibrations

System	$\nu(\text{cm}^{-1})$	$T_1(\text{ps})$	$k(10^9 \text{ s}^{-1})$	Notes
SiOH/vacuum	$\nu_{\text{OH}}=3750$	220 ± 20	4.9	Pressed SiO ₂ disk
SiOH/CCl ₄	$\nu_{\text{OH}}=3690$	159 ± 16	6.3	Dry SiO ₂ dispersion
SiOH/CF ₂ Br ₂	$\nu_{\text{OH}}=3690$	140 ± 30	7.1	"
SiOH/CH ₂ Cl ₂	$\nu_{\text{OH}}=3660$	102 ± 20	9.8	"
SiOH/C ₆ H ₆	$\nu_{\text{OH}}=3625$	87 ± 30	11.0	"
SiOH/C ₆ D ₆	$\nu_{\text{OH}}=3625$	80 ± 30	12.0	"
SiOH/H ₂ O/CCl ₄	$\nu_{\text{OH}}=3690$	56 ± 10	18.0	SiOH T_1 , $\sim 5\text{H}_2\text{O}/100\text{A}^2$ physisorbed
SiOD/vacuum	$\nu_{\text{OD}}=2760$	155 ± 16	6.5	OD T_1 with 67% OH re- placed by OD
BOH/vacuum BOH/CCl ₄	$\nu_{\text{OH}}=3700$	~ 70	~ 14.3	
SiNH ₂ /vacuum SiNH ₂ /CCl ₄	$\nu_{\text{NH}}=3460$ 3520	≤ 20	≥ 50	Pulsewidth limited signal, $\Delta T/T \sim 5\%$ for both stretches
SiOCH ₃ /vacuum	$\nu=2860$ 3000	$< 5(?)$	$> 280(?)$	No pulse saturation observed for any CH-stretching mode
OH on zeolite ZSM-5/CCl ₄ (Si/Al=3600)	$\nu_{\text{OH}}=3690$	140 ± 25	7.1	Pressed disk CCl ₄ saturated
OH on ZnO	$\nu_{\text{OH}}=3485$	≤ 10	≥ 100	$\Delta T/T_0=12\%$ pulsewidth limited
ZnO, no OH	3600-3750	≤ 10	≥ 100	Electronic excitation of free carrier absorption $\Delta T/T$ $\approx 10\%$.

is the same as on fumed SiO_2 , since the high Si/Al ratio (=3600) of this particular sample precluded any appreciable bonding of OH on aluminate sites. The very rapid relaxation of OH on the semiconductor ZnO surface may not be caused by anharmonic coupling to adjacent vibrational modes but by coupling to electronic excitations of impurity states in the ZnO.

Relaxation rates for the surface vibrations increase in the presence of solvents (solid/liquids vs. solid/vacuum interface). The increase in rate is minor for solvents like CCl_4 which have no resonant high frequency modes, ($\nu_{\text{C}-\text{Cl}}^3 = 770 \text{ cm}^{-1}$ is the highest fundamental). An increase in rate of about a factor of 2.5 occurs for benzene which has many nearly resonant ($\nu_{\text{OH} \rightarrow \text{benzene}} \nu_1 + \nu_4$, etc.) internal vibrational states which could accept some or all of the OH quantum. Alternatively, vibrational relaxation rates may increase in the presence of solvents which perturb the OH ($\nu=0 \rightarrow 1$) absorption through hydrogen bonding or van der Waals interactions. The dependence of T_1 for surface vibrations on chemical environment, temperature, and other factors previously mentioned is always qualitatively in the direction expected by analogy to T_1 data in homogeneous phases. However, standard first order perturbation theory calculations (e.g., solid state multiphonon relaxation theory) do not quantitatively agree with these trends.

During the past year a new picosecond dye laser was constructed for the purpose of generating tunable ir pulses for $\nu < 2500 \text{ cm}^{-1}$. This enables us to pump and probe interesting surface vibrations such as CO bound to metals. For vibrational relaxation on a metal surface, it is thought that a qualitatively different energy transfer mechanism, damping by excitation of electron-hole pairs in the metal, may be dominant. If this is true, then perhaps the broad spectral bandwidths ($\sim 5\text{-}50 \text{ cm}^{-1}$ FWHM) observed for high frequency vibrations on metals are really due to T_1 broadening, as has often been assumed. A direct time-resolved measurement of vibrational relaxation for a molecule on a metal surface is crucial to assessing the importance of this damping mechanism, and for understanding surface spectroscopy and kinetics.

The new laser is a synch-pumped tunable dye laser pumped by the second harmonic (532 nm) of the rejected trains of ps pulses from our actively-passively modelocked 10 Hz ps Nd-YAG laser. A single pulse from the dye laser is cavity-dumped, amplified to $\sim 500 \mu\text{J}/\text{pulse}$ and mixed in a LiIO_3 crystal with a single 532 nm pulse derived from the same 10 Hz YAG. Typically pulses of $\sim 25 \text{ ps}$ duration, $20 \mu\text{J}$, and tunable throughout the CO stretching region ($\sim 4 \text{ cm}^{-1}$ FWHM), are generated by this system. These pulses are sufficient to perform pump/probe ir saturation measurements of T_1 for CO ($\nu=1$) bound to small metal particles (e.g., Pt) on an insulator support (e.g., SiO_2). The Pt particle size (or other transition metal) can be controlled so that CO will chemisorb to either isolated metal atoms or larger crystallites. Measurement of T_1 for CO on the surface of supported metal particles should begin mid October 1986.

Initial experiments with the new laser system have involved measuring T_1 for stretching vibrations of CO bound to transition metal atoms (metal carbonyl complexes) dissolved in CCl_4 and other solvents. In terms of vibrational spectroscopy, the inorganic carbonyls are analogous to surface-bound CO (the assignment of surface CO sites as "bridge-bonded" on "terminal" frequently involves comparing the surface vibrational frequencies with corresponding metal carbonyls). Figure 3.1 shows ir pump-probe saturation data giving T_1 for the F_{1u} CO($v=1$) mode of $\text{Cr}(\text{CO})_6$ in carbon tetrachloride and hexane solutions. T_1 is very long ($T_1 \approx 490$ ps corresponds to 20,000 vibrational periods) and is clearly unrelated to the 8 cm^{-1} FWHM infrared Lorentzian bandwidth. We expect a similar T_1 lifetime for CO bound to isolated surface metal atoms on a dielectric support. A wide variety of metal carbonyls and nitrosyls are available and are excellent model compounds to answer questions about VET mechanisms, such as: is there a "heavy atom effect"; is T_1 for bridge-bonded CO different from terminal CO?; how is vibrational energy exchanged among modes of different ligands (adsorbates) bound to the same or neighboring metal atoms?

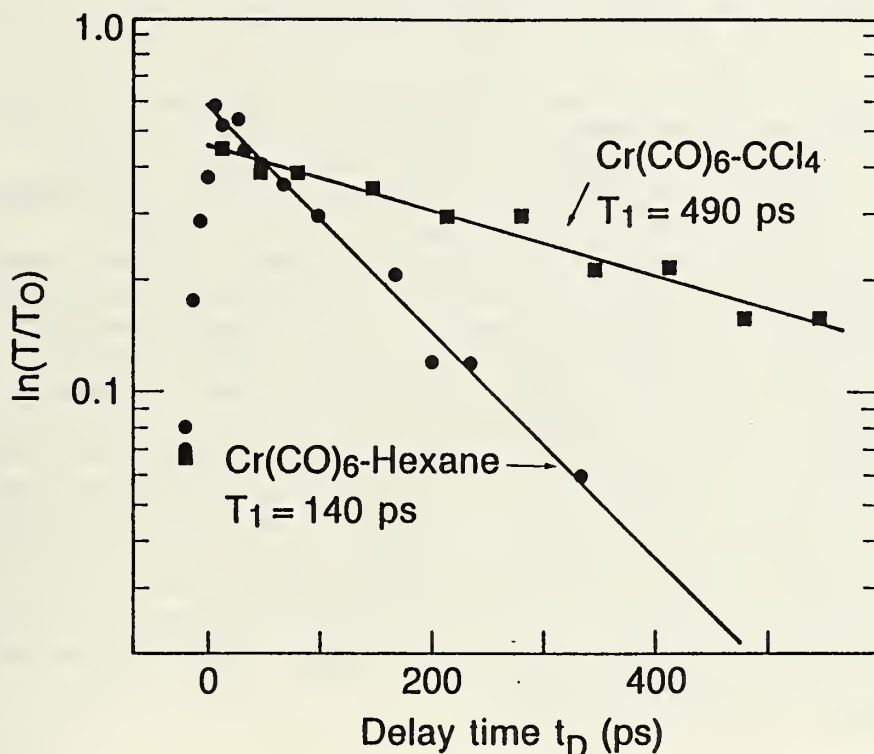


Fig. 3.1 Vibrational relaxation times for the F_{1u} CO($v=1$) mode of $\text{Cr}(\text{CO})_6$ in solutions of hexane and carbon tetrachloride.

Studies of related energy transfer processes at semiconductor surfaces have also recently begun in collaboration with Dr. Claude Sandroff of AT & T Bell Laboratories. The luminescence decay times of "exciton-like" electronic

states of extremely small ($\leq 30\text{\AA}$ diameter) and planar PbI_2 and PbBr_2 colloidal particles suspended in organic solvents are being measured. Preliminary experiments for PbI_2 and PbBr_2 in alcohol, using the third harmonic of the picosecond Nd^{+3} :YAG (355nm for PbI_2) and the second harmonic of the synchronously pumped dye laser (310 nm for PbBr_2) as excitation pulses, have yielded ca. 1100 and 900 ps lifetimes, respectively. These emission lifetimes were measured with a streak camera system. It is believed that measurements of this sort will reveal mechanisms for light-induced chemical reactions occurring at the liquid-surface interface. These include, for example, charge-transfer and oxidation-reduction reactions that are known to occur at semiconductor surfaces.

Using the LiNbO_3 OPA system, a study of the T_1 relaxation times of $\text{OH}(v=1)$ and $\text{OD}(v=1)$ vibrations of silanol, R_3SiOH , and alcohol, R_3COH , molecules in solution was completed. The results are summarized in Table 3.2. They may be compared to the surface OH results in Table I and the OH in crystalline mica results in Table 3.3. Most of the liquid phase results can be understood in terms of an isolated binary collision (IBC) model frequently used to interpret gas phase collisional VET rates. The fact that T_1 for $(\text{CH}_3)_3\text{SiOH} \leq T_1$ for $(\text{C}_6\text{H}_5)_3\text{SiOH}$, even though the latter molecule has 500 times the total density of vibrational states, shows clearly that factors other than the total vibrational state density are important in determining T_1 . The deactivation of hydroxyls of R_3MOH and R_3MOD ($\text{M}=\text{C},\text{Si}$) were simply modelled using the assumption that $\text{OH}(v=1)$ or $\text{OD}(v=1)$ energy is initially transferred to the eleven vibrations involving the OH bond and the neighboring four tetrahedral bonds of the central M atom. Data were analyzed by considering the frequencies of those particular accepting modes, and by using the propensity rules that energy transfer will be nearly resonant, and that processes involving the fewest vibrational quantum number changes (n =number changing) will be most probable. Because of their different vibrational frequencies, there are many more nearly resonant relaxation channels, involving lower values of n , for the alcohols ($n \geq 4$) than for the silanols ($n \geq 5$). This may explain why the R_3COH and R_3COD molecules relax much faster than corresponding silanols. The observation that the R_3SiOD molecules relax more slowly than the R_3SiOH species is consistent with energy transfer occurring predominantly to the SiOH bending motion, and is not consistent with transfer primarily to the Si-O stretching vibration. Similar analysis for the methanols (CH_3OH , CH_3OD , CD_3OH , CD_3OD) suggests that energy transfer to the CH (CD) stretching vibrations or to the C-O stretch are probably not dominant relaxation channels.

Table 3.2 T_1 lifetimes for the OH and OD($v=1$) stretching vibration in alcohols and silanols in dilute CCl_4 solution (≤ 0.007 mole fraction) at 298 K. Error limits are $\pm\sigma$, or 10% of T_1 , whichever is greater.

SILANOLS ^a	$\nu_{\text{OH,OD}}(\text{cm}^{-1})$	T_1 (ps)	ALCOHOL ^a	$\nu_{\text{OH,OD}}(\text{cm}^{-1})$	T_1 (ps)
Me_3SiOH	3690	205 ± 21	Me_3COH	3614	$< 6^b$
Me_3SiOD	2722	245 ± 25			
Et_3SiOH	3689	185 ± 19	Et_3COH	3622	$< 6^b$
Et_3SiOD	2722	224 ± 22	Et_3COD	2673	$< 20^b$
$\phi_3\text{SiOH}$	3675	206 ± 21	$\phi_3\text{COH}$	3609	$< 15^b$
$\phi_3\text{SiOH}$	2712	292 ± 29			
$\phi_2\text{Si}(\text{OH})_2$	3610, 3679	80 ± 15	CH_3OH	3641	$15 - 30^b$
$\phi_2\text{Si}(\text{OD})_2$	2665, 2710	134 ± 14	CH_3OD	2685	52 ± 17
			CD_3OH	3642	73 ± 7
			CD_3OD	2690	79 ± 17
			EtOH	3625	70 ± 10
			ϕOH	3610	$5 - 20^b$
			ϕOD	2665	$15 - 25^b$
			$\text{C}_6\text{F}_5\text{OD}$	2640	$< 15^b$

^aMe= $-\text{CH}_3$, Et= $-\text{CH}_2\text{CH}_3$, ϕ = $-\text{C}_6\text{H}_5$

^bLimits on T_1 were deduced from computer simulation.

Table 3.3 T_1 vibrational lifetimes of the OH($\nu=1$) stretching fundamental mode of hydroxyl ions in natural crystalline micas at 298 K. Uncertainties in T_1 are $\pm 1\sigma$. Where applicable, the samples are labelled by their Smithsonian Institution identification numbers.

Muscovite	ν_{OPA} (cm^{-1})	T_1 (ps)	Biotite	ν_{OPA} (cm^{-1})	T_1 (ps)
104935	3591	88 ± 16	82063	3691	198 ± 15
105013	3648	90 ± 15	C3647	3691	244 ± 15
105051	3591	83 ± 18	C3675-1	3691	220 ± 18
	3675	85 ± 8		3575	125 ± 11
B16862	3675	105 ± 36	Ruggles	3591	72 ± 20
Ruggles	3591	79 ± 8	Unknown	3540	64 ± 5
	3675	114 ± 13			

For comparison to the surface (Table 3.1) and liquid (Table 3.2) phase results, new results were obtained for the OH($\nu=1$) T_1 lifetime of hydroxyl ions located within the two-dimensional crystalline layers of natural Muscovite and Biotite micas. Briefly, these silicate crystals are composed of a sheet of metal cations octahedrally coordinated to OH^- ions which is in turn sandwiched between two covalently linked SiO_4 tetrahedral layers. This composite layer is further stacked upon others (creating several polymorphs) to form the mica. Excess negative charge in these stacked layers is neutralized by intercalated K^+ ions which give micas their easily cleaved sheet-like character. With Al^{+3} ions in the octahedral layer, the chemical composition of Muscovite is best represented as $[\text{K}\text{O}_3\langle\text{Si}_{3/2} + \text{Al}_{1/2}\rangle\text{O}_2(\text{OH})\text{Al}_2(\text{OH})\text{O}_2\langle\text{Si}_{3/2} + \text{Al}_{1/2}\rangle\text{O}_3]_n$. Since its aluminum ions occupy two of three possible octahedral sites (two Al^{+3} and one vacancy), Muscovite is called a dioctahedral mica. Because Biotites generally have all three octahedral sites filled (e.g., by Mg^{+2} in Phlogopite), their chemical composition may be written as $[\text{K}\text{O}_3\langle\text{Si}_{3/2} + \text{Al}_{1/2}\rangle\text{O}_2(\text{OH})\text{Mg}_3(\text{OH})\text{O}_2\langle\text{Si}_{3/2} + \text{Al}_{1/2}\rangle\text{O}_3]_n$ and they are called trioctahedral micas. Substitutions for Mg^{+2} in Phlogopite (by Fe^{+3} and Al^{+3} , for example) gives rise to other forms of the Biotite family.

T_1 values for the micas are given in Table 3.3. At room temperature, the average OH($\nu=1$) vibrational population lifetime ($T_{1\pm\sigma}$) for OH^- in Muscovite is 92 ± 13 ps. For Biotite samples, absorptions arising from two distinct lattice sites yield $T_1 = 221 \pm 23$ and 87 ± 33 ps, respectively. These energy dissipation times are comparable to those observed for the surface OH, liquid silanols, and OH in amorphous fused silica. In the micas the MOH bending

frequency is in the 800-900 cm^{-1} range (like surface OH) while the M-OH stretch in the micas is lowered to 400 - 500 cm^{-1} (much lower than the stretch in silanols or for surface OH). Thus the similarity of T_1 may again be consistent with energy transfer to the MOH bend being a dominant channel. The observed trends in T_1 (Muscovite and Biotite low frequency site vs. Biotite high frequency site) can be rationalized in terms of local site structure and hydrogen bonding. The high frequency trioctahedral Biotite sites have the longest T_1 (221 ps) and are least hydrogen bonded because their out-of-plane orientation leads to little O-HO interaction with the octahedral layer oxygens. The Muscovites and lower frequency Biotite hydroxyl sites are dioctahedral sites with broader, lower frequency absorption, reduced O-HO distance (3.5Å) and increased H-bonding and a correspondingly shorter T_1 .

The crystalline micas are also attractive samples for measuring transient vibrational populations by picosecond coherent anti-Stokes Raman scattering (CARS). Such measurements will give independent confirmation that the ir pump-probe experiments yield correct T_1 times. Also the CARS probing may determine what vibrational modes accept the energy following deactivation of the high frequency OH($v=1$) mode. The 10 Hz dye laser described above and the 532 nm doubled Nd-YAG form the CARS probe pair. The OH($v=1$) level is initially pumped by the LiNbO_3 OPA. Large CARS signals have been produced from crystalline mica when the dye laser was tuned to make the pulse pair resonant with the OH $v=0 \rightarrow v=1$ transition. We do not yet (mid September 1986) have time-resolved population data using this approach.

The preceding successfully completed experiments and those now being done are all steps toward answering the questions 1) What is T_1 , for a molecule on a metal surface? 2) What are the pathways of energy transfer (i.e., where does the energy go)? 3) How is VET at surfaces related to chemistry? With continued support from the Air Force Office of Scientific Research, we anticipate continuing progress toward understanding these and other important questions in condensed phase energy transfer.

The most significant questions for us to answer in the area of energy transfer for molecules on surfaces are: 1) What is T_1 , for a molecule on a metal surface? 2) What are the pathways of energy transfer (i.e., where does the energy go)? 3) How is VET at surfaces related to chemistry? The experiments outlined below are planned to answer these questions.

We have several different strategies for measuring T_1 for a molecule on a metal surface. One approach is to perform our usual one color IR pump/probe time-resolved bleaching experiment for molecules on supported metal clusters. Another approach involves IR excitation of a molecular (e.g., pyridine) bound to the surface of a metal (e.g., Au) particle suspended in liquid as a sol; this would be followed by anti-Stokes Raman scattering (surface enhanced) as a time dependent probe of vibrational population. These experiments require infrared and visible laser pulses of

suitable energy, bandwidth, frequency, and duration. We have two suitable laser systems which generate the difference frequency, $\omega_{IR} = \omega_1 - \omega_2$, between two visible laser pulses in non-linear crystals. For frequencies $\omega_{IR} \geq 1800 \text{ cm}^{-1}$ we use LiIO_3 and for lower frequencies $900 < \omega_{IR} < 1800$ we have tried AgGaS_2 . In addition, a new hybrid 10 Hz pulsed Nd-YAG laser, presently under construction, should generate ~8 ps, 1.06 micron pulses, and hence much shorter dye, 532 nm, difference frequency ir, and OPA ir pulses than the present apparatus produces. These shorter pulses should improve the time resolution by more than a factor of four compared to the current 10 Hz ps laser system. Ir pump-probe measurements of T_1 for $\text{CO}(v=1)$ on dispersed supported small metal particles are being attempted with this new laser source. The successful T_1 experiments on "model compounds" like the metal carbonyls will continue. Anti-Stokes Raman scattering measurements to determine the pathways (accepting modes) involved in the VET will be done, first for homogeneous model compounds such as metal carbonyls in solution and crystalline mica. It is possible that the dispersed supported metal samples may scatter so much light as to make any anti-Stokes experiments impossible. If so, we may still be able to perform such time-resolved measurements on molecules bound to the surface of colloidal metal particles in liquid suspensions.

C. Laser Diagnostics of Surface Dynamics

(D. Burgess, Jr., R. R. Cavanagh, L. B. Elwell, and D. S. King)

This program is directed at understanding energy transfer and chemical dynamics occurring at metal surfaces at a fundamental level. The approach is to apply state-resolved diagnostics, shown over the last decade in gas phase reaction and beam scattering experiments to provide a tremendous wealth of information about intermolecular potential energy surfaces to issues in surface chemistry. Thermally driven processes that have been characterized (i.e., kinetics, binding site occupation, etc.) by more conventional surface science techniques have been chosen for study because of their ubiquitous role in heterogeneous chemistry. From the viewpoint of chemical physics, elucidation of the rates and mechanisms for energy flow from a molecule into a nearby surface (dissipation) or vice versa (fluctuation) are key to a fuller, fundamental knowledge of surface controlled chemical processes.

A collaboration between CCP Molecular Spectroscopy and Surface Science Divisions has resulted in the creation of an experimental facility to perform such state-resolved studies of thermal, molecular processes at well characterized surfaces. The facility includes two ultra-high vacuum (UHV) chambers. The major chamber, for oriented single crystal work, includes traditional surface sensitive analytic tools such as mass spectrometry, ion sputtering, low-energy electron diffraction and Auger electron spectroscopy. The second chamber, a test chamber for laser desorption experiments, is much smaller in scale. Two laser systems are currently available. A near transform limited excimer-pumped dye laser is dedicated to measurements of vibrational, rotational, spin-orbit, and lambda doublet distributions, orientational effects, and kinetic energy distributions for molecules (e.g., NO) desorbing from surfaces. This system is used as the state-resolved diagnostic both for thermal and laser-induced desorption. For the

laser-induced thermal desorption (LITD) studies we are using a YAG laser (temporarily borrowed from the Center for Radiation Research) capable of producing either nanosecond or picosecond duration pulses to probe the time scale required to achieve equilibrium.

1. Adsorbate-Adsorbate Interactions: (NO + NH₃)/Pt(111) Thermal Desorption

In FY85 measurements of the internal state distributions for NO thermally desorbing from Pt(111) were measured both for an extensive (10-fold) range in NO coverage and under the influence of co-adsorbed CO. Unlike the earlier, apparently non-equilibrium dynamics exhibited by the NO/Ru(001) system, the results of the work on the NO/Pt(111) system may be summarized as follows: 1) the rotational levels and spin-orbit states are characterized by a common rotational temperature; 2) although the kinetic parameters describing the desorption process change significantly with coverage and the presence of co-adsorbed CO, the rotational degree of freedom of the desorbing NO is always nearly fully accommodated with the surface temperature; 3) there was no measurable alignment of the desorbing species.

In terms of the observable dynamics there was no manifestation of adsorbate-adsorbate interaction, i.e., no substantial deviation from full accommodation. In both the NO-NO and NO-CO systems the adsorbate interactions are weak-to-moderate in strength. The co-adsorption system (NO+NH₃)/Pt(111) was chosen for study in FY86 since it had been shown by TPD and EELS studies that there is a stable, surface bound complex formed upon co-adsorption of NO+NH₃ on cold Pt(111). Thermal desorption of NO and of NH₃ occurs simultaneously at a temperature much higher than characteristic of either species, implying that the rate-limiting step in the co-adsorbed system is dissociation of the more strongly bound complex.

Although the kinetics for NO desorption from Pt(111) were significantly altered by the interaction with co-adsorbed NH₃ there was no significant deviation from near-complete rotational accommodation with the surface. For surface temperatures of 150 to 400 K and NO coverages of 5% to saturation, the rotational temperature of the desorbed NO was 90 ± 5% of the instantaneous surface temperature and independent of the amount of co-adsorbed NH₃. This implies that disruption of the NO/NH₃ complex leads to NO molecules which are able to accommodate with the surface prior to desorption.

2. Laser-induced Desorption: NO/Pt(foil)

Thermal desorption techniques probe surface processes occurring under conditions of thermodynamical equilibrium. This is to say that external heating rates of 1-10 K/s are much slower than rates for energy transfer in condensed phases. To attempt to learn the important time scales for molecular energy transfer at surfaces we have implemented a program in laser-induced thermal desorption. Here it is hoped that sufficiently rapid

temperature jumps (heating laser pulse durations of 10^{-8} to 2×10^{-11} s) will allow desorption or other surface processes to compete favorably with energy exchange or relaxation processes characteristic of thermal processes.

A major concern in all experiments where a laser is used to heat a surface is the accurate determination of the surface temperature. Classical heat conduction equations have been employed to establish the surface temperature in the past, and are currently being used to analyze the desorption yields obtained in this laboratory. However, experimental efforts to validate the surface temperature actually achieved due to laser heating are sparse. A direct measure of the laser perturbation of the surface properties would offer the most satisfactory probe of the heating effects. Attempts at exploiting the resulting time dependent black-body radiation as a signature of the surface temperature have not been successful. The choice of our initial system for study, NO/Pt using 3-8 nanosecond heating-laser pulses, was based on our earlier results for NO/Pt thermal desorption wherein we have always observed near-complete rotational accommodation. Our naive expectation was that desorbed NO would exhibit rotational and translational accommodation and thereby give us an in situ probe of the response of such a surface in other laser-heating experiments.

The experiments were performed on a 25 x 12 x 0.25 mm polycrystalline Pt foil in a small UHV test chamber (base pressure 2×10^{-10} torr). A frequency-doubled, 3 ns FWHM YAG laser was used to heat the surface. A spatially homogeneous portion of the collimated laser beam irradiated a 1.5 mm diameter portion of the surface with 0.5 mJ/pulse at near normal incidence. The density of desorbed NO in specific (V, J, Ω) states above the surface was probed using a frequency-doubled dye laser (0.05 cm^{-1} bandwidth, 9 ns FWHM) tuned to the (0-0) or (1-1) vibronic bands of the NO A-X electronic transition. The 1 mm diameter probe beam was aligned parallel to the surface at a distance of 4 mm. LEF from desorbed molecules in a 1.5 mm long portion of the probe beam was detected with $f/2.5$ collection optics, spatial masks, spectral filters, and a solar-blind photomultiplier.

The platinum surface was initially flashed clean to 1300 K, cooled to 200 K, and then exposed to a saturation dose of NO. A background pressure of 4×10^{-9} torr NO was maintained during the experiments to stabilize the surface NO concentration, which would otherwise have been slowly depleted by the LITD process. Time of flight (TOF) distributions were obtained by scanning the time delay between the desorption laser and the probe laser in 0.1 μsec increments. At the 30 mJ/cm^2 incident energy density used, the surface temperature jump was calculated to be 120 K from the optical and thermal properties of platinum and the laser pulse FWHM. This implies a maximum surface temperature of $T_m=320$ K.

Representative TOF distributions for desorbed NO in $v=0$ with low (25 cm^{-1}) to moderate (662 cm^{-1}) rotational energy are shown in Figure 3.2. The observed LEF/TOF signals correspond to maximum molecular densities of about 5×10^{-8} torr in the probed region as determined by comparison to LEF signals with NO flowing through the chamber. The prompt onset and early maximum

exhibited by the molecules in the $J=19.5$ rotational state became increasingly more apparent as higher quantum states were probed. These data and TOF spectra for 16 other rotational states with $25 < E_R < 2162 \text{ cm}^{-1}$ suggest that there are at least two distributions of NO desorbing from the surface: a "fast" component with moderate internal excitation and a slower component with a "colder" internal energy distribution. To characterize the translational and rotational energy distributions of the desorbed NO, all of the TOF spectra were fit to the sum of two velocity distributions, each of the form $P(v) = v^4 \exp[-(a+bv+cv^2)]$, which reduces to a Maxwell-Boltzmann distribution for $b=0$.

For all quantum states with $25 < E_R < 2162 \text{ cm}^{-1}$, the slow component was fit by a distribution with a mean kinetic energy of $\langle E_T \rangle = 52 \pm 5 \text{ meV}$, while $\langle E_T \rangle$ for the fast component continuously increased from $240 \pm 35 \text{ meV}$ to $460 \pm 50 \text{ meV}$ with increasing E_R . Maxwell-Boltzmann distributions with these average energies are characterized by effective translational temperatures $\langle E_T \rangle / 2k$ of 300 K and ranging from 1400 to 2650 K, respectively. However, the observed distributions were not Boltzmann. Each had a slightly larger energy spread $\langle E_T^2 \rangle / \langle E_T \rangle^2$ than would a Maxwell-Boltzmann distribution. The relative populations for the rotational levels were determined by their magnitudes in the TOF fits. The rotational populations for states with $25 < E_R < 662 \text{ cm}^{-1}$ were well characterized by Boltzmann distributions with temperatures of 410 ± 50 and $170 \pm 20 \text{ K}$ for the fast and slow components, respectively. The energetic NO molecules contributed $21 \pm 3\%$ to the integrated desorption flux under these experimental conditions.

TOF distributions were measured for desorbed $\text{NO}(v=1, J)$ states with $E_R < 133 \text{ cm}^{-1}$. These were dominated by a single velocity distribution with $\langle E_T \rangle = 290 \pm 25 \text{ meV}$. The $\text{NO}(v=1)$ rotational distribution was estimated from an excitation spectrum taken at $3 \mu\text{sec}$ delay and including transitions from 7 different rotational levels. A value of $T_R(v=1) = 155 \pm 75 \text{ K}$ was obtained. Comparison of the integrated population in $v=1$ to the $v=0$ fast component yielded a ratio of 0.054 ± 0.027 , consistent with $T_V = 900 \text{ K}$.

To summarize the $\text{NO}/\text{Pt}(\text{foil})$ laser-induced thermal desorption results, at near saturation coverage from a platinum foil two components were observed. Although the mean kinetic energy of the less energetic component is comparable to the maximum surface temperature, its rotational temperature is significantly lower than the surface temperature. Such incomplete rotational energy accommodation has been observed in conventional TDS experiments for $\text{NO}/\text{Ru}(001)$ and discussed in terms of dynamical factors in the adsorption potentials. A dramatic departure from accommodation was exhibited by the energetic NO, with its high translational energy. While this is consistent with exit channel effects which have been invoked for thermally activated H_2 recombination and CO oxidation reactions at metal surfaces, it is also consistent with a sudden (non-thermal) desorption channel. Apparently, at heating rates of 10^{10} K/s new desorption channels compete favorably with thermalizing energy relaxation pathways even under mild temperature jump conditions. This work is supported in part by the U.S. Department of Energy.

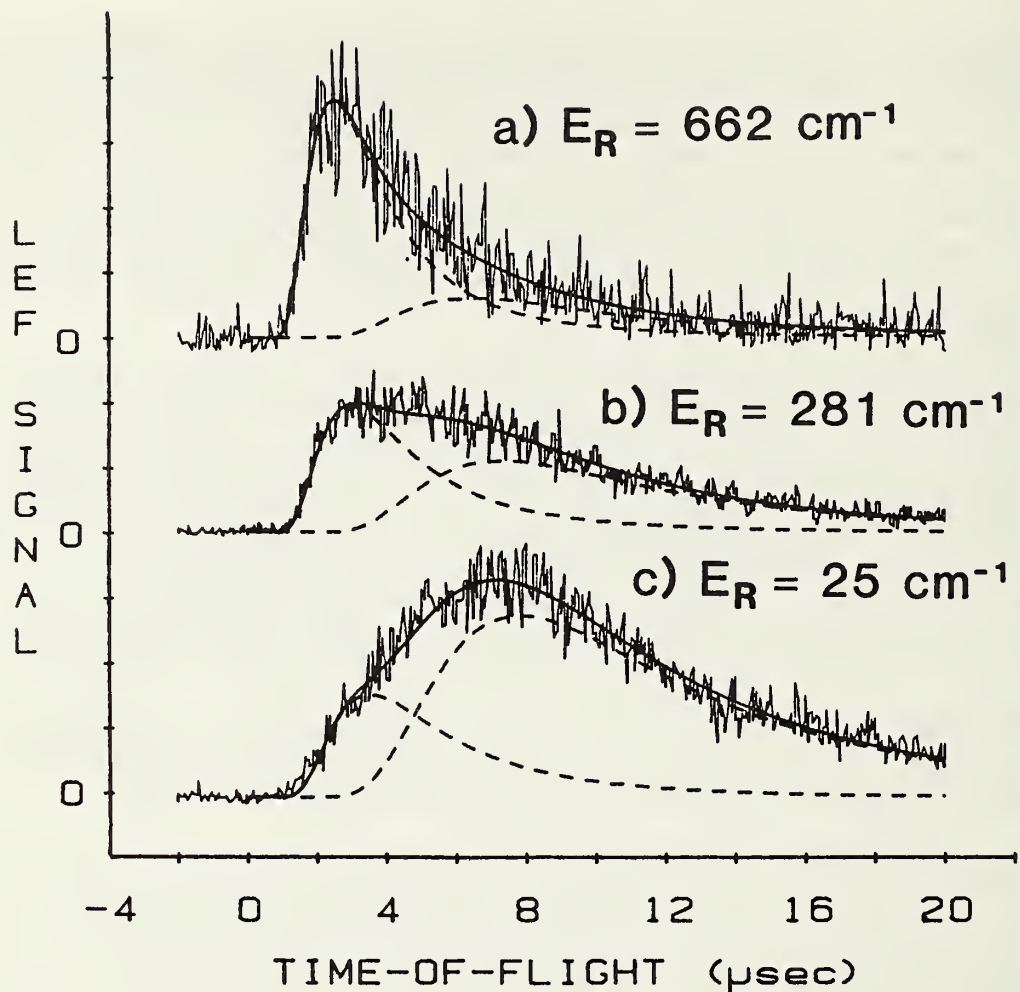


Fig. 3.2 Desorbed nitric oxide LEF signal as a function of time delay between heating and probe laser pulses for different quantum states. Spectra are normalized to NO at 294 K. Two-component fits to the data are also shown. a) $J=19.5$, $\langle E_T \rangle = 450$ and 60 meV; b) $J=12.5$, $\langle E_T \rangle = 330$ and 53 meV; c) $J=3.5$, $\langle E_T \rangle = 235$ and 47 meV.

3. Future Plans

This work will be directed towards exploring in more detail laser-induced thermal desorption (LITD). "Non-equilibrium" behavior has been observed for NO desorbing from Pt foils at low initial surface temperatures when driven by 3 ns, visible heating-laser pulses. We hope to answer speculations regarding the physical origin of this non-equilibrium dynamics (i.e., secondary desorption channels, recombinatory desorption, coverage dependent adsorbate interactions, binding site effects, or electronic effects) by exploring LITD results as a function of heating-laser pulse length, wavelength and energy, of surface morphology using single crystals, and of initial surface temperature, coverage and co-adsorbates.

One of the long range goals of this program is to study recombination reactions on surfaces. For technical reasons, this is difficult by thermal desorption techniques. Experiments currently underway entail the use of a variable pulse length heating laser (10 ns to 25 ps on loan from Radiation Physics for four months). These experiments should elucidate the contribution from recombinatory desorption to the observed NO/Pt(foil) LITD signals (described above). It is anticipated that LITD will provide a powerful technique for detailed study of recombination reactions.

D. Dynamics of van der Waals Molecules

(M. P. Casassa, L. B. Elwell, D. S. King, and J. C. Stephenson)

There has been substantial recent theoretical interest in the vibrational predissociation of van der Waals (vdW) molecules, but very few experiments that have looked at either the final product state distributions or obtained real time measurement of the dissociation lifetimes. We have recently studied the vibrational predissociation of the nitric oxide vdW dimer, including picosecond time-resolved measurements of the lifetime following excitation of the symmetric (ν_1) and antisymmetric (ν_4) stretching modes, and measurements of the complete distribution of energy in NO product fragments following ν_1 excitation.

Vibrational predissociation of van der Waals molecules occurs because, in general, the constituent molecular vibrational levels lie above the vdW bond energy. Vibrational excitation and subsequent vibrational energy flow lead eventually to rupture of the weak van der Waals bond. While such systems have had great appeal as models for vibrational dynamics, the previously available lifetime data are based on indirect measurements. In our experiments, picosecond infrared pulses excited the symmetric ($\nu_1 = 1$) or antisymmetric ($\nu_4 = 1$) stretching modes of the NO dimer. The formation times of the NO fragments ejected upon vibrational predissociation were measured by laser excited fluorescence (LEF) using picosecond time-delayed ultraviolet laser pulses. A remarkable dependence of the predissociation lifetime on the vibrational mode initially excited was observed.

The NO dimer has C_{2v} symmetry with a 2.236 Å N-N separation and a 99.6° O-N-N bond angle. The dimer bond energy is $800 \pm 150 \text{ cm}^{-1}$. Photodissociation spectra have been reported for excitations of the symmetric ν_1 (vibrational symmetry A_1) and antisymmetric ν_4 (B_2) N-O stretching fundamentals at 1870 cm^{-1} and 1789 cm^{-1} , respectively. The low frequency modes associated with the vdW bond are 90 (A_2), 170 (A_1), 198 (B_2), and 263 (A_1) cm^{-1} . We used laser-excited fluorescence (LEF) spectroscopy (using a frequency doubled CO_2 laser for photolysis and a 10 ns probe dye laser) to determine the internal state distribution and kinetic energy of the NO photofragments. For fragments with internal energy $E_{\text{int}} \leq 400 \text{ cm}^{-1}$ (representing $\geq 97\%$ of all products), the rotational states were adequately represented by a Boltzmann distribution with $T_{\text{Rot}} = 110 \text{ K}$, for both spin orbit states. The two spin orbit states, $F_1 = \text{NO } ^2\Pi_{1/2}$ and $F_2 = \text{NO } ^2\Pi_{3/2}$,

were formed with equal probability. The lambda doublet states were formed with equal probability. The average product internal energy was $\langle E_{\text{int}} \rangle = 135 \pm 25 \text{ cm}^{-1}$.

Doppler profile measurements were made for fragments in the F_2 ($J=3.5$) state. Profiles measured with the propagation direction of the probe laser parallel or perpendicular to the electric vector of the photodissociation laser were indistinguishable. This indicates the angular flux of the NO photodissociation fragments was essentially isotropic. The observed Doppler profiles were "top hat" (rectangular) in shape with $0.165 \pm 0.01 \text{ cm}^{-1}$ FWHM. The top hat shape implies a narrow kinetic energy distribution, a condition imposed by the photon energy and E_{int} distribution [assuming the dimers initially equilibrated with the beam ($T \sim 1\text{K}$)]. Computer modeling (including the fragment internal state distributions) of the observed Doppler profiles gave an average kinetic energy $\langle E_K \rangle = 400 \pm 50 \text{ cm}^{-1}$ for each NO. Conservation of energy gives a bond energy $D_0 = 800 \pm 150 \text{ cm}^{-1}$, which may be compared to the value $D_0 = 590 \pm 80 \text{ cm}^{-1}$ calculated from infrared intensity measurements.

For the lifetime measurements, dilute mixtures of NO in He or H_2 were expanded through a pulsed valve operating at 4 Hz with a .75 mm diameter orifice. The observed LEF signals scaled with expansion conditions as $X^2 P^{2.9}$, for NO mole fractions $0.005 \leq X \leq .02$ and nozzle stagnation pressures $3 \leq P \leq 10 \text{ atm}$. This is the same scaling behavior attributed to $(NO)_2$ previously. The conditions used for the lifetime measurements were shown by mass-spectrometry and final-state energy distribution measurements to produce cluster signals dominated by NO-dimer, and exhibit rotational cooling (of uncomplexed monomer) to $\sim 1 \text{ K}$.

Picosecond infrared (ir) and ultraviolet (uv) laser pulses were derived from two visible dye lasers synchronously pumped by a frequency-doubled, modelocked cw YAG laser. One dye laser was set at $\omega_1 = 17,341 \text{ cm}^{-1}$. The second dye laser was tuned to $\omega_2 = 15,471$ or $15,552 \text{ cm}^{-1}$ so that the frequency difference, $\omega_3 = \omega_1 - \omega_2$, coincided with either the ν_1 or ν_4 fundamental. Dye amplifiers pumped by a frequency-doubled, 2 ns Q-switched YAG laser amplified both lasers to produce visible picosecond pulses at 20 Hz with typical pulse energies of 0.7 mJ (ω_1) and 0.3 mJ (ω_2). Bandwidths of these pulses were 3 cm^{-1} FWHM with autocorrelation widths of 7.5 ps FWHM and a cross - correlation width of 10 ps FWHM. Infrared pump pulses of $4 \mu\text{J}$ were obtained by difference frequency mixing ω_1 and ω_2 in $LiIO_3$. The ir pulses were focused to a 0.3 mm diameter beam waist to vibrationally excite the beam-cooled $(NO)_2$. Ultraviolet probe pulses were produced by frequency-doubling ω_2 in KDP and then summing $2\omega_2$ with residual 1.064 nm from the Q-switched YAG in KD^*P . These pulses traversed a variable optical delay and were focused to a 0.15 mm beam waist colinear with the ir pump beam.

Probe pulses polarized at the magic angle to the ir pump pulses traversed the beam at a time t_D , relative to the pump pulses, exciting those NO fragments formed in the $J = 1.5-7.5$ levels of the $X^2\Pi_{3/2}$ state (P_2 band head region), resulting in LEF signals directly proportional to the number of NO

fragments formed during the time t_D . Previous studies showed that these probed states 1) are not appreciably populated by uncomplexed monomer in the expansion, 2) are formed with high probability in the $(\text{NO})_2$ ν_1 photolysis, and 3) are not favorably formed in the 1870 cm^{-1} photolysis of other NO complexes. The LEF signal and pump and probe pulse energies were recorded for each shot with a computer based data acquisition system. LEF signals were normalized to the uv probe energy. Shots with ir energy falling outside a $\pm 20\%$ acceptance window were rejected. For each data point, a delay setting was randomly selected and 100 accepted shots were averaged.

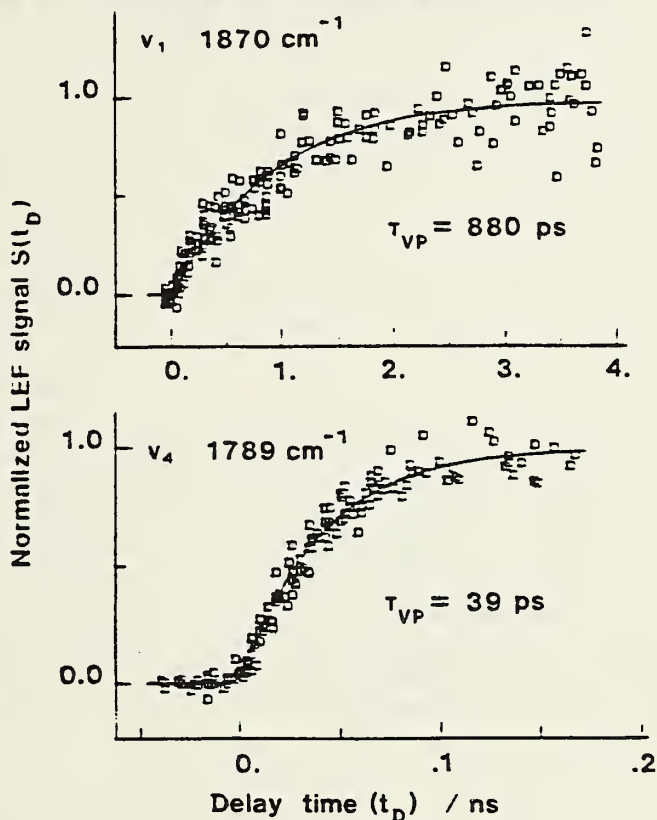


Fig. 3.3 Time-resolved appearance of NO fragments following excitations of either the symmetric (ν_1) or antisymmetric (ν_4) stretching fundamentals of the NO dimer. Note the 20-fold difference in time axes. The solid curves are least-squares fits of a simple exponential decay function with unimolecular decay rate $k_{\text{uni}} = 1/\tau_{\text{VP}}$. Although only short time measurements are included for the rapidly rising ν_4 data, there was no change in signal for delays between 150 ps and 4 ns.

Results for $(\text{NO})_2$ $\nu_1(v=1)$ and $\nu_4(v=1)$ photodissociations are shown in Fig. 3.3. A dramatic difference in dissociation rates for these two modes of nearly equal energy is immediately apparent (Note the 20-fold difference in time axes). Only short-time measurements are shown for the rapidly rising ν_4 data; no further increase in signal was observed for delays between 150 ps and 4 ns.

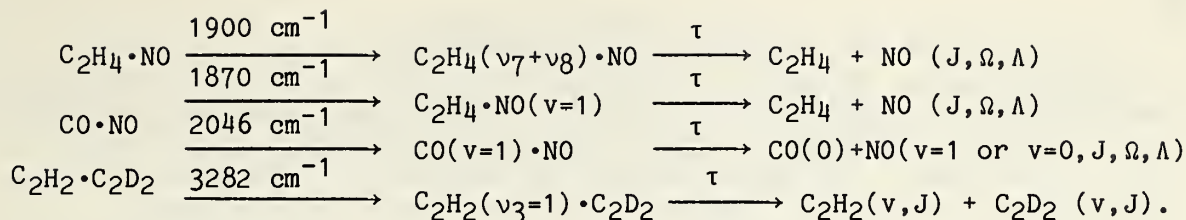
If the ir laser excited an ensemble which dissociated with a single unimolecular rate constant, $k_{\text{uni}} = 1/\tau_{\text{VP}}$, the expected fragment appearance behavior would be:

$$S(t_D) = S(t_D = \infty) [1 - \exp(-t_D/\tau_{\text{VP}})].$$

Of course non-exponential or multi-exponential decay could occur. Non-linear least-squares fits of single exponential decays to the data, shown as solid curves, yield lifetimes of 880 ± 260 ps for ν_1 and 39 ± 8 ps for ν_4 . These lifetimes represent average values for a distribution of rotational levels. Assuming that the ir bandwidth is $4\text{--}5 \text{ cm}^{-1}$ (convolution of two 3 cm^{-1} Gaussians), the pump laser interacts with all $(\text{NO})_2$ rotational levels expected to be populated in the molecular beam (If $T_{\text{ROT}} = 1 \text{ K}$, levels with $J'' \leq 3$, $K_a'' \leq 2$ account for 95% of the population). Each vibrationally-excited rotational level could have a distinct predissociation lifetime. However, with the present signal-to-noise, the data at many different expansion conditions are adequately fit by the same single exponential time constant. Including additional exponentials with different decay times did not significantly improve the fit to the data (i.e., reduce chi square).

That ν_4 (1789 cm^{-1}) decays much faster than ν_1 (1870 cm^{-1}) is inconsistent with standard statistical theories of unimolecular reaction which predict unimolecular rates to increase with reactant internal energy. On the other hand, models of vibrational predissociation involving pure V-T energy transfer correlate increased lifetime with increased energy release, and predissociation from ν_1 releases 81 cm^{-1} more energy than ν_4 . However, theory quantitatively predicts a much smaller difference (factor of ≤ 2) between ν_1 and ν_4 than was observed. In the case of $(\text{NO})_2$, the predissociation might be nonadiabatic since the $^2\Pi$ configurations of the NO fragments combine to form several low-lying electronic states in the dimer. Nonadiabatic effects have been suggested to explain the anomalously large collisional cross-section observed for vibrational deactivation of $\text{NO}(v=1)$ by $\text{NO}(v=0)$. The different overall symmetries of the ν_1 and ν_4 levels of the dimer 1A_1 ground state may constrain coupling to low lying repulsive state(s), causing the observed difference in lifetimes. Ongoing measurements of product energy distributions following ν_4 dissociation and lifetimes for states of different vibrational symmetries (e.g., combination bands involving the vdW modes) might elucidate the source of the difference in ν_1 and ν_4 predissociation rates.

Future progress in this area depends critically on our ability to obtain additional funds, either internal or from other agencies, to cover staff salaries and operations. During 1987 we hope to measure the vibrational predissociation rates following excitation of particular vibrational modes of several vdW dimers, and also to measure the distribution of energy (electronic, vibrational, rotational, translational) in the products. Candidate molecules are:



Many other vibrations in C_2H_2 , C_2D_2 , and C_2HD complexes can be studied. In several systems vibrational energy transfer across the vdW bond (a fast process according to some theoretical calculations) may occur and can be readily detected by LEF. A high resolution (e.g., transform limited, 15 ns pulses) tunable infrared laser source, similar to the low resolution ps ir difference frequency system, is necessary for obtaining good photodissociation spectra on the same molecular beams used for the time-resolved measurements.

E. Photophysical Studies of Photosensitizers

(D. S. King, in collaboration with D. F. Heller and J. Krasinski of Allied Corporation and R. S. Bodaness of National Center for Health Services Research, OHTA)

Many photosensitizers, such as hematoporphyrin derivative (HPD), are known to produce excited-singlet molecular oxygen which is then responsible for ensuing oxidation reactions. Chemically, HPD has received significant interest because it preferentially binds to tumor tissue and can be used for tumor localization (fluorescence) and photochemotherapy. Conventional tumor photolocalization techniques use blue to ultraviolet excitation sources which are severely attenuated by tissue absorptions, limiting detection and treatment to exposed surface layers. We have pursued a more universal approach which takes advantage of the two-photon spectroscopy of HPD.

Two-photon excited fluorescence spectra were taken using either a Q-switched YAG with a 20 ns output pulse duration at 1064 nm or a Q-switched alexandrite laser with 55 ns pulse duration, tunable in the 730 to 780 nm range. Second harmonic generation was also used to directly excite the sample at 532 or 375 nm. The evidence for two-photon excitation consists of both the similarity of the fluorescence spectra recorded following, for example, excitations at 1064 nm (two-photon absorption) and at 532 nm (one-photon absorption), and the quadratic intensity dependence of the two-photon fluorescence signals. Calibrations to determine the two-photon cross-sections were made from single-photon fluorescence data, using the known single-photon absorption coefficients and fluorescence quantum yields. The two-photon excitation cross-section at 750 nm (of $1.5 \times 10^{-49} \text{ cm}^4 \text{ s}$) was approximately 100-fold greater than that at 1064 nm; we attribute this to a resonant enhancement contribution from the HPD S_1 state.

In the alexandrite laser excitation experiments the HPD two-photon fluorescence was of sufficient intensity to be observed by eye in a darkened room through a single dielectric filter. This implies potential usage of such two-photon techniques for tumor localization at substantial tissue depths since there is an approximately one-thousand fold increase in tissue transmission at 750 nm as compared to 400 nm. Since the two-photon absorption rate is proportional to the square of the laser intensity, the application of picosecond laser pulses should greatly increase the efficiency of the two-photon absorption process, permitting the use of substantially reduced laser pulse energies to achieve equivalent ends. Use of 50 ps, 1 mJ pulses available from a pulsed, mode-locked alexandrite laser oscillator will only deliver 2% of the energy dose used in the present two-photon experiments, however the two-photon excitation rate should be enhanced a million-fold in relation to excitation by a 50 ns pulse of the same energy. This should lead to complete saturation of the HPD two-photon absorption. Such experiments are planned for Spring 1987.

4. QUANTUM CHEMISTRY GROUP

H. Basch, D. Beveridge, W. Fink, N. Goldgaber, P. Jasien, P. S. Julienne,
M. Krauss, B. Lengsfeld, M. Mezei, F. H. Mies, K. J. Miller,
R. Osman, W. J. Stevens, and L. Vahala

- A. Introduction
- B. Theoretical Calculations on Biomolecules
 - 1. Development of an Ab Initio Reaction Field Program
 - 2. Modeling of Fe and Mn Superoxide Dismutases
 - 3. Frozen Fragment Studies of Hydrogen Bonding
 - 4. Monte Carlo Studies of Solvated Biomolecules
 - 5. Binding of Pt Complexes to DNA
 - 6. Electronic Structure of Phosphates, Phosphoranes, and Their Analogues
 - 7. Rotational Barriers in Formamide and Acetamide
 - 8. Future Plans
- C. Quantum Chemistry of Small Molecules
 - 1. Accurate Calculations on Small Molecules
 - (a) CrO and CrO⁺
 - (b) Silicon Carbide, SiC
 - 2. Interaction Energy Curves of RR', (R,R' = He through Xe)
 - 3. Future Plans
- D. Scattering in the Presence of Radiation
 - 1. Non-adiabatic Theory of Atomic Broadening in Weak Fields
 - (a) Redistribution Calculations for Sr(¹P←¹S) + Ar
 - (b) Redistribution Calculations for Na + Rare Gas
 - (c) Lorentzian Pressure-Broadening Widths for Na

2. Nonadiabatic Theory of Redistribution in Strong Fields

(a) Collisional Redistribution of Resonant Radiation

(b) Analysis of Multiphoton Lineshape Theory in Intense Fields

3. Future Plans

E. Atomic and Molecular Scattering Theory

1. Half-Collision Amplitudes

(a) Analysis of Exact Close-Coupled Codes

(b) Multichannel Semiclassical Half Collision Amplitudes

2. Multichannel Photodissociation Amplitudes

3. Future Plans

A. Introduction

The Quantum Chemistry Group develops and applies atomic and molecular structure and scattering methods to chemical and spectroscopic problems where experiments are difficult to perform or so complicated that the theory is needed to model the results. The activities of the group encompass three broad areas: the study of the structures and properties of large biomolecules, accurate quantum mechanical calculations on small molecules, and atomic and molecular scattering theory.

The biomolecular research is a result of the NBS biotechnology initiative and represents a new direction for the group. Initial work in this area has focussed on the development of methods for accurately predicting the electronic structure, energetics, and properties of small pieces (eg., active sites) of large molecules. This research has resulted in new techniques for the decomposition of molecular electrostatic potentials and polarizabilities into transferrable fragment components that will be used to construct effective Hamiltonians for the small parts of the biomolecules to be studied quantum mechanically. During the past year, several collaborations with other groups have been initiated which will concentrate on applications of newly developed theoretical techniques to interesting problems in biochemistry. The Molecular Structure and Modeling Facility IBM4381 computer is used for these large scale calculations.

The determination of accurate electronic structures and properties for small molecules has been a central focus of the group's activities for many years. Our unique capability for handling heavy atoms through the use of effective core potentials has allowed the study of a variety of interesting molecules including transition metal oxides and heavy rare-gas dimers. The accomplishments for this year include state-of-the-art calculations on chromium oxide and silicon carbide, and a complete set of calculations of the van der Waals potentials for the homonuclear and mixed rare-gas dimers.

In the area of scattering theory, new methods have been developed for the determination of cross-sections and fragment state distributions associated with the collisional broadening and photodissociation of small molecules in the presence of both weak and strong radiation fields. In addition, significant progress has been made in the area of multichannel quantum defect theory and non-adiabatic half-collision amplitudes, with specific applications to broad-band continuum spectroscopy.

B. Theoretical Calculations on Biomolecules

1. Development of an Ab Initio Reaction Field Program (W. J. Stevens, H. Basch, and M. Krauss)

Although the methods of modern quantum chemistry and the machines on which calculations are carried out have evolved dramatically in the last ten years, it is still not feasible to determine the geometric and electronic structures of very large molecules (> 20-30 atoms) by ab initio techniques. However, in large molecules such as proteins, it may be possible to learn a great deal about chemical properties by looking at the detailed electronic structure of a small part of the molecule (the active site), while treating the remainder of the system as a perturbing environment that plays only an indirect role in the chemistry. During the past year we have modified the HONDO electronic structure program to include a reaction-field Hamiltonian that allows the study of an active molecular fragment, "A", in the field of a molecular "spectator" environment, "S". The Hamiltonian is written

$$H_A = H_A^0 + V_{AS}$$

where V_{AS} describes the interaction of the active electrons with the spectator part of the system. Assuming the interaction of "A" with "S" is non-bonding (i.e., no covalent bond, no charge-transfer), the interaction term in the Hamiltonian may be broken down into three pieces: electrostatic, polarization, and orthogonality and exchange repulsion. Our desire is to represent each of these interactions by one-electron operators in the Hamiltonian of the active part, so that the difficulty of the calculation is primarily dictated by the complexity of the active fragment "A".

Our analysis of the electrostatic potentials of the spectator molecules is based on localized molecular orbitals (LMO). Accurate SCF calculations are carried out for prototypical molecules containing specific functional groups. The molecular orbitals of the prototype are localized by some appropriate method (e.g., the Boys method). The electronic contribution to the electrostatic potential is the sum of the contributions from each LMO. The electrostatic potentials of LMOs categorized by functional groups are found to be reasonably transferrable from one molecule to another. The electrostatic potential of each LMO is approximated by a multipole expansion at its center of charge. The molecular potential is then represented by a distributed set of LMO expansions. This distributed expansion produces an accurate representation of the molecular electrostatic potential for LMO expansions that include only the centers of charge and the first few moments. We have modified the HONDO code to include the potentials of such distributed charges and second moments in the Hamiltonian, and test calculations are now being done to determine the accuracy for a variety of prototypical systems.

The polarization of "A" by "S" occurs naturally when the Schroedinger equation is solved for the wavefunction of "A" using a Hamiltonian that contains the electrostatic potential of "S". However, the determination of

accurate interaction energies requires that "S" also is polarized by the electrostatic potential of "A". In addition, there is a self-consistent effect in the mutual polarization of the two parts of the system. Fortunately, the self-consistent part of the polarization has been found to be small (~10%). For the energy contribution due to the dipole polarizability of "S" we evaluate the expression

$$\langle \Psi_A | \sum_{i,j} \vec{r}_i \cdot \vec{r}_j \alpha("S") | \Psi_A \rangle$$

where \vec{r}_i is the electric field due to electron i in fragment "A", and $\alpha("S")$ is the dipole polarizability of fragment "S". This energy term is evaluated as a perturbation once the wavefunction for "A" is known. Putting the operator directly into the Hamiltonian of "A" is not possible, because second order effects related to dispersion are improperly introduced. The polarizability of the fragment "S" is constructed from fragment LMO polarizabilities. We have developed a coupled Hartree-Fock scheme which allows the total calculated polarizability of a molecule to be rigorously represented as a sum of LMO polarizabilities. A series of calculations has shown the LMO polarizabilities for functional groups to be reasonably transferrable from one molecule to another. Distributing the LMO polarizabilities in the fragment "S" helps take into account the inhomogeneous nature of the electronic field due to "A". Higher order polarizabilities may be added in the same fashion if necessary. Currently, the HONDO code incorporates spherically averaged LMO polarizabilities in the Hamiltonian of "A", and work is proceeding to incorporate tensor representations.

Exchange repulsion and orthogonality between "A" and "S" must be included in the Hamiltonian of "A" in order to prevent the collapse of the "A" wavefunction into the "S" region. A rigorous evaluation of the exchange interaction requires two-electron operators and a knowledge of the wavefunctions of "A" and "S". In the case of atoms, it has been shown that a one-electron effective potential can be constructed which accurately mimics the exchange repulsion between the valence electrons and the frozen core. Our group has used such potentials extensively in calculations on systems containing heavy atoms. We are developing analogous procedures for molecular systems where the fragment "S" is treated like the frozen core in the atomic case. A prototypical all-electron calculation is done in which the fragment "A" is optimized with the fragment "S" held frozen. The wavefunction of "S" is taken as a product of frozen LMOs which are obtained from independent calculations on "S" alone. Then the frozen LMO exchange operators in the Hamiltonian of "A" are replaced by one-electron effective potentials. The parameters defining the potentials are adjusted until the orbitals and energies of "A" match those obtained from the all-electron calculation using the frozen "S" and the correct exchange operators. Since the derivation of the effective potentials is based on LMOs, transferability from molecule to molecule is expected. Calculations are underway to test this hypothesis.

2. Modeling of Fe and Mn Superoxide Dismutases
(R. Osman, W. J. Stevens, M. Krauss, and H. Basch)

This research is part of a long term objective to understand the biochemical and biophysical role of metals in enzymatic mechanisms of metallo-enzymes. Quantum mechanical calculations are carried out on models of the enzymes active site, with and without the substrate, in order to ascertain whether proposed mechanisms are reasonable from an energetic point of view. The complexity of the model and the sophistication of the quantum mechanical approach are chosen to produce energetics that are reliable enough to determine which of several proposed pathways may be energetically the most favorable. The electronic structure of the model active site is analyzed to provide insight into the interactions that favor one pathway over another.

Three different superoxide dismutases have been chosen for study. They are Cu,Zn-SOD, Fe-SOD, and Mn-SOD. The availability of their crystal structures enables the construction of models of their active sites. Osman and Basch have previously studied Cu,Zn-SOD (J. Amer. Chem. Soc. 106, 5710 (1984)) and have suggested a new mechanism of action that is quite different from the ones proposed previously. Their quantum mechanical calculations indicate that a single superoxide (O_2^-) cannot reduce the cupric ion because of an arginine group (Arg-141), positioned near the copper, that forms a strong hydrogen bond with the superoxide. Thus, superoxide forms a relatively stable complex with Cu,Zn-SOD that is subsequently reduced by another superoxide in solution. The reduced complex undergoes an internal oxidation-reduction coupled to a proton transfer that results in regeneration of the original enzyme and the formation of the products of the dismutation reaction. The proposed mechanism is in agreement with all known kinetic measurements of the enzymatic reaction. The mechanism is based on the special properties of the copper ion in the active site and its surroundings in the protein (particularly Arg-141).

Fe-SOD and Mn-SOD, while similar in structure to each other, are quite different in structure from the Cu,Zn-SOD. The proposed mechanism of action of these enzymes is also based on the reduction-oxidation cycle which is consistent with the kinetic studies of the dismutation reaction. However, the details of the reaction are not understood, and analogy to the Cu,Zn enzyme may not be warranted. The recent availability of crystal structures for these enzymes offers an opportunity to perform quantum mechanical calculations on models of the active sites.

We have begun the calculations by determining effective core potentials for the Fe and Mn atoms which allow their inclusion in the model active sites as valence-only systems. In addition, the core potentials have been modified to reproduce accurate $M^{+2} \rightarrow M^{+3}$ ionization potentials. Crystal structures indicate that the metal ion is pentacoordinate, with three histidines, one aspartate, and one water (or OH^-) acting as ligands. In our initial models we have replaced the histidines by ammonias and have considered only the five ligands directly bonded to the metal ion. More complex models will be

developed using a reaction field approach to incorporate regions of the enzyme that do not participate directly in the reaction but do influence the energetics by virtue of their electrostatic potentials.

3. Frozen Fragment Studies of Hydrogen Bonding (W. J. Stevens and W. Fink (UC Davis))

In a recent series of articles (J. Chem. Phys. 1983, 78, 4066; J. Chem. Phys. 1985, 83, 735; J. Chem. Phys. 1986, 84, 5687) Reed and Weinhold have proposed an energetic decomposition of hydrogen bonding interactions based on a "natural bond orbital" analysis. The conclusions reached through this analysis are that the electrostatic attraction and exchange repulsion energy components of the hydrogen bond nearly cancel each other, and the charge-transfer interaction determines the shape of the potential energy surface and the structure of the complex. The charge-transfer analysis is similar to the HOMO-LUMO charge-transfer interaction proposed by Klemperer and coworkers, but differs in that the orbitals involved are the localized lone-pair orbital as electron donor and the unoccupied X-H antibonding orbital as electron acceptor. The amount of charge transferred is very small (a few thousandths of an electron), but the energy contribution is said to be several kcal/mol. This analysis is contrary to the widely accepted proposal of Buckingham and others that the structure and energetics of hydrogen bonding is determined primarily by electrostatics.

One of the problems with a decomposition of the interaction energy between two molecules is that the orthogonality, exchange, and charge-transfer components are difficult to unravel because they all involve the overlap of the molecular wavefunctions. The analysis is also confused by a superposition effect that occurs when the virtual orbitals from the basis set of one fragment help to improve the occupied orbitals of the other fragment. Even though the analysis of Reed and Weinhold appears to be remarkably consistent for a wide variety of hydrogen bonded complexes, it is not impossible that the component of the energy that has been assigned to charge-transfer is really a mixture of other effects.

In collaboration with the group at the University of California at Davis, we have modified the HONDO program to allow for the selective freezing of molecular fragments in an all-electron calculation. It is also possible to selectively eliminate unoccupied virtual orbitals from the basis set. We have used this program to study the water dimer and to assess the importance of charge-transfer in the hydrogen bond interaction. The molecules in the dimer are labelled "A" and "B". Using a fully optimized hydrogen bonding geometry at the double-zeta plus polarization level, the energy is calculated by selectively freezing the wavefunction of either "A" or "B" and optimizing the wavefunction of the unfrozen molecule. The frozen wavefunction is obtained from a calculation on an isolated water molecule. Charge-transfer cannot occur from the frozen water to the variationally active water. We have also eliminated the virtual orbitals from the frozen water basis set so that charge-transfer cannot occur from the variationally active water into the unoccupied space of the frozen water. With all of these constraints, our

preliminary calculations have found that the hydrogen bond energy in the frozen molecule calculations is within 20% of a fully variational hydrogen bond energy. Also, a significant portion of the missing energy can be traced to the lack of polarization in the frozen molecule. Although many more hydrogen bonded systems need to be studied, our tentative conclusion is that charge-transfer does not determine the structure and energetics of hydrogen bonded complexes.

4. Monte Carlo Studies of Solvated Biomolecules (D. Beveridge, M. Mezei, W. J. Stevens, and M. Krauss)

This research project has been initiated to explore the interface between ab initio quantum mechanical studies of large molecules and simulation of molecules in the liquid state using the Metropolis Monte Carlo method. The first step in this project has been to install the Hunter College MMC program for Metropolis Monte Carlo simulations on the Molecular Structure and Modeling Facility IBM4381 computer and the Consolidated Scientific Computing System CYBER205 computer. The MMC program, developed by Mezei and Beveridge, is a state-of-the-art program for simulation of a dilute aqueous solution with a force-bias option for convergence acceleration, and a proximity analysis option for assigning the solvent molecules in each N-particle configuration of the system to individual atoms of the solute. The MMC program uses intermolecular potential functions based on several current prescriptions. These functions are hardwired into the code, but the introduction of new potentials is easily accomplished. The results of the computer simulation include the calculated thermodynamic internal energies, heat capacities, and various structural and energetic molecular distribution functions. Some new methods for free energy simulations are also included.

The accuracy of the results of computer simulations of dilute aqueous solutions is dependent on the intermolecular potential functions that are used to evaluate interaction energies and energy derivatives between molecular constituents. The functions currently used in programs such as MMC are based on pairwise-additive interaction potentials between points in the molecules (usually the atoms) that are derived either empirically or from ab initio quantum mechanical calculations. The form of the potentials is kept simple (6-12 plus a coulombic term) because of the computer time required to carry out the simulations. Potentials derived by fitting quantum mechanically calculated potential energy surfaces have been restricted to low-level SCF calculations, such as STO-3G, due to the expense of accurate calculations on complex molecules. Our high-speed computing resources and recently developed methods for simplifying ab initio calculations on large molecules (such as the reaction field approach) will enable us to examine the dependence of the Monte Carlo simulation results on the accuracy of the potentials. Benchmark calculations are planned for several small amides in aqueous solution. We will also explore the use of distributed molecular polarizabilities in the evaluation of interaction energies as a method for incorporating many-body effects in the simulation. This will be particularly important in the study of solvated ions.

Quantum mechanical calculations of the properties and reactivities of molecules in solution or of molecular fragments imbedded in very large molecular systems are limited by the statistical nature of the perturbing environment at nonzero temperatures. Part of the collaboration between the NBS and Hunter College groups will be to explore the use of snapshot distributions from converged Monte Carlo simulations to construct models of the solvent environment in reaction field studies of prototypical molecules.

5. Binding of Pt Complexes to DNA
(H. Basch, M. Krauss, K. J. Miller (RPI))

Preliminary calculations on the binding of $\text{cis-Pt}(\text{NH}_2\text{R}_2)_2$, (R=H, methyl, and cyclopropyl) to a tetramer duplex were reported in last years report but research has expanded on this problem because of new experimental results reporting the binding of $\text{Pt}(\text{NH}_3)_2$ to a pGpG segment (S. E. Sherman et al., Science 230, 412 (1985)), that suggested $\text{Pt}(\text{NH}_3)_2 \cdots \text{OP}$ H-bonds significantly stabilize the complex. This research was initiated to determine if binding energies could account for the very different anti-tumor potencies between the methyl derivative and both $\text{Pt}(\text{NH}_3)_2$ and the cyclopropyl derivative. We concluded in the preliminary results which combined SCF calculations of model binding energies with molecular mechanics conformational energy analysis that the binding energy varies smoothly with substitution. The constrained molecular mechanics energy minimization did not show direct hydrogen bonding between the amine ligand and phosphate which is a feature of the Pt-pGpG crystal structure.

Two directions are being pursued to determine if direct phosphate H-bonding is important in the duplex structure. Full cartesian coordinate geometry optimization is being pursued with a tetramer duplex bound to Pt. Achieving a global minimum is an almost impossible task but a number of local minimum structures have been examined and those which distort the H-bonding between the bases the least were examined for the substituted amines. Although a phosphate moiety is found to approach closer to ammonia ($\text{O} \cdots \text{H}$ of the order of 3.5A), an H-bond distance of approach has not been found. The second phase of this calculation is to examine SCF H-binding energies for $\text{Pt}(\text{NH}_3)(\text{R})_2$ to phosphate with associated waters in order to examine the possibilities for water either externally bonded or as a bridged water. These calculations are still in progress. The results to date do not alter the earlier conclusion that potency and binding energy are not correlated if no chemical reaction other than ligand replacement is induced by the Pt interaction with DNA.

6. Electronic Structure of Phosphates, Phosphoranes, and Their Analogues
(H. Basch, M. Krauss and W. J. Stevens)

Is the stable five coordinate vanadium complex formed in the binding of uridine vanadate to ribonuclease an analogue for a five coordinate phosphate transition state? By examining the comparative electronic structure and the proton affinities (PA) the concept of transition state analogues can be made

more precise. The relative amount of d orbital contribution and the PA of different sites will determine whether proton transfer from the protein to the site as observed for the vanadium complex reflects the phosphorane situation. At the SCF level there is a substantial difference between the electronic structure and PA of PO_3^- and VO_3^- . Electron correlation has only a small effect on PO_3^- or H_2PO_4^- but the comparable vanadium calculation has not yet been done.

Whether phosphorothioate anions will interact with proteins at either the S or O site will, in part, be determined by the electrostatic potential at each site. Although considerable experimental effort has been devoted to determining bond orders and ionicities for these molecules, the simplest way to determine the potential is to calculate it from a high quality wavefunction. Electrostatic potential maps are compared in Fig. 1 for H_2PO_4^- and $\text{H}_2\text{PO}_3\text{S}^-$ in a plane determined by O-P-O or O-P-S. The outer potential contour which determines binding behavior is shifted for S relative to O by approximately in proportion to the longer bond in P-S, reflecting the comparable ionicity of O and S. This suggests zwitterionic or H-bonds will be made initially with S which would be reinforced by the larger polarizability of S. On the other hand, there is much less difference in the outer contours of PO_3^- and PO_2S^- , reflecting the smaller fractional charge found for S in this case. Optimized geometries and PA's have been determined for all these species. Calculations have been initiated on the NMR chemical shifts for ^{31}P to correlate shifts with electronic structure and conformation.

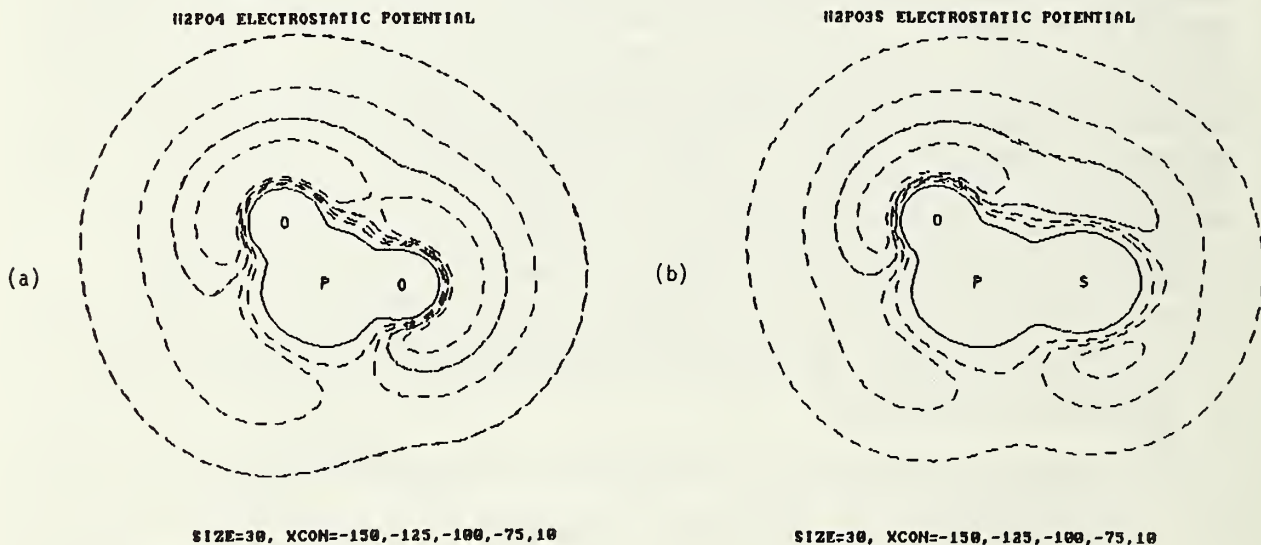


Fig. 4.1 A comparison of the electrostatic potentials of H_2PO_4^- and $\text{H}_2\text{PO}_3\text{S}^-$. The dashed contours represent potentials of -150 (innermost), -125, -100, and -50 kcal.

7. Rotational Barriers in Formamide and Acetamide
(P. G. Jasien, W. J. Stevens, and M. Krauss)

The energy barrier to rotation about an amide bond is important in the modeling of protein conformation. There have been a number of ab initio attempts to calculate the inherent barrier, but a review reveals that the accuracy was significantly limited by a lack of a complete polarization basis. The present results indicate that the inclusion of polarization functions in the basis set leads to a substantial decrease of 5 kcal/mole in the barrier height at the SCF level. Considering electron correlation and the zero point energy correction, the in vacuo rotational barriers for formamide and acetamide are predicted to be 14.2 and 12.5 kcal/mole, respectively.

8. Future Plans

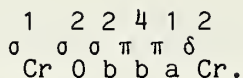
The major thrust in the biotechnology area is the development of the reaction field method. The reaction field method will be applied to the effect of solvation on the stability of amides, reactions of phosphates and their analogues, the binding of metals to DNA and protein model compounds, and the mechanism of reaction of Fe and Mn superoxide dismutase. A continuing effort is needed in evaluating the parameters and assessing the data (centroids, local polarizabilities, local quadrupoles, ...) required for the reaction field. The use of both molecular mechanics and statistical mechanics methods to determine the conformation of the environment region in the reaction field will be investigated.

C. Quantum Chemistry of Small Molecules

1. Accurate Calculations on Small Molecules
(W. J. Stevens, P. G. Jasien, and B. Lengsfeld)

(a) CrO and CrO⁺

Understanding the electronic structure of the transition metal oxides is a challenge for experimentalists and theoreticians alike. The multiple open-shell nature of the electronic wavefunction, highly degenerate constituent atoms, extreme covalent/charge-transfer mixing, and large spin-orbit splitting make the electronic states difficult to characterize theoretically and the spectra and thermodynamic behavior difficult to analyze. The CrO, CrO⁺ system is interesting from a theoretical point of view because there are a number of experimental analyses available including high-resolution spectroscopy of the ground state, photoelectron spectroscopy determining the ionization potential, and several estimates of the dissociation energies. The ground state of CrO is a ⁵Π state with the dominant valence configuration



The molecule is best described as Cr^+O^- . The singly occupied σ orbital on chromium is strongly polarized away from both the O^- and the double occupied σ_b bonding orbital. The π_b bonding orbital is quite polarized toward oxygen, and the π_a orbital is only weakly antibonding. Ionization to form the positive ion will remove an electron from either the singly occupied sigma orbital or the singly occupied pi orbital. Dyke, et al. (J. Chem. Soc., Faraday Trans. 1983, 79, 1083) have analyzed the photoelectron spectrum of CrO in terms of a single $^4\Sigma^-$ state of the ion, while our calculations show a $^4\Pi$ state only 0.1 eV above the $^4\Sigma^-$ ion ground state. Our calculated ionization potential of 7.43 eV is in reasonable agreement with the experimentally deduced value of 7.85 eV, but our ion spectroscopic constants disagree with the experimental numbers. Our best calculations (singles and doubles CI from a multiconfiguration wavefunction) predict $R_e = 1.64\text{\AA}$ ($^4\Sigma^-$), 1.62\AA ($^4\Pi$) and $\omega_e = 801\text{ cm}^{-1}$ ($^4\Sigma^-$), 895 cm^{-1} ($^4\Pi$) as opposed to 1.79\AA and 640 cm^{-1} quoted by Dyke, et al. Our values for the $^5\Pi$ ground state of CrO of $R_e = 1.647\text{\AA}$ and $\omega_e = 850\text{ cm}^{-1}$ agree reasonably well with the values of $R_e = 1.6179\text{\AA}$ and $\omega_e = 898.50\text{ cm}^{-1}$ obtained from the analysis of rotationally resolved laser-induced fluorescence spectra by Hocking, et al. (Can. J. Phys. 1980, 58, 516). Since the theoretical calculations for the neutral and ion states were carried out at the same level of accuracy, we believe that the analysis of the photoelectron spectrum is in error.

(b) Silicon Carbide, SiC

The silicon carbide molecule, SiC, is of fundamental importance in astrophysics because of the role it may play in the formation of interstellar grains. Although the triatomic molecule, SiC_2 , has been observed in the laboratory and in interstellar space, no observations of the SiC molecule have been reported. Recently, there have been a number of theoretical calculations on SiC which predict the infrared and electronic transition frequencies, but no accurate prediction of the microwave absorption frequency has been made. Radiotelescope observations of interstellar spectra are made in 128 MHz spectral windows which require several hours of data accumulation to develop a reasonable signal-to-noise ratio. At the absorption frequency of SiC (~18 GHz), the R_0 must be known to within $\pm 0.004\text{\AA}$ in order to predict the correct window for observation. Such a prediction is within the capability of modern quantum mechanical calculations.

We have performed singles and doubles CI calculations from multi-reference wavefunctions for the $^3\Pi$ ground state of SiC using a very large Slater-type basis set consisting of s,p,d, and f functions on each center. In addition to the usual d polarization functions, d and f functions were added for correlation, and their exponents were optimized in large-scale CI calculations. Five points around the bottom of the potential energy curve were calculated and fit to a Morse potential. The internuclear distances for

the calculations were chosen to symmetrically surround the minimum and to cover an energy range surrounding the lowest vibrational level. Additional points were added to ensure that the predicted Morse parameters were not sensitive to the point distribution. In all cases, the Morse fit reproduced the calculated data points to within a few wavenumbers. Several curves were generated in this way using a variety of reference wavefunctions and CI selection criteria. In the largest calculations the wavefunction consisted of more than 300,000 configurations. The several largest calculations produced R_e values that were consistent to within 0.003Å and vibrational frequencies that agreed to within a few wavenumbers.

Spin-orbit coupling splits the ground state of SiC into $\Omega = 2, 1,$ and 0 components. The $^3\Pi_2$ component is lowest in energy. Using ab initio effective spin-orbit operators developed in this laboratory, we have determined that the spin-orbit splitting in SiC is 34 cm^{-1} and nearly constant across the bottom of the potential curve. Thus, the predicted R_0 value will not be affected by spin-orbit coupling. There is a possibility that the $^3\Pi_2$ state could be perturbed by other low-lying $\Omega = 2$ electronic states. In our calculations, the closest perturbing states are $^3\Delta$ and $^5\Pi$, both of which are several thousand wavenumbers higher in energy.

The results of this study have been communicated to Dr. Michael Hollis of NASA, who will compare the predictions to known interstellar microwave lines. If a sufficiently interesting comparison is found, an application will be made for viewing time at the Kitt Peak observatory.

2. Interaction Energy Curves of RR' , ($R, R' = \text{He through Xe}$ (D. D. Konowalow and (Dept. Chem. SUNY Binghamton) M. Krauss)

Application of an ab initio hybrid model of the calculation of the rare gas dimers has yielded binding energies within 10-20% of experiment for these molecules. The discrepancy is attributed to the slow convergence in the attractive dispersion energy with high order multipoles. These calculations were performed to determine the applicability of the model to heavier systems to allow calculation of biomolecular models. Very recently an accurate correlated calculation of the binding energy of HeAr (W. Meyer et al., Phys. Rev. A33, 3807 (1986)) suggested that correlation of the fragments is important and the hybrid model potential may be questionable. Correlated atom calculations are now in progress to test this conclusion for a range of molecules. Since the hybrid model is widely used, it is necessary to examine the significance of correlation in model systems.

3. Future Plans

Accurate quantum chemistry calculations of model systems will be carried out to determine the level of accuracy required for predictive value in energetic conformations and spectroscopic properties. Electron correlation behavior in model compounds containing transition elements will continue to be studied by both ab initio and effective operator methods.

D. Scattering in the Presence of Radiation
(P. S. Julienne and F. H. Mies)

The general goal of this research is to provide calculations of radiative cross-sections and fragment state distributions associated with the collisional broadening and photodissociation of small molecules. We have developed extensive experience in calculating various nonadiabatic effects in the conventional weak-field limit, and are expanding our codes to treat the saturation of continuum transitions in intense, multiphoton fields.

Theoretical input into this program is provided by extensive sets of computer codes available to the quantum chemistry group. State of the art calculations of any necessary molecular potentials, couplings and radiative transition dipoles can be obtained. Our scattering programs have been expanded to allow for direct radiative interactions among many coupled channels. Preliminary calculations have been performed to study the pressure broadening of atomic lineshapes in both weak and strong laser fields. Our scattering codes presently provide the continuum-continuum scattering matrix elements needed in lineshape theory, and are being modified to provide the bound-continuum matrix elements required to describe photodissociation. In addition to these numerical procedures, the program involves extensive analysis of many new and exciting theoretical features introduced by very intense laser fields.

1. Non-adiabatic Theory of Atomic Broadening in Weak Fields

(a) Redistribution Calculations for $\text{Sr}(^1\text{P} \leftarrow ^1\text{S}) + \text{Ar}$
(P. S. Julienne and F. H. Mies)

We completed our close-coupled calculations of polarized light redistribution in the $\text{Sr} + \text{Ar}$ system. The calculations predict the polarization ratios of $\text{Sr}(^1\text{P})$ fluorescence following line wing excitation by either linear or circular polarized light. Ab initio calculations were used to obtain the ground and excited SrAr molecular potentials, which were adjusted modestly to give improved agreement with experiment. The radiative scattering theory gives a unified description of the absorption coefficient and subsequent fluorescence from the small detuning impact limit region to the far wings. The cross sections for depolarizing collisions of $\text{Sr}(^1\text{P}) + \text{Ar}$ were also calculated. The calculated absorption coefficient, impact broadening rate, linear and circular polarization ratios, and depolarization rate coefficients are for the most part in good agreement with a diverse set of experimental data.

(b) Redistribution Calculations for $\text{Na} + \text{Rare Gas}$
(P. S. Julienne and L. Vahala)

We have continued to calculate final state branching ratios for fine structure states and alignment/orientation for $\text{Na}(^2\text{P} \leftarrow ^2\text{S}) + \text{He, Ne, Ar}$ systems, and have obtained good agreement with experimental measurements. In

analysing the exact close-coupled data we uncovered a useful spin-uncoupling approximation of the collision dynamics and its dependence on collision velocity.

If the separation velocity of two colliding atoms is sufficiently large, the final state dynamics can be well approximated by the same recoil limit that has been successfully developed for photofragmentation. Our calculations show how the recoil limit for fine-structure branching ratios is approached for both red and blue detuning the separation velocity increases.

The recoil approximation for orientation/alignment only applies for collisions with small angular momentum (small impact parameter). The recoil limit applies when the separation time of the fragments is short compared to the characteristic times of axis rotation and spin-orbit coupling. However, by comparison to a pure 1P atom we can develop a spin-recoil approximation which treats the spin projection as fixed in space during the rapid separation to fragments while accounting for the rotation of electronic angular momentum projection Λ with the internuclear axis. Comparison of the spin-recoil model with exact close coupling results for Na + rare gas shows the applicability of the approximation.

(c) Lorentzian Pressure-Broadened Widths for Na
(P. S. Julienne and L. Vahala)

We have calculated the Lorentzian pressure-broadened widths for both the D1 and D2 lines of Na broadened by collisions with He, Ne, and Ar. In addition we have performed the first calculation of the so-called asymmetry parameter which has been widely observed in the impact regions of atomic lineshapes.

The absorption profile within the impact limit for one of the isolated 2P_j fine structure lines may be written as

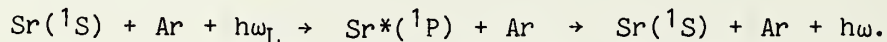
$$I(\Delta_j) = \frac{v_j(\Delta_j)/\pi}{(\Delta_j - \delta_j)^2 + v_j^2(0)}$$

where Δ_j and δ_j are the respective detunings and shift of the line. The detuning-dependent quantity $v_j(\Delta_j)$ may be shown to have a finite limit as $\Delta_j \rightarrow 0$ and exactly equals the usual impact limit broadening coefficient, including the effects of both elastic and inelastic collisions. The dependence on detuning give rise to the Lorentzian dispersion asymmetry which has been observed for Na + rare gas systems. We have calculated the radiative scattering cross section for detunings near the D1 and D2 lines for Na broadened by He, Ne, and Ar. The widths and asymmetry parameters are qualitatively in agreement with measured values. Deficiencies in the existing molecular potentials limit the expected accuracy of the scattering calculations.

2. Nonadiabatic Theory of Redistribution in Strong Fields

(a) Collisional Redistribution of Resonant Radiation (F. H. Mies)

Close-coupling codes developed for scattering in the presence of radiation fields can be used to calculate the pressure broadening and collisional depolarization of the Sr resonance transition in both the weak field and the strong field limit,



As we increase the Rabi frequency Ω_{L} and decrease the detuning Δ_{L} of the incident laser three observable properties associated with optical collision processes are obtained from such calculations, 1) Impact Limit Lineshapes. As $\Delta_{\text{L}} \rightarrow 0$ we can demonstrate that proper pressure broadened half widths, which include both elastic and inelastic collisional effects, can be rigorously extracted from close-coupled radiative scattering matrix element. The first manifestations of a.c. Stark shifts associated with the dressing of fragments by the radiation field are extracted from the numerical results, and confirm the anticipated power broadening of the Lorentzian absorption profile. This suggests that normal perturbation theory as applied to radiative interactions must be carefully scrutinized. 2) Inelastic transitions involving dressed atomic states. As Ω_{L} increases and eventually exceeds Δ_{L} the asymptotic Sr atomic states become dressed. Our fully quantal inelastic cross-sections can be used to calculate population redistribution rates in the presence of intense fields. 3) Collisional redistribution spectra in saturating fields. In strong fields we obtain the redistribution spectra for $h\nu_{\text{R}}$ in the impact limit and find the typical three-peaked Mollow lineshape due to fluorescence between dressed atomic states. Both the half-width and the polarization of the emission peaks are calculated.

(b) Analysis of Multiphoton Lineshape Theory in Intense Fields (F. H. Mies and A. Ben-Reuven)

The theory of line broadening, collisional redistribution and collision-induced multiphoton phenomena is an interdisciplinary area of research. Particularly when adding the new ingredient of strong laser fields and the resultant non-linear effects induced by saturation of resonant transitions, the analysis of such phenomena requires the integration of several diverse fields of research.

Two complementary theoretical approaches are used to describe these phenomena. The first is represented by our "optical collision" approach here at NBS where we calculate the radiative scattering matrix elements for atom-atom scattering in the presence of intense monochromatic laser fields. The calculations incorporate many subtle and sophisticated non-adiabatic and inelastic effects which are often neglected in conventional lineshape theory. However, these data that we generate must then be incorporated into very

subtle and complicated theoretical expressions for the density matrix of the interacting molecules in the field of the pumping laser fields. Only then do our calculations yield the proper description of the redistributed radiation.

The second theoretical approach, is exemplified by the unique and outstanding theoretical approach developed by Professor Ben-Reuven at Tel Aviv University. The redistribution of radiation is expressed in terms of a tetradic formalism using a Liouvillian analysis of the molecular density matrix in the presence of collisions. Fortunately, the formal ingredients of this sophisticated theory are the very scattering matrix elements that are generated by our optical collision approach.

We have begun a collaboration with Professor Ben-Reuven to explore the relationship between the tetradic description of redistribution and the close-coupled theory of scattering in strong multiphoton fields. So far we have succeeded in showing the explicit relationships required to analyze resonance fluorescence and resonant Raman lineshapes.

3. Future Plans

Our long range plans in the radiative scattering program require extensive code development combined with a careful theoretical analysis of strong field effects and multiphoton effects in the presence of collisions. In the immediate future we intend to complete the calculation of the pressure-broadening Mollow lineshape for Sr + Ar. At the completion of this relatively simple, near-resonant one-photon study we intend to explore the application of our close-coupled codes to multiphoton phenomena in strongly resonant laser fields with hopes of calculating collisional effects in four-wave mixing (PIERS-4) in Na. This will be studied in collaboration with A. Ben-Reuven at Tel Aviv University using his tetradic analysis of lineshapes.

E. Atomic and Molecular Scattering Theory

1. Half-Collision Amplitudes

(a) Analysis of Exact Close-Coupled Codes (F. H. Mies)

We have previously used a multichannel quantum defect analysis (MCQDA) of exact close-coupled radiative matrix elements to show that these can often be factored as follows:

$$S_{fi}^{\text{rad}} = N_{ff'}^- S_{f'i'}^{\text{BO}} N_{i'i}^+$$

where the 'incoming' half-collision matrix $N_{i,i}^+$ tracks the non-adiabatic scattering of the incident collision complex, and $N_{ff'}^-$ summarizes the inelastic behavior of the 'outgoing', radiatively excited collision complex.

We have speculated on the unitarity of these matrices which would justify the persistent use of the pure adiabatic Born-Oppenheimer matrix element $S_{f,i}^{BO}$, in evaluating total radiative cross-sections for continuum transitions. Based on a convincing but admittedly indirect numerical analysis of several previous studies we have been very confident in advancing the merits of this approximation. We have now modified our exact close-coupled codes to extract the exact half collision amplitudes without any commitment to unitarity. This new general capability of obtaining N^+ and N^- directly from close-coupled codes will enjoy a wide range of applicability in continuum spectroscopy and allow us to judge the validity of the unitarity condition.

(b) Multichannel Semiclassical Half Collision Amplitudes
(F. H. Mies and Y. Band)

In addition to solving the close-coupled equations exactly, we have developed a new simplified numerical procedures designed to obtain the half collision amplitude whenever the non-adiabatic couplings are restricted to classically accessible regions and the unitarity of N^+ is insured. This is equivalent to solving a set of coupled semiclassical equations. We begin by choosing a set of diagonal reference potentials tailored to the nature of the exact interaction matrix. These are used to generate a set of elastically scattered WKB reference wavefunctions. Two obvious choices that we have explored in some detail are either pure diabatic, or pure adiabatic reference potentials, although in any given situation the 'preferred' choice is usually self evident. By using a random phase approximation to neglect quickly oscillating contributions to the close coupled equations we can develop a set of first order differential equations for the half collision amplitudes which are perfectly unitary, and, in appropriate and well understood circumstances, reproduce the exact close-coupled amplitudes. This multichannel semiclassical approximation is presently being applied to a number of interest situations, including multichannel curve crossings, and asymptotic frame transformation among fine-structure states.

2. Multichannel Photodissociation Amplitudes
(P. S. Julienne)

The expansion of our multichannel close-coupling codes to calculate photodissociation cross-section is nearly complete. This gives very stable procedures for evaluating bound-continuum transitions, including all possible subtleties associated with non-adiabatic effects in molecular dissociation. A renormalized Numerov algorithm has been incorporated into the codes for the calculation of the usual continuum-continuum S-matrix elements needed for collisional problems, but more specifically for calculation of bound-continuum transition matrix elements needed for photodissociation. This algorithm is still being tested. In particular the code is designed to calculate the final state distribution of the photofragments. Ultimately these exact matrix elements can be compared to the predictions of our half collision amplitudes based on MCQDA.

3. Future Plans

Our first priority is to complete the development of the non-adiabatic photodissociation codes. The implementation of the photodissociation (and closely associated predissociation) codes will be stimulated by forthcoming studies of the Schumann-Runge predissociation of O_2 in collaboration with L. Vahala at Old Dominion University. The half collision amplitude studies will be continued and applied to an analysis of fine-structure distributions in both continuum-continuum and bound-continuum transitions. Using our new semiclassical algorithm we intend to examine its application to polyatomic curve-crossing phenomena in collaboration with Y. Ban at Ben-Gurion University. In addition, we will continue to pursue our NCQDA studies of molecular dissociation in conjunction with Professor S-h. Pan from the Chinese Academy of Science in Beijing who will be spending a year with us at NBS. In particular we will analyse the charge transfer states of alkali-halide molecules.

5. PUBLICATIONS

(a) Publications of Past Year

- Basch, H., Krauss, M., and Stevens, W. J., "Cation Binding Effect on H-Bonding," *J. Am. Chem. Soc.* 107, 7267 (1985).
- Basch, H., Krauss, M., Stevens, W. J., and Cohen, D., "Electronic and Geometric Structures of $\text{Pt}(\text{NH}_3)_2^{2+}$, $\text{Pt}(\text{NH}_2)_3\text{Cl}_2$, $\text{Pt}(\text{NH}_3)_3\text{X}$ and $\text{Pt}(\text{NH}_3)_2\text{XY}$ (X,Y = H_2O ,OH)," *J. Inorg. Chem.* 24, 3313 (1985).
- Basch, H., Krauss, M., Stevens, W. J., and Cohen, D., "Binding of $\text{Pt}(\text{NH}_3)_2^{2+}$ to Nucleic Acid Bases," *J. Inorg. Chem.* 25, 684 (1986).
- Bodaness, R. S. and King, D. S., "The Two-Photon Induced Fluorescence of the Tumor Localizing Photosensitizer Hematoporphyrin Derivative via 1064nm Photons from a 20ns Q-switched Nd-YAG Laser," *Biochem. and Biophys. Research Commun.* 126, 346 (1985).
- Casassa, M. P., Heilweil, E. J., Stephenson, J. C., and Cavanagh, R. R., "Time-Resolved Measurements of Vibrational Relaxation at Surfaces," *J. Electron. Spec.*, 38, 257 (1986).
- Casassa, M. P., Heilweil, E. J., Stephenson, J. C., and Cavanagh, R. R., "Time-Resolved Measurements of OH($\nu=1$) Vibrational Relaxation on SiO_2 Surface: Isotope and Temperature Dependence," *J. Chem. Phys.*, 84, 2361 (1986).
- Casassa, M. P., Stephenson, J. C., and King, D. S., "Vibrational Predissociation of Nitric Oxide Dimer: Total Energy Distribution in the Fragments," *J. Chem. Phys.*, 86, 2333 (1986).
- Chackerian, C., Jr., Bus, E. S., Olson, W. B., and Guelachvili, G., "Determination of $A_0 - B_0$ of CH_3D from Perturbation-Allowed Transitions," *J. Mol. Spectrosc.*, 117, 355-360 (1986).
- Dang-Nhu, M. and Pine, A. S., "Intensities des Raies d'Absorption dans la Bande Chaude $\nu_8 + \nu_{11} - \nu_{11}$ de l'Allene," *Can. J. Phys.* 64, 289-296 (1986).
- Fraser, G. T., Nelson, D. D., Jr., Peterson, K. I., and Klemperer, W., "The Rotational Spectra of $\text{NH}_3\text{-CO}$ and $\text{NH}_3\text{-N}_2$ ", *The Journal of Chemical Physics*, 84, 2472 (1986).
- Fraser, G. T., Nelson, D. D., Jr., Gerfen, G. J., and Klemperer, W., "The Rotational Spectrum, Barrier to Internal Rotation, and Structure of $\text{NH}_3\text{-N}_2\text{O}$," *The Journal of Chemical Physics*, 83, 5442, (1985).
- Fraser, G. T. and Coy, S. L., "Absorber Speed Dependence of the Coherence Relaxation Rate of the $J=0-1$ Transition of N_2O ," *The Journal of Chemical Physics*, 83, 5687 (1985).

- Fraser, G. T., Lovas, F. J., Suenram, R. D., Nelson, D. D., Jr., and Klemperer, "Rotational Spectrum and Structure of $\text{CF}_3\text{H-NH}_3$," *The Journal of Chemical Physics*, 84, 5983 (1986).
- Heilweil, E. J., Casassa, M. P., Cavanagh, R. R., and Stephenson, J. C., "Time-Resolved Vibrational Energy Relaxation of Surface Adsorbates," *J. Vac. Sci. Technol.* B3, 1471 (1985).
- Heilweil, E. J., Casassa, M. P., Cavanagh, R. R., and Stephenson, J. C., "Vibrational Energy Decay of Surface Adsorbates," *Proceedings of Time-Resolved Vibrational Spectroscopy Conference* (Springer-Verlag: *Proceedings in Physics*, A. Laubereau and M. Stockburger, eds., Vol. 4, pg. 71, 1985).
- Hillman, J. J., Jennings, D. E., Olson, W. B., and Goldman, A., "High Resolution Infrared Spectrum of Hydrogen Peroxide: The ν_6 Fundamental Band," *J. Mol. Spectrosc.*, 117, 46-59 (1986).
- Hougen, J. T., "A Generalized Internal Axis Method for High Barrier Tunneling Problems, as Applied to the Water Dimer," *J. Mol. Spectrosc.*, 114, 395-426 (1985).
- Hougen, J. T., "Symmetry beyond Point Groups in Molecular Spectroscopy," *J. Phys. Chem.* 90, 562-568 (1986).
- Howard, B. J. and Pine, A. S., "Rotational Predissociation and Libration in the Infrared Spectrum of Ar-HCl ," *Chem. Phys. Lett.* 112, 1-8 (1986).
- Jacox, M. E., "Comparison of the Ground-State Vibrational Fundamentals of Diatomic Molecules in the Gas Phase and in Inert Solid Matrices," *J. Mol. Spectrosc.*, 113, 286 (1985).
- Jacox, M. E., "Reaction of F Atoms with the Methyl Halides. Vibrational Spectra of CH_3XF and of $\text{H}_2\text{CX-HF}$ Trapped in Solid Argon," *J. Chem. Phys.* 83, 3255 (1985).
- Jasien, P. G. and Stevens, W. J., "Ab Initio Study of the Hydrogen Bonding Interactions of Formamide with Water and Methanol," *J. Chem. Phys.* 84, 3271 (1986).
- Jasien, P. G. and Stevens, W. J., "Calculated Proton Affinities for Some Molecules Containing Group VIA Atoms," *J. Chem. Phys.* 83, 2984 (1985).
- Jennings, D. E., Weber, A., and Brault, J. W., "Raman Spectroscopy of Gases with a Fourier Transform Spectrometer: The Spectrum of D_2 ," *Appl. Opt.* 25, 284 (1986).
- Julienne, P. S. and Mies, F. H., "Analytic Multichannel Theory of Molecular Dissociation," in *Electron and Atomic Collisions*, ed. D. C. Lorents, W. E. Meyerhof, and J. R. Petersen (North Holland, Amsterdam, 1986), p. 725.

- Karpas, Z., Stevens, W. J., Buckley, T. J., and Metz, R., "Proton Affinity and Gas-phase Ion Chemistry of Methyl Isocyanate, Methyl Isothiocyanate, and Methyl Thiocyanate," *J. Phys. Chem.* 89, 5274 (1985).
- Krauss, M., Stevens, W. J., and Basch, H., "Relativistic Effective Potential SCF Calculations of AgH and AuH," *J. Comp. Chem.* 6, 287 (1985).
- Lovas, F. J., "Recommended Rest Frequencies for Observed Intersellar Molecular Microwave Transitions - 1985 Revision," *J. Phys. Chem. Ref. Data*, 15, 251-303 (1986).
- Maki, A. G., Wells, J. S., and Hinz, A., "Heterodyne Frequency Measurements on the 12°0-00°0 Band of OCS," *Int. Journal of Infrared and Millimeter Waves*, 7, 909-917 (1986).
- Mantell, D. A., Cavanagh, R. R., and King, D. S., "Internal States and Distributions of NO Thermally Desorbed from Pt(111): Dependence on Coverage and Co-Adsorbed CO," *J. Chem. Phys.* 84, 5131 (1986).
- Mialocq, J.-C. and Stephenson, J. C., "Picosecond Laser Study of the Collisionless Photodissociation of Dimethylnitramine at 266 nm," *Chem. Phys. Lett.* 123, 390 (1986).
- Mialocq, J.-C. and Stephenson, J. C., "Picosecond Laser Induced Fluorescence Study of the Collisionless Photodissociation of Nitrocompounds at 266 nm," *Chem. Phys.* (1986).
- Miller, K. J., Taylor, E. R., Basch, H., Krauss, M., and Stevens, W. J., "A Theoretical Model for the Binding of Cis-Pt(NH₃)₂²⁺ to DNA," *J. Bio. Struct. Dynam.* 2, 1157 (1985).
- Nelson, D. D., Jr., Fraser, G. T., and Klemperer, W., "Ammonia Dimer: A Surprising Structure," *The Journal of Chemical Physics*, 83, 6201 (1985).
- Ohashi, N., Lafferty, W. J., and Olson, W. B., "Fourier Transform Spectrum of the Torsional Band of Hydrazine," *J. Mol. Spectrosc.*, 117, 119-133 (1986).
- Perry, J. W., Woodward, A. M., and Stephenson, J. C., "Picosecond Coherent Anti-Stokes Raman Scattering (CARS) Study of Vibrational Dephasing of Carbon Disulfide and Benzene in Solution," *SPIE Proceedings* 620, (1986).
- Pine, A. S. and Howard, B. J., "Hydrogen-Bond Energies of the HF and HCl Dimers from Absolute Infrared Intensities," *J. Chem. Phys.* 84, 590-596 (1986).
- Rosenkrantz, M. E. and Krauss, M., "Damped Dispersion Interaction Energies for He-H₂, Ne-H₂, and Ar-H₂," *Phys. Rev.* A32, 1402 (1985).

- Suenram, R. D., Lovas, F. J., and Pickett, H. M., "The Microwave Spectrum and Molecular Conformation of Peroxynitric Acid (HOONO_2)," *J. Mol. Spectrosc.*, 116, 406-421 (1986).
- Suenram, R. D., Lovas, F. J., and Pickett, H. M., "Fluoromethanol: Synthesis, Microwave Spectrum and Dipole Moment," *J. Mol. Spectrosc.* 119, (1986).
- Thompson, G. A., Maki, A. G., and Weber, A., "Infrared Tunable Diode Laser Spectroscopy of the $\Delta v = 2$ Band of $^7\text{Li}^{127}\text{I}$," *J. of Mol. Spectrosc.* 118, 540-543 (1986).
- Thompson, G. A., Maki, A. G., and Weber, A., "The Infrared Spectrum of GeO ," *J. Mol. Spectrosc.*, 116, 136-142 (1986).
- Thompson, G. A., Maki, A. G., and Weber, A., "Infrared Spectrum of LiI ," *J. Mol. Spectrosc.*, 118, (1986).
- Weber, A. (ed.), "Technical Activities 1985 - Molecular Spectroscopy Division," NBSIR 86-3313 (1986).
- Wofford, B. A., Bevan, J. W., Olson, W. B., and Lafferty, W. J., "Rovibrational Analysis of ν_3 $\text{HCN} \cdots \text{HF}$ Using Fourier Transform Spectroscopy," *J. Mol. Spectrosc.*, 83, 6188-6192 (1985).
- Wofford, B. A., Bevan, J. W., Olson, W. B., and Lafferty, W. J., "Rovibrational Analysis and Vibrational Predissociation in the ν_2 Band of HCN Dimer," *J. Chem. Phys.* 85, 105-108 (1986).
- Wofford, B. A., Jackson, M. W., Bevan, J. W., Olson, W. B., and Lafferty, W. J., "Rovibrational Analysis of an Intermolecular Hydrogen-bonded Vibration: The ν_1^1 Band of $\text{HCN} \cdots \text{HF}$," *J. Chem. Phys.* 84, 6115-6118 (1986).
- Vahala, L. L., Julienne, P. S., and Havey, M. D., "Nonadiabatic Theory of Fine Structure Branching Cross-Sections for NaHe , NaNe , and NaAr Optical Collisions," *Phys. Rev. A* 34, 1856 (1986).

(b) Publications in Progress

- Basch, H., Krauss, M., and Stevens, W. J., "Cation Binding Effect on Imidazole Tautomerism, Intern. J. Quant. Chem. (in press).
- Bodaness, R. S., Heller, D. F., Krasinski, J., and King, D. S., "Two-photon Laser-Induced Fluorescence of the Tumor Localizing Photosensitizer Hematoporphyrin Derivative: Resonance Exchanged 750nm Two-photon Excitation into the Near UV-Soret Band," J. Biol. Chem. (in press).
- Burgess, D., Jr., King, D. S., and Cavanagh, R. R., "Kinetics and Dynamics of the Ammonia/Nitric Oxide Coadsorbate System on Pt(111)," in preparation for submission to Surface Science.
- Burgess, D., Jr., Mantell, D. A., Cavanagh, R. R., and King, D. S., "Dynamics of the Laser-induced Thermal Desorption of Nitric Oxide from a Platinum Foil," J. Chem. Phys. (in press).
- Burkholder, J. B., Hammer, P. D., Howard, C. J., Maki, A. G., Thompson, G. A., and Chackerian, C., Jr., "Infrared Frequency and Intensity Measurements of the ClO Radical," (manuscript in preparation).
- Casassa, M. P., Stephenson, J. C., and King, D. S., "Vibrational Predissociation of the Nitric Oxide Dimer," Faraday Discuss. Chem. Soc. 82, (1986) (in press).
- Casassa, M. P., Stephenson, J. C., and King, D. S., "Picosecond Measurements of the Dissociation Rates of the Nitric Oxide Dimer $\nu_1(\nu=1)$ and $\nu_4(\nu=1)$ Levels," J. Chem. Phys. (submitted).
- Fraser, G. T., and Pine, A. S., "Van der Waals Potentials from the Infrared Spectra of Rare Gas-HF Complexes," The Journal of Chemical Physics, (in press).
- Fraser, G. T., Suenram, R. D., and Lovas, F. J., "Nearly Free Internal Rotation in Ar-CH₃Cl," The Journal of Chemical Physics (in press).
- Heilweil, E. J., Casassa, M. P., Cavanagh, R. R., and Stephenson, J. C., "Population Lifetimes of OH($\nu=1$) and OD($\nu=1$) Stretching Vibrations of Alcohols and Silanols in Dilute Solution," J. Chem. Phys., (in press).
- Heilweil, E. J., "Vibrational Population Lifetimes of OH($\nu=1$) in Natural Crystalline Micas" Chem. Phys. Letters (in press).
- Hinz, A., Wells, J. S., and Maki, A. G., "Heterodyne Frequency Measurements on the Nitric Oxide Fundamental Band," J. Mol. Spectrosc. (submitted).
- Hinz, A., Wells, J. S., and Maki, A. G., "Heterodyne Measurements of Hot Bands and Isotopic Transitions of N₂O Near 7.8 μ m," Zeitschrift fur Physik D, (submitted).

- Hougen, J. T., "Hydrogen Migration Tunneling Effects in the Rotational and Vibrational Spectrum of Protonated Acetylene $C_2H_3^+$," J. Mol. Spectrosc. (submitted).
- Jackson, M. W., Wofford, B. A., Bevan, J. W., Olson, W. B., and Lafferty, W. J., "Infrared Spectrum of the Overtone Band $2\nu_{50}$ in the Hydrogen Bonded Complex HCN-HF," J. Chem. Phys. (in press).
- Jackson, M. W., Wofford, B. A., Bevan, J. W., Olson, W. B., and Lafferty, W. J., "Rovibrational Analysis of the C-H stretching Band and its Overtone in the Hydrogen-bonded Heterodimer HCN--HF," J. Chem. Phys. (in press).
- Jacox, M. E., "Comparison of the Electronic Energy Levels of Diatomic Molecules in the Gas Phase and in Inert Solid Matrices," J. Mol. Struct. (in press).
- Jasien, P. G., Stevens, W. J., and Krauss, M., "Ab Initio Calculations of the Rotational Barriers in Formamide and Acetamide: The Effects of Polarization Functions and Correlation," J. Mol. Struct. Theochem. (in press).
- Jasien, P. G. and Stevens, W. J., "Theoretical Studies of Potential Gas-phase Charge Transfer Complexes: $NH_3 + HX$ ($X = Cl, Br, I$)," Chem. Phys. Letters (in press).
- Jennings, D. E., Weber, A., and Brault, J. W., "FTS-Raman Flame Spectroscopy of High-J Lines in H_2 and D_2 ," (submitted).
- Julienne, P. S. and Mies, F. H., "Nonadiabatic Theory of Atomic Line Broadening: Redistribution Calculations for $Sr('P \leftarrow 'S) + Ar$," Phys. Rev. A (in press).
- Julienne, P. S. and Vahala, L. L., "Close Coupled Theory of Fine Structure Transitions in Collisional Redistribution," in Spectral Lineshapes, Vol. 4, ed., by R. Exton (in press).
- Lafferty, W. J. and Olson, W. B., "The High Resolution Infrared Spectra of the ν_2 and ν_3 Bands of HOCl," J. Mol. Spectrosc. (in press).
- Lafferty, W. J., Suenram, R. D., and Lovas, F. J., "The Microwave Spectra of the $(HF)_2$, $(DF)_2$, HFDF and DFHF Hydrogen Bonded Complexes," J. Mol. Spectrosc. (in press).
- Lindsay, D. M., Thompson, G. A., and Wang, Y., "ESR Spectra of $Cu_3(^2A_1)$ in an N_2 Matrix, J. Phys. Chem., (in press).
- Lovas, F. J., Suenram, R. D., Ross, S., and Klobukowski, M., "Rotational Structural Ab Initio and Semirigid Bender Analysis of the Millimeter Wave Spectrum of H_2CO-HF ," J. Mol. Spectrosc. (in press).
- Lovas, F. J. and Suenram, R. D., "Design and Operation of a Pulsed Beam Fourier Transform Microwave Spectrometer, Measurements on OCS and Rare Gas-OCS Complexes," J. Chem. Phys. (in press).

- Maki, A. G., "High Resolution Measurements of the ν_2 Band of HNO_3 and the ν_3 Band of trans-HONO," (submitted).
- Mies, F. H., Julienne, P. S., Band, Y. B., and Singer, S. J., "A Converged Analysis of Radiative Matrix Elements," J. Phys. B., (in press).
- Monten, K. M., Walmsky, C. M., Henkel, C., Wilson, T. L., Snyder, L. E., Hollis, J. M., and Lovas, F. J., "Torsionally Excited Methanol in Hot Molecular Cloud Cores," Astron. Astrophys. (in press).
- Nelson, D. D., Jr., Fraser, G. T., Peterson, K. I., Zhao, K., Klemperer, W., Lovas, F. J., and Suenram, R. D., "The Microwave Spectrum of the $K=0$ States of Ar- NH_3 ," The Journal of Chemical Physics (submitted).
- Ohashi, N. and Hougen, J. T., "The Torsional-Wagging Tunneling Problem and the Torsional-Wagging-Rotational Problem in Methylamine," J. Mol. Spectrosc. (in press).
- Olson, W. B., Hunt, R. A., Maki, A. G., and Brault, J. W., "Hydrogen Peroxide: Rotational Constants of the Ground State and the Lowest Torsional Component of the First Excited Torsional State," (submitted).
- Pine, A. S. and Looney, J. P., " N_2 - and Air-Broadening in the Fundamental Bands of HF and HCl," J. Mol. Spectrosc. (in press).
- Schaeffer, R. D., Lovejoy, R. W., Olson, W. B., and Tarrago, G., "High Resolution Spectrum of $^{28}\text{SiH}_3\text{D}$ from 1450 to 1710 cm^{-1} ," (submitted).
- Suenram, R. D. and Lovas, F. J., "The Microwave Spectrum and Structure of the Argon --- Acrylonitrile van der Waals Complex," (submitted).
- Thompson, G. A., Olson, W. B., Maki, A. G., and Weber, A., "Fourier Transform Infrared Spectrum of the Fundamental Band of LiCl at 830°C," (submitted).
- Wofford, B. A., Bevan, J. W., Olson, W. B., and Lafferty, W. J., "Rovibrational Analysis of the ν_5 Vibrational Band in the HCN-HF Hydrogen Bonded Cluster," (submitted).

6. TALKS

- Casassa, M. P., "Picosecond Measurements of Vibrational Relaxation of Chemisorbed Molecules," Laser Users Group Seminar, NBS, February 1986.
- Casassa, M. P., "Time- and State-Resolved Studies of van der Waals Molecule Predissociation," Gordon Conference, August 1986.
- Casassa, M. P., "Picosecond Measurements of Vibrational Predissociation of van der Waals Dimers," Symposium on Clusters and Cluster Ions, Baltimore, MD, September 1986.
- Casassa, M. P., "Picosecond Studies of van der Waals Molecule Vibrational Predissociation," Surface Science Lunch Bunch Seminar, NBS, September 1986.
- Casassa, M. P., "Picosecond Studies of Vibrational Predissociation in van der Waals Molecules," Symposium on State-to-state Chemistry, ACS National Meeting, Anaheim, CA, September 1986.
- Fraser, G. T., "van der Waals Potentials from the Infrared Spectra of Rare Gas-HF Complexes," 41st Symposium on Molecular Spectroscopy, Columbus, OH, June 1986.
- Fraser, G. T., "Rotational Spectrum, Internal Rotation, and Structure of Ar-CH₃Cl," 41st Symposium on Molecular Spectroscopy, Columbus, OH, June 1986.
- Fraser, G. T., "van der Waals Potentials from the Infrared Spectra of Rare-Gas-HF Complexes," 41st Symposium on Molecular Spectroscopy, Columbus, OH, June 1986.
- Fraser, G. T., "Infrared and Microwave Spectroscopy of Weakly Bound Complexes," 20th Mid-Atlantic Regional Meeting of the American Chemical Society, Symposium on Clusters and Clusters Ions, Baltimore, MD, September 1986.
- Fraser, G. T., "Nearly Free Internal Rotation in Ar-CH₃Cl," NATO-Advanced Research Workshop on Structure and Dynamics of Weakly Bound Molecular Complexes, Maratea, Italy, September 1986.
- Fraser, G. T., "Rotational Spectrum and Structure of CF₃H-NH₃," NATO-Advanced Research Workshop on Structure and Dynamics of Weakly Bound Molecular Complexes, Maratea, Italy, September 1986.
- Heilweil, E. J., "Picosecond Vibrational Dynamics of Hydroxyl Groups in Condensed Phase Systems," National Institutes of Health, January 1986.
- Heilweil, E. J., "Picosecond Vibrational Dynamics of Hydroxyl Groups in Condensed Phase Systems," Chemistry Department, Physical Chemistry Seminar, University of Illinois, Urbana, IL, February 1986.

- Heilweil, E. J., "Population Lifetimes of OH(v=1) and OD(v=1) Vibrations in Alcohols, Silanols and Crystalline Micaceous," Ultrafast Phenomena Conference, Snowmass, CO, June 1986.
- Heilweil, E. J., "Picosecond Vibrational Dynamics of Hydroxyl Groups in Condensed Phase Systems," Gordon Conference on Vibrational Spectroscopy, Wolfeboro, NH, August 1986.
- Hougen, J. T., "Symmetry Beyond Point Groups in Molecular Spectroscopy," Duke University, Durham, NC, November 1985.
- Hougen, J. T., "Hydrogen Migration Tunneling Effects in the Rotational and Vibrational Spectrum of Protonated Acetylene," University of California at Irvine, March 1986.
- Hougen, J. T., "Overview of Molecular Spectroscopy at NBS," Jet Propulsion Laboratories, Pasadena, CA, March 1986.
- Hougen, J. T., "Hydrogen Migration Tunneling Effects in the Rotational and Vibrational Spectrum of Protonated Acetylene," NBS, Boulder, CO, March 1986.
- Hougen, J. T., "Hydrogen Migration Tunneling Effects in the Rotational and Vibrational Spectrum of Protonated Acetylene, $C_2H_3^+$," 41st Symposium on Molecular Spectroscopy, Ohio State University, Columbus, OH, June 1986.
- Hougen, J. T., "Far-Infrared Spectrum of Methylamine and the Group Theoretical Treatment of Its Large Amplitude Motions," 41st Symposium on Molecular Spectroscopy, Ohio State University, Columbus, OH, June 1986.
- Hougen, J. T., "Hydrogen Migration Tunneling Effects in the Rotational and Vibrational Spectrum of Protonated Acetylene, $C_2H_3^+$," 9th International Conference on High Resolution Infrared Spectroscopy, Liblice (near Prague), Czechoslovakia, September 1986.
- Hougen, J. T., "The Role of Tunneling Models in Analyzing High-Resolution Spectra of Weakly Bound Molecular Complexes," NATO-Advanced Research Workshop on Structure and Dynamics of Weakly Bound Molecular Complexes, Maratea, Italy, September 1986.
- Jacox, M. E., "Vibrational Spectra of Free Radicals Formed by the Reaction of F Atoms with Small Molecules," Department of Chemistry, Bryn Mawr College, Bryn Mawr, PA, November 1985.
- Jacox, M. E., "Vibrational Spectra of Free Radicals Formed by the Reaction of F Atoms with Small Molecules," AT & T Bell Laboratories, Murray Hill, NJ, December 1985.
- Jacox, M. E., "Vibrational Spectra of Free Radicals Formed by the Reaction of F Atoms with Small Molecules," Delaware Valley Section, Society for Applied Spectroscopy, Philadelphia, PA, February 1986.
- Jacox, M. E., "Vibrational Spectra of Free Radicals Formed by the Reaction of F Atoms with Small Molecules," Department of Chemistry, University of Colorado, Boulder, CO, February 1986.

- Jacox, M. E., "Matrix Isolation Spectroscopic Studies of the Reaction of F Atoms with Small Molecules," Symposium on Matrix Isolated Species, Central Regional American Chemical Society Meeting, Bowling Green, OH, June 1986.
- Jacox, M. E., "Spectroscopy of Free Radicals Formed in the Early Stages of Nitramine Decomposition," U.S. Army Research Office Workshop on Combustion Probes for the Solid Nitramines, Combustion Research Facility, Sandia National Laboratory, Livermore, CA, June 1986.
- Jacox, M. E., "Comparison of the Electronic Energy Levels of Diatomic Molecules in the Gas Phase and in Inert Solid Matrices," 41st Symposium on Molecular Spectroscopy, Columbus, OH, June 1986.
- Jacox, M. E., "The $A\ ^2\Pi - X\ ^2\Sigma^+$ Near Infrared Absorption Spectrum of HC_2 Isolated in Solid Argon," 41st Symposium on Molecular Spectroscopy, Columbus, OH, June 1986.
- Julienne, P. S., "Close Coupled Theory of Fine Structure Transitions in Collisional Redistribution," 8th International Conference on Spectral Line Shapes, College of William and Mary, Williamsburg, VA, June 1986.
- Julienne, P. S., "Close Coupled Theory and Analytic Models for Collisional Redistribution," Department of Atomic Physics, University of Newcastle, Newcastle-upon-Tyne, England, July 1986.
- Julienne, P. S., "Close Coupled Calculations on Laser Assisted Collisions," Max Planck Institute for Quantum Optics, Garching, West Germany, July 1986.
- Julienne, P. S., "Scattering Theory of Photoassisted Collisions: Application to Alkali and Alkaline Earth Atoms Colliding with Rare Gas Atoms," and "Half Collision Analysis of Photoassisted Collisions: Development of Physical Insight," Department of Physics, University of Kaiserslautern, Kaiserslautern, West Germany, August 1986.
- Julienne, P. S., "Close Coupling Calculations of Atomic Line Profiles and Collisional Redistribution for 1P and 2P Transitions," Observatoire de Paris, Meudon, France, September 1986.
- King, D. S., "Molecule-Surface Dynamics," Rice University, Department of Chemistry and Rice Quantum Institute, Rice University, Houston, TX, November 1985.
- King, D. S., "Two-Photon Excitations of the Tumor-Localizing Photosensitizer HPD," International Laser Science Conference, Dallas, TX, November 1985.
- King, D. S., "Dynamics of the Molecular-Surface Interaction," JILA Symposium, Boulder, CO, March 1986.

- King, D. S., "Thermal and Laser-Induced Desorption Dynamics," Cornell University, Department of Chemistry, Cornell University, Ithaca, NY, March 1986.
- King, D. S., "Dynamics of the Photodissociation of van der Waals Dimers," Virginia Commonwealth University, Chemistry Department, Richmond, VA, March 1986.
- King, D. S., "Vibrational Predissociation of NO-containing van der Waals Dimers," ACS Symposium on Dynamics of Clusters, National Meeting, NY, April 1986.
- King, D. S., "Photodissociation of van der Waals Dimers," Brookhaven National Laboratory, Chemistry Department, Long Island, NY, April 1986.
- King, D. S., "NO/Pt Interactions: Thermal- and Laser-Induced Desorption," IBM, Yorktown Heights, NY, April 1986.
- King, D. S., "Vibrational Predissociation Dynamics of the Nitric Oxide Dimer," NBS Staff Research Seminar Series, NBS-Gaithersburg, May 1986.
- King, D. S., "Dynamics of the Vibrational Predissociation of the Nitric Oxide Dimer," Mid-Atlantic Regional Meeting of ACS, Baltimore, MD, September 1986.
- King, D. S., "Vibrational Predissociation Dynamics of van der Waals Dimers," Faraday Soc. Disc. on Photodissociation Dynamics, Bristol, England, September 1986.
- King, D. S., "Vibrational Predissociation Dynamics of van der Waals Dimers," NATO-Advanced Research Workshop on Structure and Dynamics of Weakly Bound Molecular Complexes, Maratea, Italy, September 1986.
- Krauss, M., "Pt Binding to DNA," Chemistry Department, Drexel University, Philadelphia, PA, May 1986.
- Krauss, M., "Pt(NH₂R)₂ Binding to a tetramer Duplex of DNA," Meeting of the American Society of Biological Chemists, Washington, D.C., June 1986.
- Lafferty, W. J., "Sub-Doppler Resolution Infrared Spectroscopy of the Carbon Dioxide Dimer," Mid-Atlantic Regional Meeting of ACS, Baltimore, MD, September 1986.
- Lovas, F. J., "Microwave Spectrum and Properties of the Methanol-Formamide Complex," Mid-Atlantic Regional Meeting of ACS, Baltimore, MD, September 1986.
- Maki, A. G., "High Resolution Measurements and Analysis of the ν_2 , ν_3 , ν_4 , ν_5 , and $2\nu_9$ Bands of Nitric Acid," 41st Symposium on Molecular Spectroscopy, Ohio State University, Columbus, OH, June 1986.

- Maki, A. G., "New Infrared Frequency and Intensity Measurements on Chlorine Monoxide (ClO)," 41st Symposium on Molecular Spectroscopy, Ohio State University, Columbus, OH, June 1986.
- Mies, F. H., "Collisional Redistribution of Intense Laser Radiation," Department of Chemistry, Tel Aviv University, Tel Aviv, Israel, February 1986.
- Mies, F. H., "Collisional Redistribution of Intense Laser Radiation," Department of Chemical Physics, Weizmann Institute, Rehovot, Israel, February 1986.
- Mies, F. H., "Collisional Redistribution of Intense Laser Radiation," Department of Physics, Bar Ilan University, Ramat-Gan, Israel, March 1986.
- Mies, F. H., "Collisional Redistribution of Intense Laser Radiation," Department of Chemistry, Ben Gurion University, Beer Sheva, Israel, March 1986.
- Olson, W. B., "Experimental Values for the Rotational Constants of the OG and 1G Torsional Components of the Vibrational Ground State of H₂O₂, and the Matrix Element Coupling Them," 41st Symposium on Molecular Spectroscopy, Ohio State University, Columbus, OH, June 1986.
- Pine, A. S., "High-Resolution Infrared Spectroscopy of Hydrogen-Bonded and van der Waals Complexes," Department of Chemistry, Johns Hopkins University Baltimore, MD, November 1985.
- Pine, A. S., "High-Resolution Spectroscopy of van der Waals and Hydrogen-Bonded Complexes," NBS Staff Research Seminar, NBS Gaithersburg, MD, May 1986.
- Pine, A. S., "N₂ and Air Broadening in the Fundamental Bands of HF and HCl," 41st Symposium on Molecular Spectroscopy, Ohio State University, Columbus, OH, June 1986.
- Pine, A. S., "Vibrational Anomalies and Dynamic Coupling in Hydrogen-Bonded van der Waals Molecules," NATO-Advanced Research Workshop on Structure and Dynamics of Weakly Bound Molecular Complexes, Maratea, Italy, September 1986.
- Stephenson, J. C., "Picosecond Studies of Vibrational Energy Transfer: Surfaces, Solids, and Liquids," AFOSR Contractors Meeting, Dayton, OH, November 1985.
- Stephenson, J. C., "Picosecond Studies of Vibrational Energy Transfer: Surfaces, Solids, and Liquids," Department of Chemistry, University of Pittsburgh, PA, March 1986.
- Stephenson, J. C., "Picosecond Studies of Vibrational Energy Transfer: Surfaces, Solids, and Liquids," Department of Chemistry, Cornell University, April 1986.

- Stephenson, J. C., "Picosecond Studies of Vibrational Energy Transfer: Surfaces, Solids, and Liquids," Department of Chemistry, U. C. Berkeley, Berkeley, CA, June 1986.
- Stephenson, J. C., "Picosecond Studies of Vibrational Energy Transfer: Surfaces, Solids, and Liquids," International Quantum Electrons Conference, San Francisco, CA, June 1986.
- Suenram, R. D., "Rotational Spectra and Structural Determinations of Several van der Waals Complexes," Rice University, Department of Chemistry Colloquium, Houston, TX, March 1986.
- Suenram, R. D., "Rotational Spectra and Structural Determinations of Several van der Waals Complexes," 11th Annual Austin Symposium on Molecular Structure, Austin, TX, March 1986.
- Suenram, R. D., "Rotational Spectrum of the Hydrogen Bonded Formamide-Water Complex," Mid-Atlantic Regional Meeting of ACS, Baltimore, MD, September 1986.
- Suenram, R. D., "Structures of the Ar...Acrylonitrile and Ar...Formamide van der Waals Complexes," NATO-Advanced Research Workshop on Structure and Dynamics of Weakly Bound Molecular Complexes, Maratea, Italy, September 1986.
- Suenram, R. D., "Rotational Spectrum of the Hydrogen Bonded Formamide-Water and Formamide-Methanol Complexes," NATO-Advanced Research Workshop on Structure and Dynamics of Weakly Bound Molecular Complexes, Maratea, Italy, September 1986.
- Thompson, G. A., "Infrared Spectroscopy of High Temperature Diatomics," Rome Air Development Center, Griffisse Air Force Base, NY, May 1986.
- Thompson, G. A., "High Temperature Spectroscopy of Alkali Halides and Hydrides at High Temperature," Advanced Fuel Research, Inc., East Hartford, CT, May 1986.
- Thompson, G. A., "Infrared Spectroscopy of High Temperature Diatomics," Photometrics, Inc., Boston, MA, May 1986.
- Thompson, G. A., "High Resolution Infrared Spectroscopy of LiCl at 800°C," 41st Symposium on Molecular Spectroscopy, Ohio State University, Columbus, OH, June 1986.
- Weber, A., "Research in High Resolution Molecular Spectroscopy at NBS," ENEA, Centre Ricerche Energie Frascati, Frascati, Rome, Italy, September 1986.
- Weber, A., "Research in High Resolution Molecular Spectroscopy at NBS," Physics Department, University of Florence, Florence, Italy, September 1986.
- Weber, A., "Research at NBS in High Resolution Spectroscopy of Weakly Bound Molecular Complexes," Physics Department, University of Giessen, Giessen, Germany, October 1986.

7. MOLECULAR SPECTROSCOPY DIVISION SEMINARS

- Balasubramanian, K., Department of Chemistry, Arizona State University, Tempe, NJ, "Electronic Structure of Molecules Containing Heavy Atoms" May 1986.
- Ben-Reuven, A., School of Chemistry, Tel-Aviv University, Tel-Aviv, Israel, "New Challenges in the Study of Spectral Line Shapes," September 1986.
- Bevan, J., Chemistry Department, Texas A&M University, College Station, TX, "Dynamical Behavior in Linear Hydrogen-Bonded Interactions," November 1985.
- Beveridge, D., Department of Chemistry, Hunter College, New York, NY, "Aqueous Hydration of Biological Molecules: Free Energy Simulations," February 1986.
- Clough, S. A., Air Force Geophysics Laboratory, Hanscom AFB, MA, "Line Shapes and Molecular Collisional Broadenings with Applications to Atmospheric Problems," February 1986.
- Cook, M., Naval Research Laboratory, "Electronic Structure of the $\text{MoFe}_3\text{S}_4(\text{SH})_6^{3-}$ Ion: A Model for the Nitrogenase Active Site," October 1985.
- DeFrees, D., Molecular Research Institute, San Jose, CA, "Theoretical Studies of Interstellar Chemistry," November 1985.
- Fink, W. H., Chemistry Department, National Science Foundation, Washington, D.C., "Influence of External Potentials of H-Bonding," December 1985.
- Graner, G., Universite de Paris-Sud, Orsay, France, "Recent Work in Molecular Spectroscopy at Laboratoire d'Infrarouge," June 1986.
- Harris, D., Chemistry Department, University of California, Santa Barbara, CA, "Spectroscopy and Structure of MgOH : A Quasi-Linear Molecule," December 1985.
- Harrison, J., Chemistry Department, Michigan State University, East Lansing, MI, "Electronic and Geometric Structure of Transition Metal-Containing Cations," August 1986.
- Herman, R., Department of Physics, Penn State University, PA, "Velocity-changing Effects on Collisional Lineshapes," May 1986.
- Kok, R., University of Georgia, Athens, GA, "Molecular Mechanics and Ab Initio Calculations on Some Organic and Organo-metallic Compounds," October 1985.
- Konowalow, D. D., Ballistics Research Laboratory, Aberdeen, MD, "High Spin States of He_2 ," July 1986.

- Lester, W., Department of Chemistry, University of California, Berkeley, CA, "Quantum Monte Carlo of Electronic Structure," August 1986.
- Lisy, J., Chemistry Department, University of Illinois, IL, "Vibrational Predissociation Spectroscopy of Molecular Clusters," March 1986.
- Malvezzi, M., Gordon McKay Laboratory, Harvard University, MA, "Picosecond Laser Excitation, Melting, and Vaporization of Solid Surfaces," April 1986.
- Mautner, M., Chemical Kinetics Division, NBS, Gaithersburg, MD, "Cluster Ions and The Ionic Hydrogen-Bond," January 1986.
- Mialocq, J.-C., Centre d'Etudes Nucleaires de Saclay, Department de Physico-Chimie, France, "Ultrafast Molecular Dynamics Studied with Picosecond Lasers," June 1986.
- Miller, A. E. S., Department of Chemistry, Bryn Mawr College, Bryn Mawr, PA, "Electronic Structure of Transition-Metal Hydrides," March 1986.
- Mollendal, H., Universiteteti Oslo, Oslo, Norway, "Microwave Spectra of 1,4 defluoro -2-butyne and Several Molecules with Intra-molecular Hydrogen Bonds," March 1986.
- Osman, R., Department of Physiology and Biophysics, Mt. Sinai School of Medicine, New York, NY, "A New Mechanism of Action of Superoxide Dismutase," November 1985.
- Rappe, A. K., Department of Chemistry, Colorado State University, CO, "Studies on $2\pi + 2\pi$ Reactions: Allowed Reactions Involving Transition Metal Complexes," October 1985.
- Rosenkrantz, M., Ballistic Research Laboratory, Aberdeen, MD, "Application of Quantum Chemistry to Molecules of Atmospheric Interest," October 1985.
- Sandroff, C., AT & T Bell Communications, "Layered Semiconductor Colloids and Their Uses: Interfacial Science, Cluster Chemistry and New Solid Materials," December 1985.
- Saykally, R., Chemistry Department, University of California, Berkeley, CA, "Laser Spectroscopy of Molecular Ions and van der Waals Molecules," May 1986.
- Schrötter, H.-W., Sektion Physik, Universität München, West Germany, "High Resolution CARS and Inverse Raman Spectroscopy," August 1986.
- Scoles, G., Department of Chemistry, University of Waterloo, Waterloo, Canada, "Infrared Laser Molecular Beam Spectroscopy of Molecule-Noble Gas Clusters," April 1986.

Shapiro, M., Chemical Physics Department, Weizmann Institute of Science, Rehovot, Israel, "Coherent Control of Unimolecular Reactions," January 1986.

Shuker, R., Physics Department, Ben Gurion University of the Negev, Beer Sheva, Israel, "Laser Induced Cherenkov and Non-linear Effects in Sodium Vapor," June 1986.

Smalley, R., Chemistry Department, Rice University, Houston, TX, "New Results with Supersonic Cluster Beams," November 1985.

Sutter, D. H., Institut für Physikalische Chemie, Universität Kiel, Kiel, Olshausenstrasse, Germany, "Microwave Zeeman and Fourier Transform Studies at Kiel," February 1986.

Toennies, J. P., Max-Planck-Institut für Stromungsforschung, Göttingen, West Germany, "State Resolved Molecular Beam Scattering Experiments on Atom-molecule Inelastic Collisions," March 1986.

Vidal, C. R., Institut für Extraterrestrische Physik, Max-Planck-Institut für Physik und Astrophysik, Bayern, West Germany, "Laser Intracavity Absorption," April 1986.

Watts, R. O., The Australian National University, Canberra, Australia, "Molecular Structure and Dynamics from Molecular Beam Experiments," April 1986.

8. VISITING SCIENTISTS

The Molecular Spectroscopy Division has been host in the past year to the following scientists who have worked with NBS scientists on problems of mutual interest.

Adams, George, A., Ballistics Research Laboratory, works with M. Krauss on electronic structure codes for the chemistry and spectroscopy of large molecules.

Basch, Harold, Bar Ilan University, Israel, is engaged in research on metal interactions with biomolecules. He works with M. Krauss.

Bodaness, Robert S., National Institutes of Health, works with D. S. King on laser photosensitization processes in biological samples.

Craig, N., Oberlin College, works with W. J. Lafferty on the Fourier transform Infrared spectrum of 1,2-difluorethylene.

Fink, W. H., National Science Foundation, works with W. J. Stevens on the development of model potentials and their application to large molecules.

Gillies, C. W., Chemistry Department, Rensselaer Polytechnic Institute, works with F. J. Lovas and R. D. Suenram on pulsed beam Fourier transform microwave spectroscopy of hydrogen bonded molecules.

Hollis, Jan Michael, NASA/Goddard Space Flight Center, works with F. J. Lovas and R. Suenram on software development for automated microwave spectrometer and collaborates on astronomical studies.

Jennings, Donald E., NASA/Goddard Space Flight Center, works with A. Weber on a project to do Raman spectroscopy of gases with the Fourier transform spectrometer of the National Solar Observatory (Kitt Peak).

Konowalow, Daniel D., Professor at SUNY-Binghamton, New York, works with M. Krauss on studies of electronic structure of alkali and alkaline earth molecules.

Lengsfeld, Byron H., Ballistic Research Laboratory, works with M. Krauss on electronic structure codes for the chemistry and spectroscopy of large molecules.

Ohashi, Nobukimi, Kanazawa University, Physics Department, Japan, works with J. T. Hougen, W. J. Lafferty, and W. B. Olson on high resolution infrared spectroscopy and theory of methylamine.

Osman, R., Mt. Sinai School of Medicine, New York, works with W. J. Stevens on the application of ab initio quantum chemistry to biochemical modeling.

Sattler, Joseph L., Harry Diamond Laboratories, U.S. Army, collaborates with W. J. Lafferty and A. Maki on precise line frequency measurements in the infrared.

Vahala, Linda L., Physics Department, Old Dominion University, Norfolk, VA, works with P. S. Julienne on the theory of molecular line broadening and final state branching ratios for the resonance transitions of alkali atoms perturbed by rare gas collision partners.

Zozom, Jennifer, Chemistry Department, Rensselaer Polytechnic Institute works with Drs. F. J. Lovas and R. D. Suenram on pulsed beam Fourier transform microwave spectroscopy of hydrogen bonded molecules.

U.S. DEPT. OF COMM. BIBLIOGRAPHIC DATA SHEET (See instructions)		1. PUBLICATION OR REPORT NO. NBSIR 86-3483	2. Performing Organ. Report No.	3. Publication Date NOVEMBER 1986
4. TITLE AND SUBTITLE Technical Activities 1986 Molecular Spectroscopy Division				
5. AUTHOR(S) A. Weber, ed.				
6. PERFORMING ORGANIZATION (If joint or other than NBS, see instructions) NATIONAL BUREAU OF STANDARDS DEPARTMENT OF COMMERCE WASHINGTON, D.C. 20234			7. Contract/Grant No.	8. Type of Report & Period Covered
9. SPONSORING ORGANIZATION NAME AND COMPLETE ADDRESS (Street, City, State, ZIP)				
10. SUPPLEMENTARY NOTES <input type="checkbox"/> Document describes a computer program; SF-185, FIPS Software Summary, is attached.				
11. ABSTRACT (A 200-word or less factual summary of most significant information. If document includes a significant bibliography or literature survey, mention it here) This report summarizes the technical activities of the NBS Molecular Spectroscopy Division during the Fiscal Year 1986. The activities span experimental and theoretical research in high resolution molecular spectroscopy, quantum chemistry and laser photochemistry, and include the development of frequency standards, critically evaluated spectral data, applications of spectroscopy to important scientific and technological problems, and the advancement of spectroscopic measurement methods and techniques. A listing is given of publications and talks by the Division staff.				
12. KEY WORDS (Six to twelve entries; alphabetical order; capitalize only proper names; and separate key words by semicolons) biomolecules; energy transfer; high resolution molecular spectroscopy; hydrogen bonded molecules; laser photo chemistry; picosecond spectroscopy; quantum chemistry; spectral frequency standards; trace atmospheric species; van der Waals molecules.				
13. AVAILABILITY <input checked="" type="checkbox"/> Unlimited <input type="checkbox"/> For Official Distribution. Do Not Release to NTIS <input type="checkbox"/> Order From Superintendent of Documents, U.S. Government Printing Office, Washington, D.C. 20402. <input checked="" type="checkbox"/> Order From National Technical Information Service (NTIS), Springfield, VA. 22161			14. NO. OF PRINTED PAGES 113	
			15. Price \$16.95	

